



9TH Hardwood Proceedings

Part II.

With Special Focus on “An
Underutilized Resource:
Hardwood Oriented
Research”

2021

Sopron, Hungary

Editors:

Róbert Németh,

Peter Rademacher,

Christian Hansmann,

Miklós Bak, Mátyás Báder

9TH HARDWOOD PROCEEDINGS – PART II.

**WITH SPECIAL FOCUS ON “AN UNDERUTILIZED RESOURCE:
HARDWOOD ORIENTED RESEARCH”**

Editors: Róbert Németh, Peter Rademacher, Christian Hansmann, Miklós Bak, Mátyás Báder

Constant Serial Editors: Róbert Németh, Miklós Bak

ISSN 2631-004X (Hardwood Conference Proceedings)

UNIVERSITY OF SOPRON PRESS

SOPRON, 2021

9TH HARDWOOD PROCEEDINGS – PART II.

WITH SPECIAL FOCUS ON “AN UNDERUTILIZED RESOURCE:
HARDWOOD ORIENTED RESEARCH”

Volume 9 – Part II.

Editors: Róbert Németh, Peter Rademacher, Christian Hansmann, Miklós Bak, Mátyás Báder

Constant Serial Editors: Róbert Németh, Miklós Bak



UNIVERSITY OF SOPRON PRESS

SOPRON, 2021

9TH HARDWOOD PROCEEDINGS – PART II.
Sopron, 2021

Editorial board

Prof. Dr. Róbert Németh
Dr. Peter Rademacher
Dr. Christian Hansmann
Dr. Miklós Bak
Dr. Máttyás Báder

University of Sopron – Hungary
FATE - Wood Science Association – Hungary
Mendel University in Brno – Czech Republic
Wood K Plus – Austria
University of Sopron – Hungary
University of Sopron – Hungary

Scientific committee

Prof. Dr. Dr. h.c. Peter Niemz
Prof. Dr. Željko Gorišek
Prof. Dr. George I. Mantanis
Prof. Dr. Bartłomiej Mazela
Prof. Dr. Julia Mihailova
Prof. Dr. Holger Militz
Prof. Dr. Joris Van Acker
Prof. Dr. Ali Temiz
Dr. Milan Gaff
Dr. Galina Gorbacheva
Dr. Henrik Heräjärvi
Dr. Andreja Kutnar
Dr. Rastislav Lagana
Dr. Goran Milić
Dr. Lê Xuân Phuong
Dr. Emilia-Adela Salca
Dr. Vjekoslav Živković

ETH Zürich – Switzerland / Luleå University of
Technology – Sweden
University of Ljubljana – Slovenia
University of Thessaly – Greece
Poznań University of Life Sciences – Poland
University of Forestry – Bulgaria
Georg-August University Göttingen – Germany
Ghent University – Belgium
Karadeniz Technical University – Turkey
Czech University of Life Sciences – Czech Republic
Bauman Moscow State Technical University – Russian
Federation
Natural Resources Institute Finland (LUKE) – Finland
InnoRenew CoE – Slovenia
TU Zvolen – Slovak Republic
University of Belgrade – Serbia
Vietnam National University of Forestry – Vietnam
“Transilvania” University of Brasov – Romania
University of Zagreb – Croatia

Graphic design

Ágnes Vörös

University of Sopron – Hungary

Webservices

András Somos

University of Sopron – Hungary

University of Sopron Press, 2021

Responsible for publication: Prof. Dr. Attila Fábrián, rector, University of Sopron

ISBN 978-963-334-399-9 (online)

ISSN 2631-004X

Cover image: photograph of an oak glued-laminated timber sample by Miklós Bak, 2020

The manuscripts have been peer-reviewed by the editors and have not been subjected to linguistic revision.

© All rights reserved

Content

Opportunities and challenges for hardwood based engineered wood products <i>Joris Van Acker</i>	5
Opportunities and challenges coming with hardwood use for structural applications <i>Johannes Konnerth, Christian Huber, Peter Bliem, David Obernosterer, Pia Solt-Rindler, Georg Jeitler, Michael Grabner, Ulrich Müller, Hendrikus van Herwijnen, Maximilian Pramreiter</i>	15
Illegal logging and trade of illegally-derived forest: Africa and the sustainable market <i>Olajide Joseph Alaba</i>	16
Experimental results of monitoring wood drying and the occurrence of drying cracks in real-time in hardwoods <i>Hanna Botter-Kuisch, Jan Van den Bulcke, Jan M. Baetens, Joris Van Acker</i>	17
Sound analysis of mechanical wood cutting processes as a basis for adaptive process control <i>Mehieddine Derbas, Stephan Frömel-Frybort, Christian Laaber, Martin Riegler</i>	25
Effect of specimen moisture content on wood degrading capability of <i>Fuscoporia contigua</i> in vitro testing <i>István Eső, Norbert Horváth</i>	33
Novel test set-up for detailed analysis of wood cutting processes <i>Stephan Frömel-Frybort</i>	37
A short background to hardwood resources and properties in Ghana <i>James Govina, Róbert Németh</i>	38
An introduction of Ghana's hardwood products and market specialties <i>James Kudjo Govina, Róbert Németh</i>	47
Conduction of heat in the high temperature modified oak wood <i>Richard Hrčka, Barbora Slováčková</i>	49
Selected elastic properties of thermally treated beech wood <i>Rastislav Lagaňa, Andrej Janeka, Tomáš Andor</i>	56
A study of the surface properties of a solid wood coating system with self-healing microcapsules <i>Rastislav Lagaňa, Ján Svocák, Jozef Kúdela</i>	61
Oriented investigations on the application of NIR spectroscopy for the evaluation of the bonding quality of glued laminated timber from hardwood <i>Peter Niemz, Jakub Sandak, Juana Mai, Andreas Hänsel</i>	68
Develop an app to quickly identify popular timber species traded in Hanoi, Vietnam <i>Le Xuan Phuong, Vu Manh Tuong, Nguyen Thi Loan, Dong Thanh Hai, Le Minh Tuyen</i>	69
Substitution of softwood by hardwood species in the MDF process <i>Pinkl Stephan, Bugelnig N, Drexler F, Fitzthum R, Führer J, Höchtel S, Kolbitsch L, Loike C, Malzl L, Meixner R, Pilz N, Rudolf K, Schnepps J, Vasovic D, Vennemann J, Yang Y, Gindl-Altmatter W, Konnerth J, Martin Riegler</i>	75
Electric guitar neck from densified poplar? Experimental and numerical analysis <i>Sebera Václav, Mikuljan Marica, Niemelä J. Arne, Prislán Rok, Mrissa Michael, Kutnar Andreja, Pečnik G. Jaka</i>	76
Influence of soil in oak root system on its response to bending <i>Sebera Václav, Tippner Jan, Paulic Vinko, Praus Luděk, Vojáčková Barbora, Brabec Martin, Milch Jaromír</i>	83
Armillarioid root rot invasion: possibilities of silvicultural and chemical control <i>Liqiong Chen, Danish Shahab, Orsolya Kedves, Simang Champramary, Boris Indic, Viktor Dávid Nagy, Csaba Vágvölgyi, László Kredics, György Sipos</i>	90
Porosity of beech and oak heartwood degraded by <i>trametes versicolor</i> , L. Lloyd (<i>Fagus sylvatica</i> , L. and <i>Quercus petraea</i> , Matt. Liebl) <i>Barbora Slováčková</i>	98

Opportunities and challenges for hardwood based engineered wood products

Joris Van Acker

UGent-Woodlab, Laboratory of Wood Technology, Department of Environment, Ghent University,
Coupure Links 653, 9000 Ghent, Belgium, email: joris.vanacker@ugent.be

Keywords: Engineered wood products, hardwood species, green building

ABSTRACT

Since it becomes clear that we will need to be more bio-economy oriented in the future, there is a clear need to assess the potential of the wood resource as well as to prioritise some wood products. Application of timber and wood-based products in the construction sector has major merits in relation to the sustainable developments goals as defined by the United Nations and complying with the Green Deal of the EU.

Both the fact that hardwoods are underutilised in the construction sector and the many innovative engineered wood products that are now part of the forestry wood industry chain, create opportunities for a promising future.

The interest in new green building products has increased substantially over the last decades. There is extra emphasis on the utilization of hardwoods linked to the increased role of broadleaved tree species in forestry. This consistently increased focus on green development is mainly due to the public concern of the impact of global warming. There are quite some companies, institutes and authorities that have started making efforts on sustainable timber buildings. Glue laminated timber (GLT, glulam) and the introduction of cross laminated timber (CLT) are now established engineered wood products (EWPs) and are critical assets in green timber building constructions. These products are mainly based on softwoods, however hardwood species could be key to further green innovations. There are critical advantages in using hardwoods in the construction sector, especially when considering production output efficiency and sustainability. Firstly, there are opportunities in increasing the use of common hardwood products like plywood by means of focussing on construction end use. Secondly, other more specific structural engineered wood products like veneer and strand based LVL, LSL and I-joists should be regarded as additional tools to incorporate more hardwoods in green building alongside the massive timber options based on CLT and glulam.

INTRODUCTION

Wood has played an important role as a construction product for thousands of years due to its availability, flexibility and sustainable character. These advantages and a continuously growing demand, resulted in solid wood products with large dimensions from (semi-) natural forests, which have been intensively harvested. In order to apply wood in a more efficient way and rule out the inherent variability, engineered wood products are more widely used for many different end-uses.

The potential of forest production in both volume and quality is key to the future of the forest-based sector. Additionally, there is a growing impact of socio-economic parameters with a general concern to the adequate and sustainable supply of resources. Timber, wood, lignocellulosic biomass, or whatever name we give the material coming from forestry and related sectors, is an eminent renewable resource with high potential for sustainability and an excellent ecosystem service for our modern society. The balance between wood material use and bioenergy use will inevitably lead to higher competition for the same resource and could evolve into critical shortage. Vertical integration alongside a better tree and wood quality concept should lead to a more structured approach dealing with whether some wood products need to be prioritized and how we could deal with substitution of man-made (building) materials requiring more energy to be produced. This should be combined with the important option to produce green energy based on woody biomass.

Engineered wood products (EWP) are made from timber/lumber, veneers, strands, or from other small wood elements that are bound together with structural resins to form lumber-like structural products. Wood-based products have evolved over time, above all thanks to the development of new adhesives and to the glue-lamination technology that have made it possible to overcome some dimensional and behavioral

limitations inherent in solid wood, paving the way for structural applications and allowing modern wooden materials to acquire a level of reliability in design and use that make them comparable with those used in building and in the construction sector.

To enable an increased use of wood products for the building sector there is a need to include engineered wood products based on hardwoods. The modern engineered wood products (EWPs) suitable for wood constructions are an excellent tool in order to develop sustainable strategies for green building over the coming decades. In this framework, the raw material can also easily come from plantations based on fast growing hardwood species.

HARDWOOD AS RESOURCE

Trends

Traditionally, the output of roundwood in the EU is dominated by coniferous trees. In 2019, coniferous trees accounted for 69 % of all roundwood harvested in the forests of EU-27 countries. This share has remained stable throughout 2000–2019 (Eurostat data). In 2019 a Joint Vision was published providing sustainable choices in a climate-friendly future for Forest-based Industries (Eustafor 2019), and indicating a.o. to meet the increasing demand for raw materials by maximising new secondary streams and ensuring primary raw material supply from sustainably managed forests. Increasing the broad-leaved tree fraction in European forests mitigates hot temperature extremes and hence facilitates an increase of the broad-leaved tree fraction (BTF) in forests. This is a promising management strategy to enhance the provision of ecosystem services and to adapt to climate change (Schwaab et al. 2020). The importance of structurally diverse forests for the conservation of biodiversity and provision of a wide range of ecosystem services has been widely recognised (Storch et al. 2018). Hardwood forests are Europe's largest overlooked renewable resource. Broadleaved tree species account for 43% or 15.0 billion m³ of the European growing stock in forests. Hardwoods present the natural forest ecosystems in the largest part of Europe. Historically, hardwoods were widely used in construction, furniture, flooring, commodities, paper etc. Nowadays however, the forest-based industries in Europe are predominately based on softwood use. The largest share of hardwood today is mainly used inefficiently for energy generation. To valorise better the rich hardwood resource of Europe, it is essential to connect the forestry chain with the transforming industries and the final customers. Hardwoods represent the primary opportunity to foster a long-term strategic pathway for sustainable development of the emerging forest-based circular bio-economy and thus respond to major key societal and environmental global challenges (von Lengefeld and Kies 2018).

Beech and birch

Hardwood species like beech or birch with high stocks in the European forests are hardly used for products with high added value. The amount of hardwood forests has increased so that now, in Europe, almost 50% of forests are covered with hardwood species. Plywood lost most of its market share for furniture and even for house construction due to the competition by Oriented Strand Boards (OSB), Particle Boards (PB) and Medium Density Fibre Boards (MDF). In view of price competitiveness, the future of plywood production will rely mostly on hardwood (Berthold et al. 2017). Birch plywood has been the flagship of Finnish wood-based panel industries since 1910 (Kumar and Verkasalo 2019). However, both beech and birch have extra potential usage beyond plywood.

Hybrid Poplar

During the last century, fast-growing poplar clones have mainly been selected with a focus on specific end uses like the production of matches, plywood or pulp-based products. Today, a lot of new poplar and also willow clones are intended for short rotation coppice, and criteria for selection have been in part adjusted. The wood resource obtained from the fast-growing tree species is considered important to enable a higher production in the future and hence selection and breeding of these deciduous trees has been a major part of silvicultural and even agricultural frameworks. Furthermore, in many ways, poplar trees can be considered to be the best potential alternative to softwood species for engineered wood products (Van Acker et al. 2016). The applications related to biomass for energy and other less tree quality dependent end uses should be part of an integrated approach.

Mainly hybrid poplar is used in man-made plantations and agroforestry worldwide. The high environmental adaptability, high growth rate and short rotation period (often less than 20 years) make poplar one of the most efficient tree species in terms of sustainability. The development of engineered construction products based on poplar wood fits within the larger strategies to use more hardwoods for construction. The use of wood from fast-growing plantations contributes to enhance their important role for economy, society and environment, which is linked to a sustainable management and processing. The construction sector is essential to maximize this potential by creating added value to the whole chain through high performing EWP (Fig. 1).



Figure 1: Hybrid Poplar Engineered Wood Products as output of different processing and quality parameters

ENGINEERED WOOD PRODUCTS

Green building

Engineered wood products with focus on constructing with wood are eminent to focus on green building. Hildebrandt et al. (2017) underpinned the contribution of wood-based construction materials for leveraging a low carbon building sector in Europe. This will contribute to the creation of carbon sinks (Amiri et al. 2020) and will allow to bring ecosystem thinking to sustainability-driven wooden construction business (Viholainen et al. 2021).

Milner (2009) underlined the overall importance of sustainability of engineered wood products in construction. The changing timber resource has changed the way we use wood (McKeever 1997). One major change has been the introduction of engineered wood products, which can use the available timber resource more efficiently. EWPs allow the use of small diameter, low quality logs, the use of previously underutilized species, like some hardwoods. EWPs are designed to substitute directly for solid sawn wood products in many applications.

Sawn wood based: Glulam and CLT

Glued-Laminated Timber (GLT), Glulam, is an engineered stress-rated product made by gluing together 50 mm or thinner pieces of lumber. Cross-laminated timber (CLT) is a wood panel product made from gluing together layers of solid-sawn lumber, i.e., lumber cut from a single log. Each layer of boards is usually oriented perpendicular to adjacent layers and glued on the wide faces of each board, usually in a symmetric way so that the outer layers have the same orientation. Lightweight yet strong, CLT offers design flexibility and low environmental impacts – it outperforms concrete in terms of energy, air pollution and water pollution. Despite being 5 times lighter than concrete, CLT has a comparable strength per weight ratio to concrete.

Veneer based: Plywood and LVL

Softwood plywood is the “original” engineered wood product. Laminated Veneer Lumber (LVL) is a structural composite lumber product designed to compete with solid sawn lumber, particularly large dimension lumber. Primary uses include headers, beams, and rafters in construction and flanges for wood I-joists. Laminated Veneer Lumber (LVL) is similar in certain respects to glulam and plywood. It is fabricated by laminating thin sheets of veneer (0.25–0.4 cm thick) bonded together with durable adhesive. The veneer plies are usually laid up with all the wood fibres running in one direction and aligned parallel to the length of the member.

Strand based: OSB and LSL

Oriented Strand Board (OSB) is a non-veneer structural panel, manufactured from thin reconstituted wood strands or wafers and competes directly with softwood plywood in many construction applications. Aspen-OSB is an established product since decades in North-America. Specific strength and stiffness are interesting characteristics, but the ability to select quality trees with a major impact on production yield are also an asset.

Laminated Strand Lumber (LSL) is a non-veneer panel product manufactured by compressing wood strands of between 0.76 and 1.3 mm thickness coated with adhesive under heat. Hence, Oriented Strand Lumber is a similar product. Parallel Strand Lumber (PSL) is a lumber composite material produced from long strands or veneer strips. The strands are dried, coated with a waterproof adhesive and bonded together under pressure and heat. The strands are usually also aligned so that the wood grain is parallel to the length of the member. LVL, PSL and LSL are collectively known as Structural Composite Lumber (SCL).

The potential of using strand-based products as alternative for veneer-based ones has been demonstrated in wood I-joists. The prefabricated EWP type I-joist is a structural, load carrying substitute used for floor and roof framing applications. The final product can be a straight beam or a complex, curved structural member. The wood I-joist is composed of an OSB or plywood web and two LVL, OSB, or lumber flanges.

HARDWOOD ENGINEERED WOOD PRODUCTS

Trends

Most engineered components in North America are manufactured from softwoods, such as Douglas-fir, the southern pines, or spruce–pine–fir lumber (Ross and Shmulsky 2021). Significant research and development efforts have been devoted toward investigating the use of lower grade hardwood resources in engineered materials and components. Studies aimed at developing appropriate drying technologies, lumber grading procedures, and various engineered materials and components have been conducted. The publication by Ross and Erickson (2020) is a compilation of results obtained from research and development studies focusing on using low-grade hardwood materials in engineered components. Not only basic information is provided about this resource: availability, mechanical properties, log grading techniques, and appropriate drying methods, but it also summarizes studies that examine the use of this resource in trusses, laminated veneer lumber, I-joists, and other applications.

The hygroscopic behaviour of engineered timber, both glued-laminated (glulam) timber and laminated veneer lumber (LVL) made of softwood and hardwood, showed the impact of water vapor diffusivity. This underlines that for both drying and swelling/shrinkage performance the wood species characteristics are very relevant (Chiniforush et al. 2019).

The main issues with using hardwoods for CLT production, compared to softwood operations, are quick dulling of cutting tools because of higher hardwood density and a longer pressing time (Adhikari et al. 2020). Other factors, such as moisture content, various dimensions of the lumber, and the caustic nature of some species, were highlighted as limitations for the use of hardwood lumber in CLT panels. The primary concern of the manufacturers was the availability of hardwood lumber in the required quality and quantity. Although virtually all CLT structures are manufactured using softwood species, there is growing interest in the possibility of manufacturing CLT panels out of hardwoods in North America. Research on hardwood CLT is scarce but existing results suggest that it is technically feasible (Espinoza and Buehlmann 2018). Crovella et al. (2019) compared the mechanical properties of lower grade softwood and hardwood CLT panels. Because of their availability, mechanical properties and distinctive appearance, there is a growing interest for the use of hardwood species in structural products such as glued-laminated timber. Based on

assessing bonding and structural grading of northern hardwoods white ash (*Fraxinus americana* L.), yellow birch (*Betula alleghaniensis* Britt.) and white oak (*Quercus alba* L.) are considered promising species for the manufacture of Canadian hardwood glulam (Morin-Bernard et al. 2021).

Research on four green-glued Eucalyptus products (green roof trusses, face-laminated beams, edge-laminated planks and panels, and CLT) and some of the processing steps involved, was reviewed by Wessels et al. (2020). *Eucalyptus globulus* is one of the hardwood species growing in Europe and high strength finger-joints using 1C-PUR adhesive were developed for high performance engineered laminated products (Lara-Bocanegra et al 2017).

Aicher et al. (2018) reported on hardwood glulam (GLT) beams produced industrially from European hardwoods like oak, beech, sweet chestnut and ash as well as the tropical species as teak, keruing, melangangai and light red meranti.

Olorunnisola (2018) provides a review of design of structural elements with tropical hardwoods and underlines the importance of Engineered Wood Products.

Gilbert et al. (2018) reported on mechanical properties perpendicular to the grain and in shear of glued rotary peeled veneers, as would be encountered in veneer-based structural products, of three species recovered from juvenile (early to mid-rotation) subtropical hardwood plantation logs. This allowed to perform a reliability analysis of Laminated Veneer Lumber (LVL) beams manufactured (Gilbert et al. 2019). Shukla and Kamdem (2008) investigated the properties of laminated veneer lumber (LVL) made with low density hardwood species using cross-linked polyvinyl acetate (PVAc) adhesive and thin veneers of silver maple, yellow poplar and aspen.

Glulam based on beech, poplar, ...

European hardwood species such as beech, oak and ash present a potential alternative to commonly used softwoods in glued engineered wood products. Also birch glulam is commercially available. Although mainly amino- and phenoplast adhesives are used for bonding these hardwoods, there is an interest to use one-component polyurethane (1C-PUR) adhesives as an alternative especially when combined with a primer pretreatment (Luedtke et al. 2015).

Due to its average mechanical properties, poplar, a fast-growing species, has been disfavored compared to stronger species for several decades. Glued laminated timber (GLT) beams made with this species revealed a very promising mechanical behaviour as bending strength tests evidenced a ductile behavior on more than 70% of the beams (Monteiro et al. 2020). Poplar was considered due to the increase of availability in Portuguese forest and its relative low density combined with good mechanical properties (Martins et al. 2017).

Cross Laminated Timber based on beech, poplar, ...

Normally, CLT is made from softwood. In Canada, Essoua and Blanchet (2017) benchmarked with the most important wood species black spruce (*Picea mariana* M.) to assess CLT based on large leaf beech (*Fagus grandifolia* Ehrh.) glued with different polyurethane adhesives. Brunetti et al (2020) showed that strength grading was very effective for beech timber, as both machine grading, as well as visual grading, worked properly with good quality boards and with weaker pieces and the yields reflected the quality of the raw material. Dubois et al. (2020) reports on several positive properties of birch CLT.

Wang et al. (2018) indicated that the rolling shear properties increase with distance to the pith when using fast growing poplar wood as the cross-layers in CLT. With the expansion of CLT material throughout the global construction community, an effort is being made to explore the use of regionally produced CLT materials from Iran, including the testing of fast-grown poplar (*Populus alba*) (Hematabadi et al. 2020).

Laminated Veneer Lumber based on beech, poplar, ...

Knorz and Van de Kuilen (2012) made a high-capacity engineered wood product-LVL of European Beech (*Fagus sylvatica* L.), named BauBuche, which is a laminated veneer lumber made from locally sourced beech manufactured exclusively by Pollmeier.

An innovative model based only on local grain angle measurements proved to be more efficient than models taking into account the veneer density. It can be used to sort veneer during the peeling process and grade the production of beech LVL panels to optimize their mechanical properties even for low-quality veneer (Viguiet et al. 2018).

Aspen (*Populus tremuloides*) is a relatively new substitute species in North America for LVL production. It is worthy to note that two LVL mills in Canada pioneered the manufacture of aspen LVL. The success of these mills demonstrate that poplars are very suitable for LVL production. A novel laminated veneer lumber (LVL) was produced with poplar fibrosis veneers and phenolic formaldehyde. Tests were conducted to evaluate the properties of this product with different densities (ranging from 0.8 to 1.2 g cm⁻³). The mechanical properties and water resistance were observed to be superior to those values of the traditional LVL (Wei et al. 2019).

Combined products

Glued laminated timber (glulam) is most often made of coniferous, specifically spruce wood. It is possible to combine outer lamellas from hardwood with inner lamellas from softwood in a glulam cross-section. The combined cross-section appeared to be more advantageous especially in cases of smaller beam depth (Balász et al. 2020).

To enlarge the source of raw materials and improve the mechanical properties of CLT, some local hardwood species can be included. Li et al. (2020) explored the feasibility of using construction-oriented strand board (COSB) to fabricate hybrid CLT (HCLT).

The great beech forests extension in Europe has recently led to investigate the possible application of this hardwood species for the production of CLT panels. Beech-Corsican pine timber and melamine-based adhesive was used to check mechanical performances

of CLT panels both in the homogeneous and hybrid configurations (Sciomenta et al., 2020).

Experimental investigations on timber-concrete composite members made of beech LVL with notched connection. Thanks to the improved mechanical properties of beech wood, high strength and stiffness values were recorded (Boccardo et al. 2017). Shear transfer in beech LVL-concrete composites with inclined coach screw connectors was reported on by Sebastian et al. (2018).

Nguyen et al. (2018) worked on a methodology to optimise the manufacturing strategy of structural cross-banded laminated veneer lumbers (LVL-C) manufactured by blending Australian native-forest spotted gum (*Corymbia citriodora*) with plantation southern pine (Caribbean pine (*Pinus caribaea* var. *hondurensis*) and slash pine (*Pinus elliottii* var. *elliottii*)) veneers.

Modified hardwood EWPs

The concept of service life prediction (SLP) is of major importance for the utilisation of wood and wood products.

Glulam beams, which were made from hydrothermally treated poplar (*Populus deltoides*) showed that the hydrothermal treatment reduced the cross-sectional moisture induced stresses as well as relevant moisture gradients and it also caused an increase of the bending strength as well as stiffness of the treated wood and the glulam beams (Mirzaei et al. 2017).

Rotary cut beech (*Fagus sylvatica* L.) veneers were treated with four different lignin phenol formaldehyde (LPF) solutions using dimethyl sulfoxide (DMSO) as a solvent. Such technical lignins can, to a certain extent, be used as a substitute for standard PF resin for the production of beech LVL (Fleckenstein et al. 2018).

Barnes et al. (2018) assessed thermally modified plywood, oriented strand board, laminated strand lumber, and laminated veneer lumber as a posttreatment using a closed, pressurized treatment method. These heat treatments caused a reduction in weight loss when subjected to laboratory soil block durability tests.

Thermo-mechanically compressed wood dowels were used as a joint element alternative to the traditional glue and metallic fasteners to design novel engineered wood products (EWPs), namely adhesive-free laminated beams and cross-laminated timber panels (El Houjeyri et al. 2021).

Van Acker et al. (2020) presented some innovative approaches to increase service life of poplar lightweight hardwood construction products (Table 1).

Table 1: Options to increase service life of Engineered Wood Products (EWP)

Component	EWP	Durable wood	Vacuum pressure ¹	Glue-line additive	Surface spray ²	Thermal modification	Chemical modification	Resin ³	Coatings
Strand	OSB	-	-	±	+	+	+	+	-
	LSL	-	-	±	±	-	-	+	-
Veneer	Plywood	+	+	+	+	+	±	+	+
	LVL	±	±	+	±	±	±	+	+
Timber	CLT	+	+	-	+	+	±	±	+
	GLT	+	+	-	±	±	±	±	+

Legend: +: existing option, ±: feasible option, -: less probable option

¹: deep impregnation with biocides; ²: surface biocide application with potential diffusion, e.g. borates; ³: analogue to glue used for production or a hydrophobing agent; Abbreviations: EWP = engineered wood product; OSB = oriented strand board; LSL = laminated strand lumber; LVL = laminated veneer lumber; CLT = cross laminated timber; GLT = glue laminated timber or glulam.

CONCLUSIONS

While there is still a strong reliance on softwood production, there is a clear need to involve also hardwoods in the value chain for building with timber. In this context, fast growing hardwood plantations have a strong potential to furthermore increase and complement the regional production of forests, especially in view of an increasing demand for wood raw materials in the emerging bio-economy, limiting raw wood materials transportation. EWPs can be produced using fit-for-purpose processing for building with wood complying with requirements on performance related to durability (service life), fire safety, earthquake resistance, high-rise and low energy construction, among others. EWPs will contribute to the main advantages of building with wood: (1) Fast: short building time, often 30% faster, (2) Light: very good strength to stiffness ratio, and (3) Green: sustainable especially when using bioenergy. This makes EWP increasingly important for contemporary construction and renovation of buildings and infrastructures. EWPs based on sawn wood like Glulam or GLT (Glued Laminated Timber), CLT (Cross Laminated Timber), veneer based panels and beams like plywood or LVL (Laminated Veneered Lumber) and strand based products OSB (Oriented Strand Board), LSL (Laminated Strand Lumber) and the similar OSL (Oriented Strand Lumber) and derived I-joists are ready for a large-scale use in structural and functional applications - for massive timber constructions, prefabricated thermally insulated walls and timber frame structures, respectively - on full compliance with current standards and rules.

A larger use of hardwoods in the building sector will underpin sustainability and environmental objectives related to greenhouse gas emission and significantly contribute to the circular economy in particular through the improvement of a better vertical integration between cultivation and wood industry as part of the future bio economy. The latter is particularly interesting for rural communities in low wood production countries. Engineered wood products (EWPs) for high-valued building applications, both for new structures and renovation, can contribute to implement a new generation of zero waste - positive environmental impact building systems based on products specially designed in order to optimize mechanical performance, thermal insulation, service life and seismic behavior. In this framework, the wood resource derived from (fast growing) hardwood species and transformed in EWPs fit-for-purpose materials are able to cover multi-story buildings and go beyond 25 m span structures, addressing the demand for new and sustainable construction products, which meet the challenges of modern society concerning performance and sustainability. The above raw material can provide complementary products to the softwood-based ones with a clear link to local home-grown timber production with very high growth rate.

REFERENCES

- Adhikari, S., Quesada, H., Bond, B., & Hammett, T. (2020). Potential of Hardwood Lumber in Cross Laminated Timber in North America: A CLT Manufacturer's Perspective. *Mass Timber Construction Journal*, **3**(1), 1-9.
- Aicher, S., Ahmad, Z., & Hirsch, M. (2018). Bondline shear strength and wood failure of European and tropical hardwood glulams. *European Journal of Wood and Wood Products*, **76**(4), 1205-1222.
- Amiri, A., Ottelin, J., Sorvari, J., & Junnila, S. (2020). Cities as carbon sinks—classification of wooden buildings. *Environmental Research Letters*, **15**(9), 094076.
- Balász, I., Pešek, O., & Bukovská, P. (2020). Hardwood-Softwood Combination in Glued Laminated Timber Cross-Section. *Transactions of VSB - Technical University of Ostrava Civil Engineering Series. Section Building Structures & Structural Mechanics*, **20**, 1, 5-12.
- Barnes, H. M., Aro, M. D., & Rowlen, A. (2018). Decay of thermally modified engineered wood products. *Forest Products Journal*, **68**(2), 99-104.
- Berthold, D., Meinlschmidt, P., & Ritter, N. (2017). Hardwood processing in Germany – Challenges and opportunities for the wood based panel industry. In: *6th International Scientific Conference on Hardwood Processing Proceedings*, Veikko Möttönen and Emilia Heinonen (eds.), p. 97-108.
- Boccardo, L., Zweidler, S., Steiger, R., & Frangi, A. (2017). Bending tests on timber-concrete composite members made of beech laminated veneer lumber with notched connection. *Engineering Structures*, **132**, 14-28.
- Brunetti, M., Nocetti, M., Pizzo, B., Aminti, G., Cremonini, C., Negro, F., ... & Mugnozza, G. S. (2020). Structural products made of beech wood: quality assessment of the raw material. *European Journal of Wood and Wood Products*, **78**(5), 961-970.
- Chiniforush, A. A., Akbarnezhad, A., Valipour, H., & Malekmohammadi, S. (2019). Moisture and temperature induced swelling/shrinkage of softwood and hardwood glulam and LVL: An experimental study. *Construction and Building Materials*, **207**, 70-83.
- Chiniforush, A. A., Valipour, H., & Akbarnezhad, A. (2019). Water vapor diffusivity of engineered wood: Effect of temperature and moisture content. *Construction and Building Materials*, **224**, 1040-1055.
- Crovella, P., Smith, W., & Bartczak, J. (2019). Experimental verification of shear analogy approach to predict bending stiffness for softwood and hardwood cross-laminated timber panels. *Construction and Building Materials*, **229**, 116895.
- Dubois, H., Verkasalo, E., & Claessens, H. (2020). Potential of birch (*Betula pendula* Roth and *B. pubescens* Ehrh.) for forestry and forest-based industry sector within the changing climatic and socio-economic context of Western Europe. *Forests*, **11**(3), 336.
- El Houjeyri, I., Thi, V. D., Oudjene, M., Ottenhaus, L. M., Khelifa, M., & Rogaume, Y. (2021). Coupled nonlinear-damage finite element analysis and design of novel engineered wood products made of oak hardwood. *European Journal of Wood and Wood Products*, **79**(1), 29-47.
- Espinoza, O., & Buehlmann, U. (2018). Cross-laminated Timber in the USA: Opportunity for hardwoods? *Current Forestry Reports*, **4**(1), 1-12.
- Essoua, G. G. E., & Blanchet, P. (2017). Cross laminated timber made from large-leaf beech: Production, characterization and testing. In: *6th International Scientific Conference on Hardwood Processing Proceedings*, Veikko Möttönen and Emilia Heinonen (eds.), p. 208-212.
- Fleckenstein, M., Biziks, V., Mai, C., & Militz, H. (2018). Modification of beech veneers with lignin phenol formaldehyde resins in the production of laminated veneer lumber (LVL). *European journal of wood and wood products*, **76**(3), 843-851.
- Gilbert, B. P., Husson, J. M., Bailleres, H., McGavin, R. L., & Fischer, M. F. (2018). Perpendicular to grain and shear mechanical properties of veneer-based elements glued from single veneer sheets recovered from three species of juvenile subtropical hardwood plantation logs. *European Journal of Wood and Wood Products*, **76**(6), 1637-1652.
- Gilbert, B. P., Zhang, H., & Bailleres, H. (2019). Reliability of laminated veneer lumber (LVL) beams manufactured from early to mid-rotation subtropical hardwood plantation logs. *Structural Safety*, **78**, 88-99.

- Hematabadi, H., Madhoushi, M., Khazaeyan, A., Ebrahimi, G., Hindman, D., & Loferski, J. (2020). Bending and shear properties of cross-laminated timber panels made of poplar (*Populus alba*). *Construction and Building Materials*, **265**, 120326.
- Hildebrandt, J., Hagemann, N., & Thrän, D. (2017). The contribution of wood-based construction materials for leveraging a low carbon building sector in Europe. *Sustainable cities and society*, **34**, 405-418.
- Knorz, M., & Van de Kuilen, J. W. G. (2012). Development of a high-capacity engineered wood product-LVL made of European Beech (*Fagus sylvatica* L.). In: WCTE 2012: *World Conference on Timber Engineering*, Auckland, New Zealand.
- Kumar, A., & Verkasalo, E. (2019). Wood-based panel industries in Finland—current status and development potential. *Pro Ligno* **15**, 4, 185-192.
- Kuzman, M. K., Klarić, S., Barčić, A. P., Vlosky, R. P., Janakieska, M. M., & Grošelj, P. (2018). Architect perceptions of engineered wood products: An exploratory study of selected countries in Central and Southeast Europe. *Construction and Building Materials*, **179**, 360-370.
- Lara-Bocanegra, A. J., Majano-Majano, A., Crespo, J., & Guaita, M. (2017). Finger-jointed *Eucalyptus globulus* with 1C-PUR adhesive for high performance engineered laminated products. *Construction and Building Materials*, **135**, 529-537.
- Li, Q., Wang, Z., Liang, Z., Li, L., Gong, M., & Zhou, J. (2020). Shear properties of hybrid CLT fabricated with lumber and OSB. *Construction and Building Materials*, **261**, 120504.
- Luedtke, J., Amen, C., van Ofen, A., & Lehringer, C. (2015). 1C-PUR-bonded hardwoods for engineered wood products: influence of selected processing parameters. *European Journal of Wood and Wood Products*, **73**(2), 167-178.
- Martins, C., Dias, A. M. P. G., & Cruz, H. (2017). Glulam made by Poplar: delamination and shear strength tests. In: *6th International Scientific Conference on Hardwood Processing Proceedings*, Veikko Möttönen and Emilia Heinonen (eds.), pp. 222-231.
- McKeever, D. B. (1997). Engineered wood products: a response to the changing timber resource. *Pacific Rim Wood Market Report*, **123**(5), 15.
- Milner, H. R. (2009). Sustainability of engineered wood products in construction. In: *Sustainability of construction materials*, pp. 184-212. Woodhead Publishing.
- Mirzaei, G., Mohebbi, B., & Ebrahimi, G. (2017). Glulam beam made from hydrothermally treated poplar wood with reduced moisture induced stresses. *Construction and Building Materials*, **135**, 386-393.
- Monteiro, S. R., Martins, C., Dias, A. M., & Cruz, H. (2020). Mechanical performance of glulam products made with Portuguese poplar. *European Journal of Wood and Wood Products*, **78**(5), 1007-1015.
- Morin-Bernard, A., Blanchet, P., Dagenais, C., & Achim, A. (2021). Glued-laminated timber from northern hardwoods: Effect of finger-joint profile on lamellae tensile strength. *Construction and Building Materials*, **271**, 121591.
- Nguyen, H. H., Gilbert, B. P., McGavin, R. L., & Bailleres, H. (2019). Optimisation of cross-banded laminated veneer lumbers manufactured from blending hardwood and softwood veneers. *European Journal of Wood and Wood Products*, **77**(5), 783-797.
- Olorunnisola, A. O. (2018). *Design of structural elements with tropical hardwoods*. Springer International Publishing.
- Ross, R., & Shmulsky, R. (2021). *Some Mechanical Properties of Hardwood-Based Particle Composite Materials*. General Technical Report USDA FPL-GTR-283, 1-6.
- Schwaab, J., Davin, E. L., Bebi, P., Duguay-Tetzlaff, A., Waser, L. T., Haeni, M., & Meier, R. (2020). Increasing the broad-leaved tree fraction in European forests mitigates hot temperature extremes. *Scientific reports*, **10**(1), 1-9.
- Sebastian, W. M., Piazza, M., Harvey, T., & Webster, T. (2018). Forward and Reverse shear transfer in beech LVL-concrete composites with singly inclined coach screw connectors. *Engineering Structures*, **175**, 231-244.
- Sciomenta, M., Spera, L., Bedon, C., Rinaldi, V., Fragiaco, M., & Romagnoli, M. (2021). Mechanical characterization of novel Homogeneous Beech and hybrid Beech-Corsican Pine thin Cross-Laminated timber panels. *Construction and Building Materials*, **271**, 121589.
- Shukla, S. R., & Kamdem, D. P. (2008). Properties of laminated veneer lumber (LVL) made with low density hardwood species: effect of the pressure duration. *Holz als Roh-und Werkstoff*, **66**(2), 119-127.

- Storch, F., Dormann, C. F., & Bauhus, J. (2018). Quantifying forest structural diversity based on large-scale inventory data: a new approach to support biodiversity monitoring. *Forest Ecosystems*, **5**(1), 1-14.
- Van Acker, J., Defoirdt, N., & Van den Bulcke, J. (2016). Enhanced potential of poplar and willow for engineered wood products. In: *Proceedings of the 2nd Conference on Engineered Wood Products Based on Poplar/Willow Wood*. León, Spain, pp. 187-210.
- Van Acker, J., Jiang, X., & Van den Bulcke, J. (2020). Innovative Approaches to Increase Service Life of Poplar Lightweight Hardwood Construction Products. In: *XV International Conference on Durability of Building Materials and Components (DBMC 2020)*. Current Topics and Trends on Durability of Building Materials and Components, Serrat, C., Casas, J.R. and Gibert, V. (eds).
- Viguier, J., Bourgeay, C., Rohumaa, A., Pot, G., & Denaud, L. (2018). An innovative method based on grain angle measurement to sort veneer and predict mechanical properties of beech laminated veneer lumber. *Construction and Building Materials*, **181**, 146-155.
- Viholainen, N., Kylkilähti, E., Autio, M., Pöyhönen, J., & Toppinen, A. (2021). Bringing ecosystem thinking to sustainability-driven wooden construction business. *Journal of Cleaner Production*, **292**, 126029.
- von Lengefeld, A. K., & Kies, U. (2018). Teaming-up for the European Hardwoods Innovation Alliance (EHIA): Take your action! In: *8th Hardwood conference proceedings*, Sopron, pp. 15-16.
- Wang, Z., Dong, W., Wang, Z., Zhou, J., & Gong, M. (2018). Effect of macro characteristics on rolling shear properties of fast-growing poplar wood laminations. *Wood Research*, **63**(2), 227-238.
- Wei, Y., Rao, F., Yu, Y., Huang, Y., & Yu, W. (2019). Fabrication and performance evaluation of a novel laminated veneer lumber (LVL) made from hybrid poplar. *European Journal of Wood and Wood Products*, **77**(3), 381-391.
- Wessels, C. B., Nocetti, M., Brunetti, M., Crafford, P. L., Pröller, M., Dugmore, M. K., ... & Naghizadeh, Z. (2020). Green-glued engineered products from fast growing Eucalyptus trees: a review. *European Journal of Wood and Wood Products*, **78**(5), 933-940.

Opportunities and challenges coming with hardwood use for structural applications

Johannes Konnerth¹, Christian Huber¹, Peter Bliem², David Obernosterer³, Pia Solt-Rindler², Georg Jeitler³, Michael Grabner¹, Ulrich Müller¹, Hendrikus van Herwijnen², Maximilian Pramreiter¹

¹ BOKU University of Natural Resources and Life Sciences Vienna, Institute of Wood Technology and Renewable Materials, Konrad Lorenz Strasse 24, 3430 Tulln, Austria, johannes.konnerth@boku.ac.at

² Wood Kplus, Kompetenzzentrum Holz GmbH, Altenberger Strasse 69, 4040 Linz, Austria

³ Hasslacher Holding GmbH, Feistritz 1, 9751 Sachsenburg, Austria

Keywords: Mechanical properties, yield, alternative disintegration, material comparison, adhesive bonding.

ABSTRACT

Building in timber is increasing in importance and becoming a huge trend supported by European governments to contribute to the aim of a drastic CO₂ reduction in the atmosphere by storage and substitution. The building sector is the major consumer for solid wood, so far dominated by softwood species. Inherent log wood raw material characteristics and current ways of processing solid wood are the reason for a relatively low yield of finished building products out of logs.

Aiming for improved resilience, silviculture is changing species composition in European forests resulting in increasing share in hardwood species available on a long term. Substantial substitution of softwood by hardwood species is expected to not only dramatically influence high quality logwood quantity. Manufacturers will also have to deal with significant differences in material properties when using hardwood compared to softwood, and even within individual wood species, resulting in new challenges during production. Additionally, the sector will have the opportunity to create products with new sets of properties and aesthetics. In the current ambient of change, wood science and industry is forced to foster new utilizations pathways to account for individual species and assortment inherent wood characteristics, in order to cope with the expected increasing gap of raw material availability, properties and expected demand.

Illegal logging and trade of illegally-derived forest: Africa and the sustainable market

Olajide Joseph Alaba¹

¹ Chairman, BlackCamel Energy Ltd/Forest Products Traceability Network

Email: joseph.africanwood@gmail.com. Phone: +2348160008570

Keywords: Forest, timber legality standard, logging, Africa and Western countries

ABSTRACT

Illegal logging is considered as a problem in Nigeria and Africa at large. Nigeria is being ranked as a high risk nation due to unregulated practices. It is being constituted as a threat for sustainability of forest management. In timber production-supply-consumption cycle, illegal logging mainly occurs in phase of forest felling, where it is difficult to identify and control all possible cases. The percentage of illegal logging is calculated as proportion of registered illegal cuttings and total cuttings in the country. Data capturing is a huge problem due to lack of modern capturing equipment and training. Seeking to reduce illegal logging, Forest Products Traceability Network has created a standard in conjunction with all stakeholders in Nigeria to work on improvement of forestry related legislation. The standard which is in alignment with the FSC and PEFC forest and forest products management standard will be used as yardstick to measure legal and illegal timber in the country. Why illegal logging thrived is because there is market for the illegally harvested timber. If illegalities must be eradicated, there should be a better alternatives for practices. Therefore, if premium market for timber products are assured, illegalities will easily be eradicated and people will embrace legality. Promoting trade of legal timber in the US market is the best alternative and strong factor in making legality thrive in Africa. Unfortunately, EU, US and most Western countries that frowns on unsustainable practices are the ones indirectly promoting illegal logging especially in Nigeria. They buy from Asians (China, Vietnam, Indian) thinking they are buying from a managed forest and thereby not faulting any forestry laws. However, the fact is that these Asians buys from Nigeria and the rest of African countries illegally. Take it to their country and green washed them for sales to the EU, United States and other Western countries. Introducing the Nigerian legal logs to the EU and US sustainable timber market will not only boost transparency and traceability but will boost genuine promotion of a friendly environment and transparent adoption of the EUTR and United States Government Lacey Act for timber imports.

Experimental results of monitoring wood drying and the occurrence of drying cracks in real-time in hardwoods

Hanna Botter-Kuisch^{1,2}, Jan Van den Bulcke², Jan M. Baetens³, Joris Van Acker²

¹ Department of Infrastructure, Anton de Kom University of Suriname, Leysweg 86, POB 9212, Paramaribo, Suriname, email: hanna.kuisch@uvs.edu

² UGent-Woodlab, Laboratory of Wood Technology, Department of Environment, Ghent University, Coupure Links 653, 9000 Ghent, Belgium, email: hanna.kuisch@ugent.be, jan.vandenbulcke@ugent.be, joris.vanacker@ugent.be

³ Department of Data analysis and mathematical modelling, Ghent University, Coupure Links 653, 9000 Ghent, Belgium, email: jan.baetens@ugent.be

Keywords: Hardwood drying, real-time monitoring, cracks, wood anatomy, electrical resistance, temperature, shrinkage

ABSTRACT

Drying is a fundamental step in solid wood processing, yet it is very challenging. This is even more valid for several tropical hardwood species, mainly because of high incidence of potential drying defects negatively affecting the final product quality. Successful kiln drying depends largely on the diffusivity and permeability of the wood species, which in turn depends on several variables. Despite many research efforts, predicting kiln-drying schedules for a given wood species is not fully feasible. The main reason is that important spatio-temporal variables such as moisture and temperature gradients, and wood anatomical features are considered insufficiently in predictive modelling frameworks. We expect that the monitoring and controlling of the drying process up to the limit states can be used for any wood species.

To understand the influence of variables determining these limit states we developed an experimental measurement set-up consisting of heat-resistant load cells mounted in an oven to continuously record the weight of the wood specimens dried at 100 °C. In addition, specimens are equipped with custom-made electrodes and thermistors to determine the electrical resistance (ER), which relates to the moisture content (MC), and the temperature, respectively. To determine the onset and development of cracks, as well shrinkage of the cross section at the end grain, a camera is mounted to acquire images of the wood specimens during drying.

This paper presents the experimental results of a tropical hardwood species *Dicorynia guianensis* and a temperate hardwood species *Quercus robur*, using this experimental methodology. The results show that the general trends observed for average MC, ER, temperature, crack development and shrinkage of the cross section at end grain as a function of drying time, are similar for both wood species. The differences in an observed trend are due to the wood anatomical structure of a wood species.

This methodology enables to unveil interrelationships between the measured variables and changes of the wood anatomical structure, of utmost importance for the fine-tuning and prediction of kiln-drying schedules. Currently, more tropical hardwood species and multiple specimens are being tested using this methodology. Here, we present a proof-of-concept.

INTRODUCTION

Since long wood has been used as a renewable and durable material in the building and construction sector. In Suriname this has resulted in a profound practical knowledge on how to use wood, mainly tropical hardwood, in optima forma. Unfortunately, the use of hardwood as a building and construction material has declined substantially in Suriname (Tropenbos 2011). This is not in line with development strategies for a country with a forested area of more than 90%. Given proper education on logging, wood processing and usage, the forests in Suriname can be a continuous source of renewable and sustainable materials for current and future generations of Suriname (Tropenbos 2011).

At present, sawing is the major processing technique in Suriname, whereas drying of wood, which constitutes a basic wood processing technique and is a major starting point for creating added value, is seriously underdeveloped. Some of the advantages of dried wood are: 1) no risk of fungal activity in wood having a moisture content (MC less than 20%), 2) dried wood is about twice as strong and stiff as wet wood, 3) dried wood weighs 40% to 50% less than wet, undried wood, 4) timber products made from properly dried wood will not or hardly shrink during use, while products made from wet wood often shrink significantly as the wood dries, and 5) further processing steps like gluing and finishing are much easier to achieve with dry wood (Denig, 2000).

Drying of tropical hardwood species is very challenging due to the great variety in their anatomical structures and many defects that are prone to occur. In general, many tropical hardwoods are of very high density in contrast to softwood species often used for construction all over the world, and can contain high levels of wood extractives that hamper drying and increase the risk for shrinkage cracks during drying. In addition, specific anatomical features of hardwood, such as the presence of spiral grain and abundant parenchyma, pose a further challenge often resulting in dimensional distortion of the timber during drying, rendering them useless for further use. Furthermore, some tropical hardwood species should be dried fast and preferably immediately after sawing as fresh sawn wood in the hot and humid environment of the tropics is prone to biological attack by insects, fungi, and to oxidation, all of which lower the economic value significantly. Although the basic processing steps for wood drying are relatively simple and straightforward, incorrect drying can lead to increased defects making the final product sometimes no longer fit for purpose.

Kiln drying of wood is the most preferred drying method because it is reliable and fast. A kiln drying schedule, indicating a desired temperature, humidity and air velocity for the dryer, is tuned to the wood species and timber dimensions at hand. Such a schedule is a carefully developed compromise between the need to dry wood quickly and the need to avoid drying defects due to severe drying conditions (Denig 2000). Therefore, the occurring drying stresses in wood must be kept within limits to prevent failure of the wood tissue (Panshin and De Zeeuw 1970). The level of critical stresses resulting in wood failure varies among wood species. Thereby, selecting a proper schedule for wood species with no drying information is quite difficult. In the case of Suriname, kiln drying schedules are known for about 25 tropical hardwood species, whereas more than 300 commercial hardwood species are of interest. Selecting a suitable schedule for the remaining hardwood species, but especially for any wood species, can be achieved by applying the 'trial-and-error' method or by a prediction method, of which the latter will be most effective.

According to Botter-Kuisch et al. (2020), different research groups contributed to find suitable drying methods in order to keep the level of critical stresses below the point at which wood failure might occur. They presented a literature overview of investigated variables for wood exposed to different drying conditions and concluded that these studies insufficiently considered important variables in the predictive modelling framework. Besides the variables mentioned in literature, spatio-temporal variables such as moisture and temperature gradients, as well wood anatomical features during drying must be considered according to these researchers. Therefore, they developed an experimental set-up that allows real-time monitoring of several variables for any hardwood species. The variables measured in real-time using this experimental methodology are:

1. drying rate: determined by the average moisture loss of the entire wood specimen as a function of time,
2. local MC gradient: inferred from the electrical resistance (ER) gradient,
3. wood temperature gradient,
4. onset and development of cracks at the end grain, and
5. shrinkage of the cross section.

This paper presents the experimental results of a tropical hardwood species *basralocus* (*Dicorynia guianensis*) and a temperate hardwood species oak (*Quercus robur*), using the experimental methodology described in detail by Botter-Kuisch et al. (2020).

EXPERIMENTAL METHODS

Sampling of specimens

Two wood species were selected for this paper: a temperate hardwood species European oak (*Quercus robur*) originating from Charleville-Mézières in France (Europe), and a tropical hardwood species basralocus (*Dicorynia guianensis*) originating from Tibiti located in Central Surinam (South America). Specimens of five different trees were tested for the wood species basralocus and specimens of three different trees for the wood species oak. The quartersawn beams cut from these logs were all green. The beams, containing only heartwood and without visible defects, were planed to a final cross section of 50 x 50 mm². The length of the drying specimens (further referred to as D-specimens) was 120 mm. The length of the specimens used to determine the MC of the D-specimens was 50 mm (further referred to as M-specimens). The sequence of cutting these specimens from the beam is illustrated in Fig. 1. The end grain of all D-specimens was sanded and polished with an orbit sander.

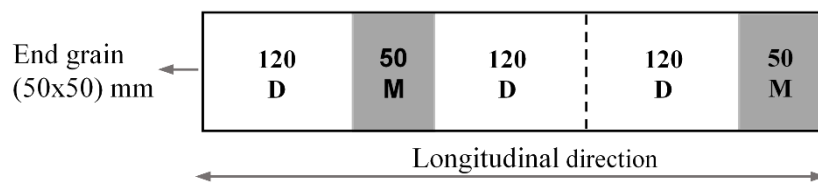


Figure 1: Drying specimens (D: 50 × 50 × 120 mm³) used in experimental set-up and specimens used for determining MC (M: 50 × 50 × 50 mm³) cut from a quartersawn beam (Botter-Kuisch et al. 2020)

Each test run contains four D-specimens. In two of these specimens, electrodes and thermistors were mounted (further referred to as the wired (DW) specimens), and the other two specimens served as reference (DR) specimens. Of all four D-specimens, the mass of the entire specimen was recorded during drying. The number and type of specimens tested for each wood species is given in Table 1 along with the average MC.

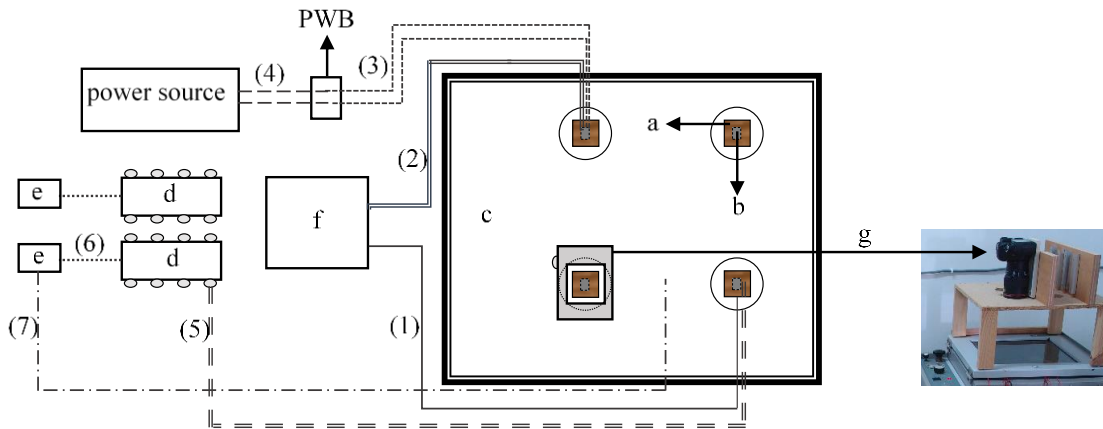
Table 1: Number of reference (DR) and wired (DW) specimens tested, and average MC of the wood species

Wood species	DR-specimens	DW-specimens	Total	Average MC ^a [%]
basralocus	16	16	32	63.5 ± 5.6
oak	6	6	12	70.7 ± 8.2

^aCalculated from the M-specimens

Experimental Methodology

Experiments were carried out using the custom-built set-up illustrated in Fig. 2 and described in detail in Botter-Kuisch et al. (2020). The maximum temperature of the oven was set to 100 °C to dry the wood specimens. Images of the polished end grain cross section of the wood specimens during drying were acquired by camera mounted on top of the oven.



- (1) — Thermistor in wood connected to GP2 data logger
- (2) — 2 Signal cables (positive and negative) of load cell connected to GP2 data logger
- (3) 2 Excitation cables (positive and negative) of load cell soldered to a printed wiring board (PWB)
- (4) — — Electrical wires soldered to PWB and connected to power source
- (5) = = 2 Custom-made electrodes in wood connected to Gigamodule
- (6) Interface cable to connect Gigamodule to Thermofox data logger
- (7) _ . _ Thermistor in oven connected to Thermofox data logger

Figure 2: Scheme of the custom-built experimental set-up to monitor wood variables in real-time during high-temperature drying. Wood specimens (a) were mounted on heat-resistant load cells (b), in an oven with a glass door (c) heated at 100 °C. Furthermore, the scheme illustrates data loggers, more specifically two Material Moisture Gigamodules (d) along with two Thermofox Universal modules (e) for measuring ER in the wood specimen, a GP2 Data Logger (f) for measuring temperature and mass of the wood specimens. On top of the oven, a camera (g) was mounted to acquire images of the polished end grain with the aim to monitor crack development during drying and to visualize and quantify wood anatomical features (Botter-Kuisch et al. 2020)

The variables were measured in real-time following the methodology developed by Botter-Kuisch et al. (2020):

1. In order to determine the average moisture loss, the DW- and DR-specimens were mounted on heat-resistant load cells in the oven to continuously record the mass of the wood specimens dried at 100 °C. These load cells were connected to the GP2 data logger.
2. In order to determine the local MC gradient, the DW-specimens were equipped with custom-made electrodes inserted at different positions at both a depth of 25 mm (core measurements) and a depth of 5 mm (surface measurements) of the specimen. The electrical wires of these electrodes were connected to the Gigamodule to measure the ER, and the Gigamodule was connected to the external Thermofox data logger to record the measured data during drying.
3. In order to determine the temperature gradient, two thermistors were inserted in each DW-specimen, at both a depth of 25 mm (core measurement at the centre of the specimen) and a depth of 10 mm (surface measurement near the end grain). These thermistors were connected to the GP2 data logger to record the temperature in the wood specimen during drying.
4. In order to determine the onset and development of cracks at the end grain, a camera that could be moved manually to different positions, was mounted on top of the oven to acquire images of the wood specimens inside the oven during the drying experiment. The end cracks visible in the different images were quantified and analysed using Fiji.
5. In order to determine the shrinkage of the cross section at end grain, as well the tangential and radial shrinkages, the same images were analysed using Fiji.

This paper presents only the results of the positions of the electrodes and thermistors mounted in the DW-specimens that are shown in Fig. 3, which are at the centre and near the end grain on both the front and the back of the specimen.

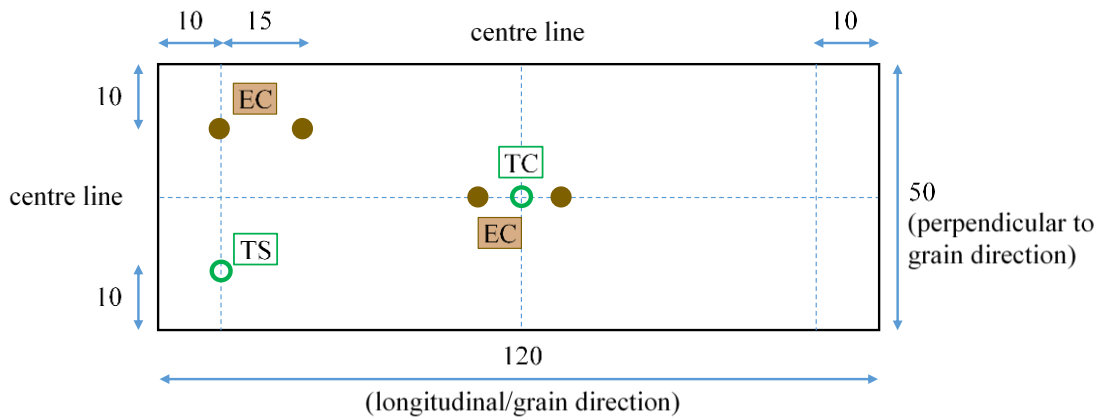


Figure 3: Schematic view of selected positions (at the centre and near the end grain) of the custom-made electrodes (pairs EC 1 and EC2) and heat-resistant thermistors (TC1 – core measurement and TS2 – surface measurement) mounted in the wired specimen. EC: pairs electrodes at the upper face for core measurements at a depth of 25 mm. At the bottom face and at corresponding positions electrodes (ES) were mounted for surface measurements at a depth of 10 mm. All dimensions in this scheme are in mm

RESULTS AND DISCUSSION

The results of the measured variables are presented in the same sequence as mentioned in the previous section. Regarding the image analysis of the end cracks in Fiji, only the results of basalocus are presented in this paper, because the images of the oak specimens are currently being processed and analysed.

MC as a function of drying time

The average MC as a function of drying time of the DR-specimens for both wood species is presented in Fig. 4. The steepness of these curves reflects the drying rate.

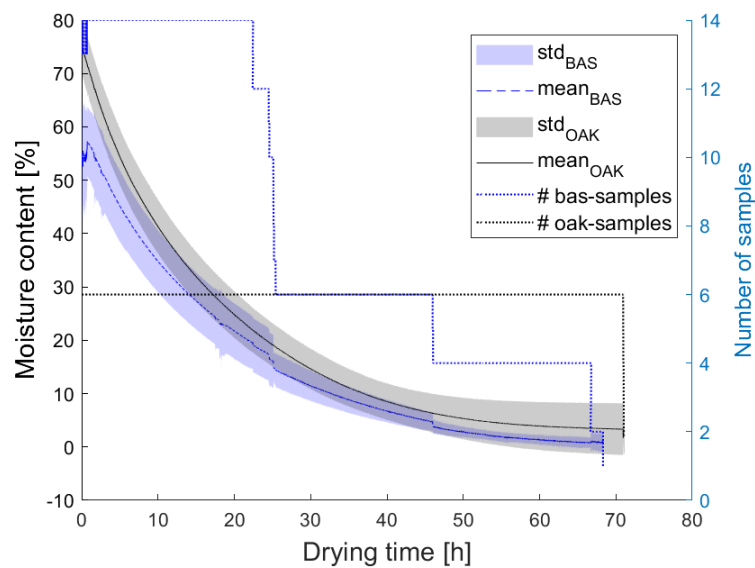


Figure 4: Average MC during drying of the reference (left) and wired (right) specimens for both wood species

ER as a function of drying time

The ER at different positions is illustrated in Fig. 5. The ER of both wood species near the end grain measured at the corner of the upper face and at the core (EC2 in Fig.3) or at the surface shows a faster increase compared to the ER measured at the centre of the specimens and at the core (EC1 in Fig. 3) or at the surface. This implies that in the longitudinal direction of the wood the ER increases during drying moving from the centre to the end grain that means a decrease in MC. In addition, the ER at the core (upper row in Fig. 5) increases slower than at the surface (bottom row in Fig. 5) for both wood species. This implies that in the transverse direction of the wood, moving from the core to the surface, the MC decreases faster during drying at the outer layers. These observations agree with literature (Skaar 1988, Simpson 1991). Also a slight difference is observed between the steepness of the basalocus and oak curves, especially at the core measurements (upper row in Fig. 5). The influence of the wood species is currently being investigated and is therefore not presented in this paper.

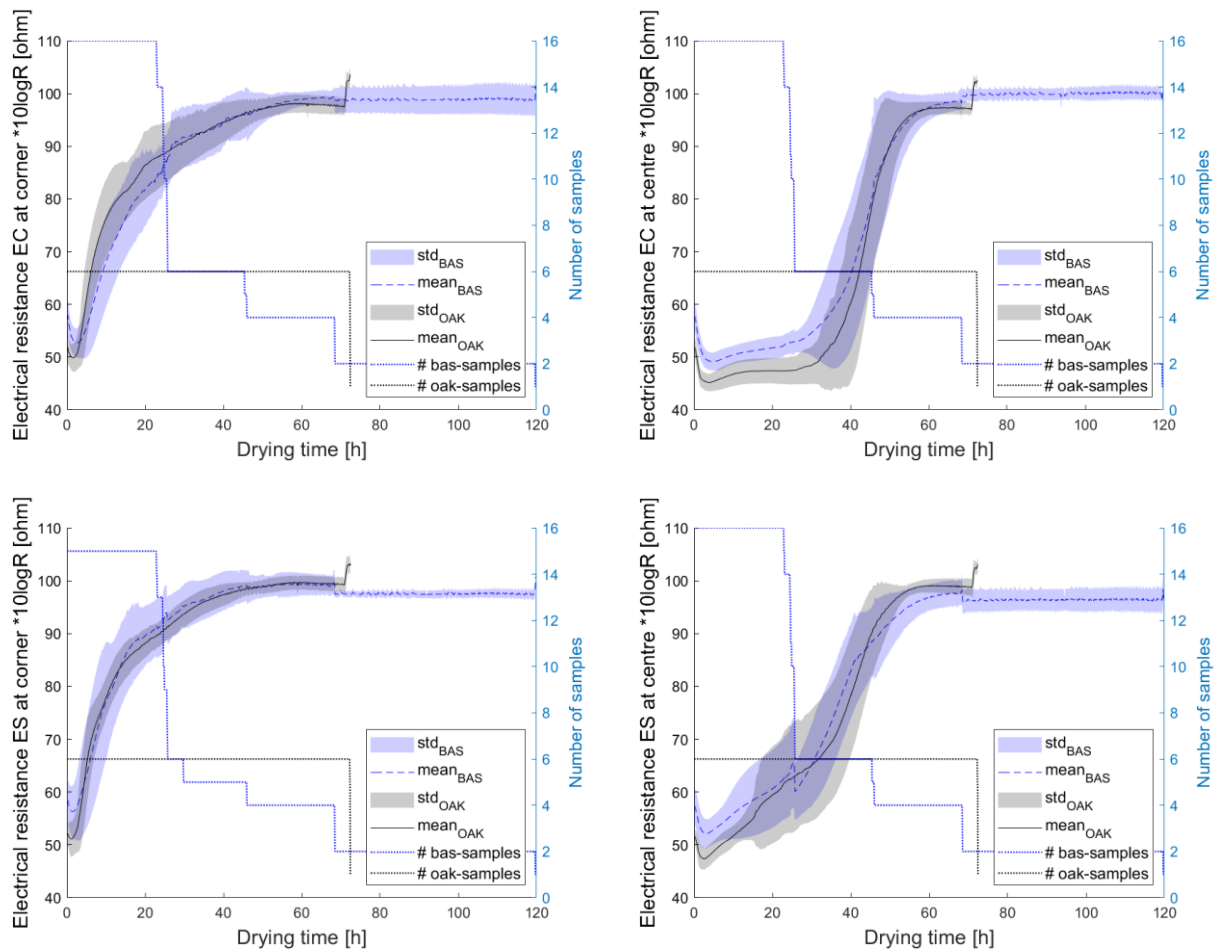


Figure 5: ER during drying near the end grain (left) and at the centre (right) of the specimens for both wood species. Upper row: ER measurements at the core (at a depth of 25 mm: EC). Bottom row: ER measurements at the surface (at a depth of 5 mm: ES)

Temperature as a function of drying time

The local temperature measured at both the core and surface is presented in Fig. 6 for both wood species. Similar to the results of the ER, temperature increase in the core at the centre is slower than at the surface near the end grain.

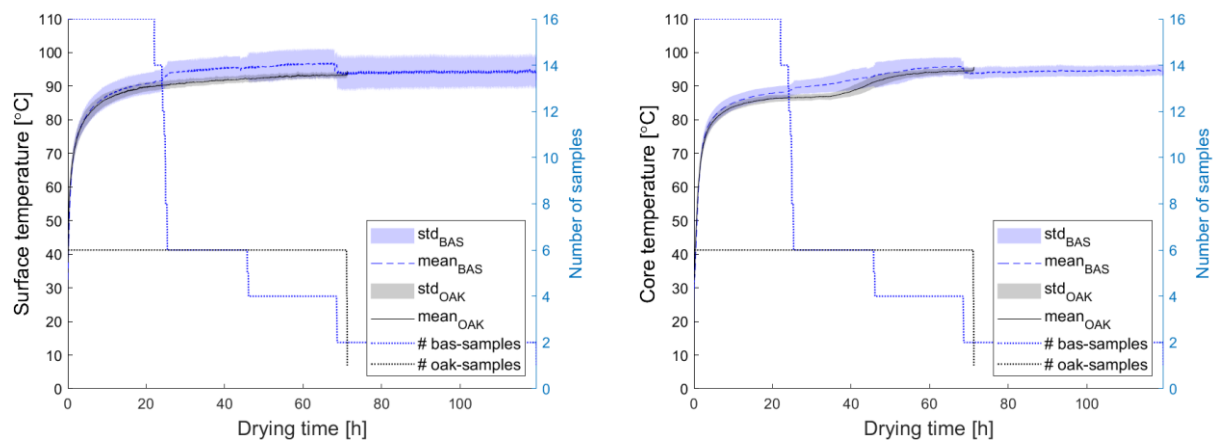


Figure 6: Temperature during drying near the end grain (left) and at the centre (right) of the specimen for both wood species. Measurement at the surface (at a depth of 10 mm: TS) and at the core (at a depth of 25 mm: TC)

Crack development and shrinkage during drying

The development of the end cracks for both wood species is presented in Fig. 7 at three of the distinctive moments described by Botter-Kuisch et al. (2020). These are t_0 (specimen at wet condition), t_1 (first cracks observed) and t_3 (maximum number of cracks). In addition, an image after one day (circa 24 hours) of drying is also presented in the last column.

t = 0 h Shrinkage area = 0%	t = 0.5 h 0.45%	t = 2.5 h 1.97%	t = 23.5 h 8.71%
t = 0 h Shrinkage area = 0%	t = 0.5 h 1.07%	t = 3 h 3.71%	t = 22 h 8.41%

Figure 7: Crack development at end grain of a basralocus specimen (upper row) and an oak specimen (bottom row) during the first 24 hours of drying. The drying time (t) is also indicated, as well the shrinkage of the cross section at end grain

For both wood species, all cracks followed the rays in the radial direction. However, cracks in the tangential direction (Fig. 8 left) were also observed on the end grain of basralocus specimens, which were never observed for oak.

The results of the quantified and analysed cracks in Fiji for 19 basralocus specimens are given in Table 2. The cracks in oak are currently being analysed.

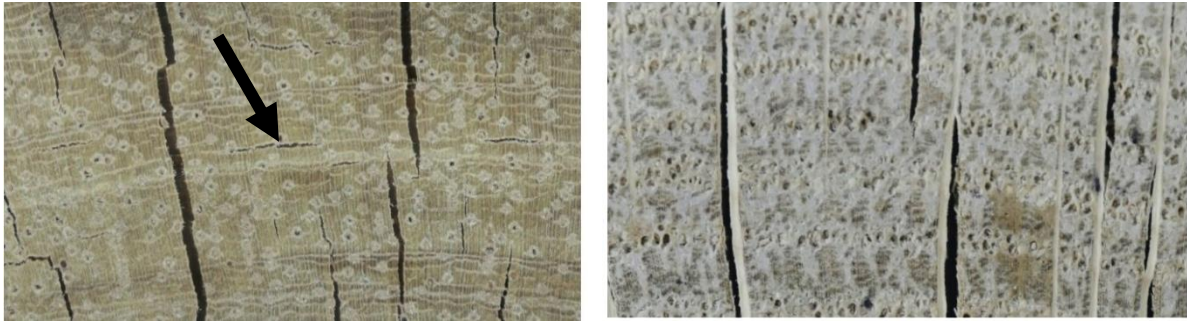


Figure 8: Cracks following the rays at the end grain of a basralocus specimen (left) and an oak specimen (right). Cracks in the tangential direction are indicated with an arrow in basralocus. Also the wood tissue is clearly visible

Table 2: Analysis of widest cracks at moment t_3 of 19 basralocus specimens

Wood species	Number of cracks	Length of cracks [mm]	Width of cracks [mm]
Average	67±27	10.0±6.7	0.5±0.2
Minimum	18	2.9	0.2
Maximum	128	30.2	1.2

CONCLUSIONS

The results show that the general trends observed for the average MC, ER, temperature, onset and development of cracks, as well shrinkage of the cross section at end grain as a function of drying time, are similar for both the basralocus and oak specimens tested using the described methodology. The influence of mainly the wood anatomical structure of these wood species is reflected in the slope of the different curves. The experimental set-up enables to unveil interrelationships between the measured variables and differences in wood anatomical structure of different species. Currently, more tropical hardwood species are being tested using this methodology. These results will be used for model building in the near future and can be of utmost importance for the fine-tuning and prediction of kiln-drying schedules.

REFERENCES

- Botter-Kuisch, H.P., Van den Bulcke, J., Baetens, J.M. and Van Acker, J. (2020) Cracking the code: real-time monitoring of wood drying and the occurrence of cracks. *Wood Science and Technology*, **54**, 1029–1049. <https://doi.org/10.1007/s00226-020-01200-6>.
- Denig, J., Wengert, E.M. and Simpson, W.T. (2000) *Drying Hardwood Lumber*. General Technical Report FPL–GTR–118, 138 p, Madison, Wisconsin.
- Panshin, A.J. and De Zeeuw, C. (1970) *Textbook of Wood Technology: Structure, identification, uses, and properties of the commercial woods of the United States and Canada*, Vol. 1, 3rd ed. McGraw-Hill, New York.
- Simpson, W.T. and Sagoe, J.A. (1991) *Relative drying times of 650 tropical woods: estimation by green moisture content, specific gravity, and green weight density*. General Technical Report FPL–GTR–71, 27 p, Madison, Wisconsin.
- Skaar, C. (1988) *Wood-Water Relations*. Springer, Berlin Heidelberg.
- Tropenbos (2011) Verslag workshop Domestic Timber Market: Inzichten en Ontwikkelingen. 10-12 november 2010, 80 p, Colakreek, District Para. Paramaribo, Suriname.

Sound analysis of mechanical wood cutting processes as a basis for adaptive process control

Mehieddine Derbas¹, Stephan Frömel-Frybort¹, Christian Laaber², Martin Riegler¹

¹ A-3430 Tulln, Konrad Lorenz Straße 24, Wood K plus - Competence Centre for Wood Composites and Wood Chemistry, m.derbas@wood-kplus.at

² A-2351 Wiener Neudorf, Brown-Boveri-Straße 8, Laaber GmbH

Keywords: Acoustic emissions, signal processing, machining, in-process control, in-process monitoring

ABSTRACT

The optimization of wood machining processes through online control is an essential step to ensure high manufacturing quality. The monitoring of acoustic emissions during wood machining is a comprehensive method to identify process conditions (LEMASTER ET AL. (1982)). In the present study, acoustic emissions were measured during wood machining with an optical microphone from Xarion GmbH with a constant range from 10 Hz to 1 MHz and a dynamic range from 50 dB to 150 dB (A) sound pressure level.

To identify the effects of different wood characteristics and process parameters on the acoustic emissions during machining, two approaches of signal analysis were applied. First, the conventional approach in signal processing was used, which relies on feature analysis. Second, a novel approach relying on principal component analysis to analyse the frequency spectrum was developed.

The experiments focused on the effect of the cutting speed and the wood species. A significant region separation could be seen when using the mentioned analysis methods.

INTRODUCTION

Due to the complex structure of wood, many different influencing variables must be considered during machining. Heterogeneity does not exclusively exist between species, but also within small samples, where major structural alterations, such as knots and changes in the fibre direction can be detected (MOHRING ET AL. (2019)). These individual characteristics in wood induce significant consequences on the machining process and on the quality of machining. Next to wood characteristics, process parameters influence the chip formation mechanism, e.g. by different fibre directions that the cutting edge is encountering (GOTTLÖBER (2014)). The mentioned disadvantages impose manufacturing flaws and sub-optimal cutting processes as well as unscheduled downtime due to e.g. tool breakage that accounts for 7 to 20% of the total interruptions. The challenge in this case is to develop an in-process control method that relies on in-process monitoring, so that the process can be adjusted accordingly to ensure good quality (VETRICHELVAN ET AL. (2015)).

Traditional machining process monitoring techniques, such as force or power consumption monitoring, have proven ineffective in addressing this problem. Because these techniques lack the statistical degree of freedom required to solve a problem with a large number of input variables or causes. Acoustic emission monitoring however, is the most capable technique to monitor the process efficiently (MARCHAL ET AL. (2009)). However, the harsh environmental conditions due to dust and ambient noise, make this type of surveillance very challenging for conventional equipment.

The present research focuses on the measurement and analysis of acoustic emissions. To analyse the acoustic emissions during wood milling processes, an optical microphone collects acoustic information, which is analysed by a conventional and a statistical approach. The key hypothesis of this study is that the acoustic emissions that are generated during machining include sufficient information to establish significant correlations with material properties, process parameters and tool health.

EXPERIMENTAL METHODS

Analysis

The first approach is based on traditional signal processing methods. Signal features were calculated, visualised and examined. Two domains are defined in this case: the time domain and the frequency domain. Only one signal feature is calculated for each domain:

- Time domain: Root mean square values (RMS) represents the loudness of the acoustic emissions:

$$TD_{rms} = \sqrt{\frac{\sum_{j=1}^n x_j^2}{n}} \quad (1)$$

- Frequency domain: Mean frequency is the weighted average of the frequencies and their respective response and it represents the weighted frequency of the signal:

$$FD_{mf} = \frac{\sum_{j=1}^n (f_j \cdot P_j)}{\sum_{j=1}^n P_j} \quad (2)$$

Whereby:

- FD_{mf} : weighted mean frequency in the frequency domain
- TD_{rms} : root mean square value of the signal in the time domain
- x : signal
- n : length of the signal
- j : index of the element inside the signal
- f : frequency spanning from 10 Hz to 1 MHz
- P : power spectrum

The second method is a novel approach for analysing the frequency spectra of individual cuts statistically by principal component analysis (PCA). The feature matrix was constructed by arranging the cuts in the rows and the frequencies in the columns (Fig. 1).

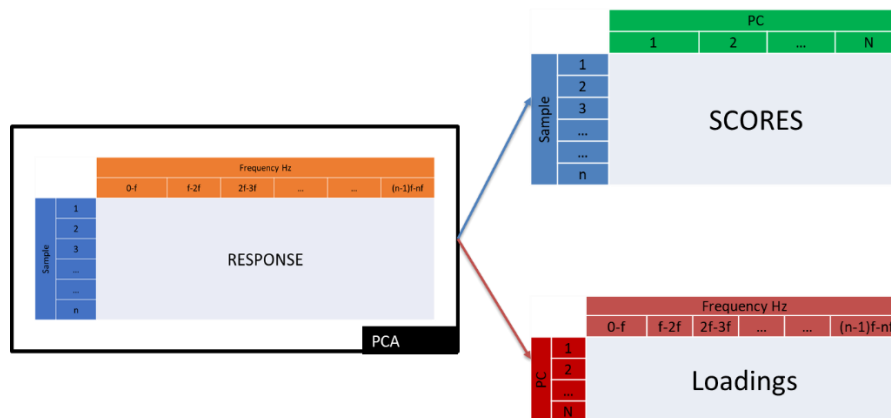


Figure 1: Feature matrix (left) and PCA components – scores and loadings (right)

Prior to analysis, a parametric function was used to extract the cuts that are found inside each dataset (Fig. 2). A cut is defined as the duration when the cutting edge of the tool is inside the workpiece. The motivation behind this separation comes from the fact that the spindle is accounting for a significant amount of redundant emissions that will have the same information across all the experiments.

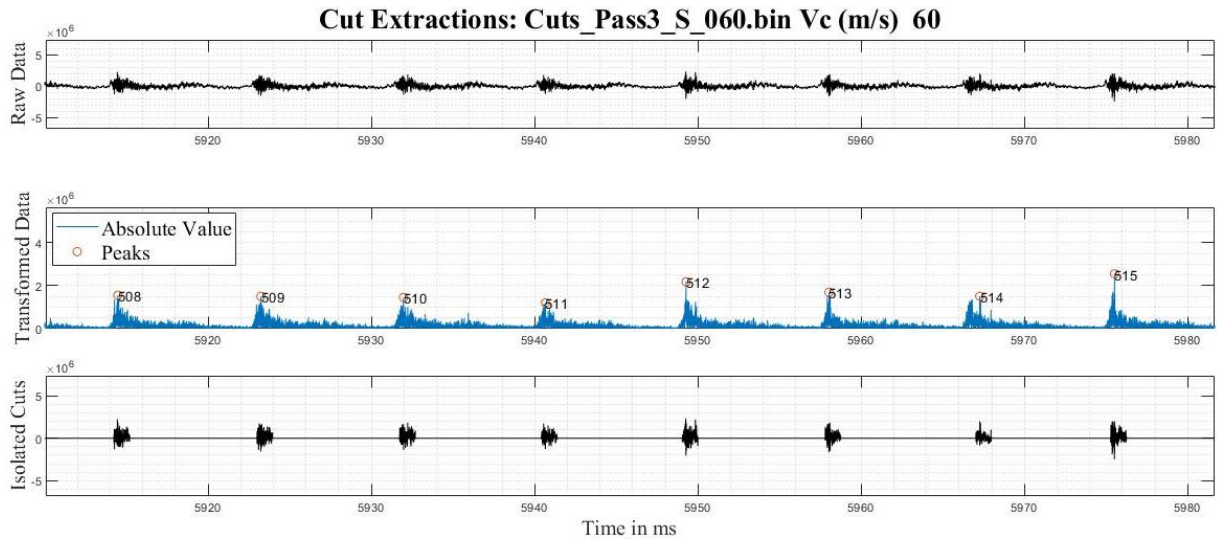


Figure 2: Steps for cut extraction; raw data (top) was transformed to intermediate values (middle) and individual cuts were isolated (bottom)

Isolated cuts were initially analysed by descriptive statistics. Scatter plots proved to be the most effective visualisation and comparison tool for detecting an area separation for different dataset variations (Fig. 3, left).

A Gaussian ellipse, commonly known as an error ellipse, was plotted around the scatter plots to emphasize the separation. This is an excellent tool for displaying the correlation between the calculated features from the two proposed methods and for highlighting possible clusters.

As a more detailed analysis, Singular Value Decomposition (SVD) of the covariance matrix between the two signal features determines the orientation and size of the ellipsoid (Fig. 3, right). The longitudinal direction of the ellipse is the direction of the first eigenvector. The second eigenvector is perpendicularly oriented to the longitudinal direction.

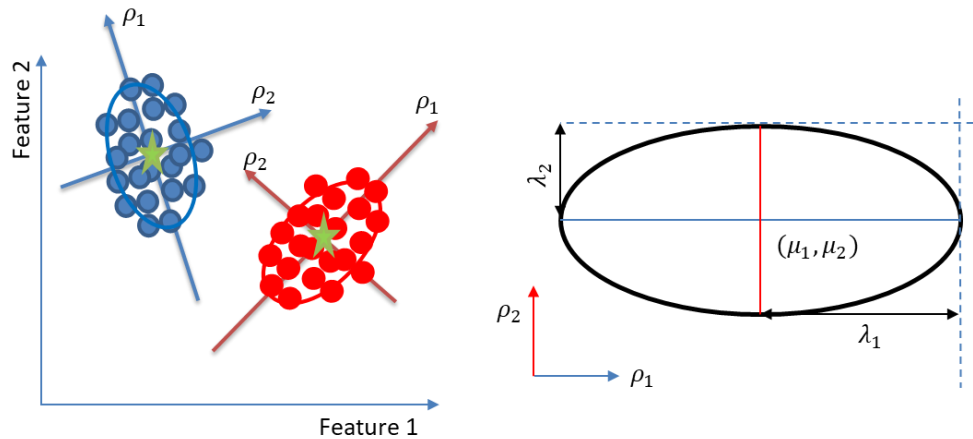


Figure 3: Descriptive statistics for comparing data sets based on gaussian ellipses

Whereby:

- ρ_1 : the first eigenvector
- ρ_2 : the second eigenvector
- λ_1 : the first eigenvalue
- λ_2 : the second eigenvalue
- μ_1 : the mean of the first feature
- μ_2 : the mean of the second feature

Equipment

Sensor

The ETA250 optical microphone from Xarion GmbH was used. This microphone can monitor sound from 10 Hz to 1 MHz with a constant sensitivity across the mentioned frequency range. The signal acquired was sampled at a rate of 2 MHz according to the Nyquist–Shannon sampling theorem and with a data type of “int32” giving the signal a high precision.

The sensor was placed on a sensor arm at a distance of roughly 200 mm from the machining process (Fig. 4). Afterwards, the sensor was aligned properly to ensure that the high frequency components are collected by the sensitive surface of the sensor.

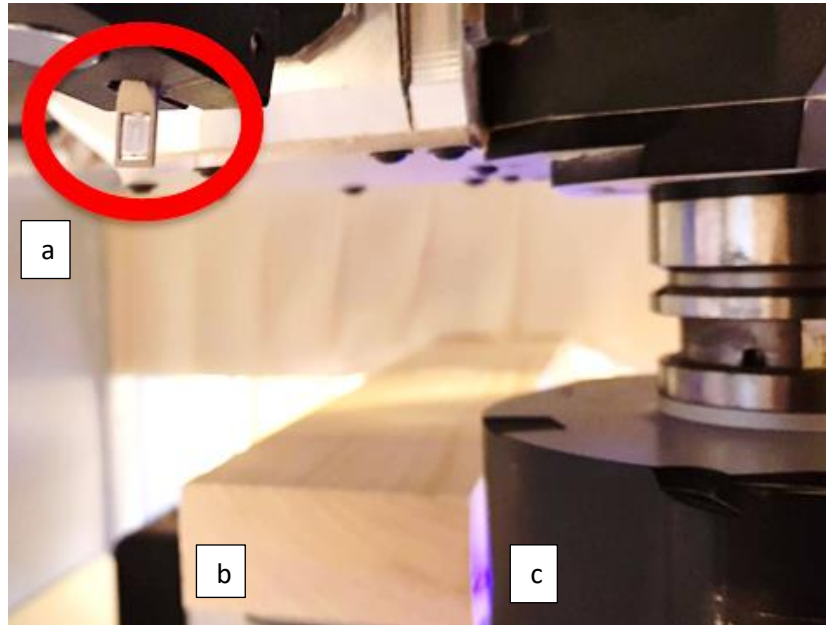


Figure 4: Experimental setup; sensor (a), workpiece (b), tool (c)

Machine and Cutting Tool

A 5 axis CNC BMG 110 machining centre from HOMAG Group was used in order to machine the wood samples.

A single-knifed cutting tool from Leitz Group was used, with a diameter of 165 mm and a cutting width of 80.4 mm (Fig. 5).



Figure 5: Leitz cutting tool

Samples

The samples were two uniform boards of beech and two uniform boards of spruce. The boards were 1,000 mm long, 120 mm wide and 45 mm thick (Fig. 6). The fibres were all in the longitudinal direction, though some deviations occurred due to the presence of knots. Knot locations were also documented in order to see if any changes can be observed in the data in the knot regions.

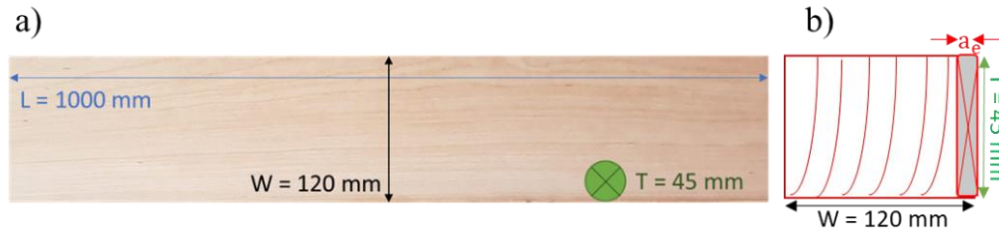


Figure 6: a) top view of a beech sample, b) right view of a beech sample, the rectangle with the width a_e and length T represents the volume machined

Process Parameters

Process parameters were chosen based on the notion that this is an exploratory study, therefore repeating border values is sufficient to obtain statistically significant data with minimum standard error. (GUTHRIE ET AL. (2012)). The values for the feed speed and for the spindle speed were selected with the aim to keep the feed per tooth and the average chip thickness unchanged. Hence, two values of cutting speed were chosen with the values shown in Table 1.

Table 1: Process parameters

V_c [m/s]	Number of Teeth [-]	Feed Speed [m/min]	Spindle Speed [RPM]	h_m [mm]
60	1	6.4	6945	0.16
100	1	10.7	11575	0.16

Each experiment was repeated three times to ensure statistical robustness and relevance.

RESULTS AND DISCUSSION

Conventional Approach

The RMS value (loudness) and the mean frequency (tone) of each individual cut were calculated by using formula (1) and (2). In Fig. 7, these two signal features are plotted against each other.

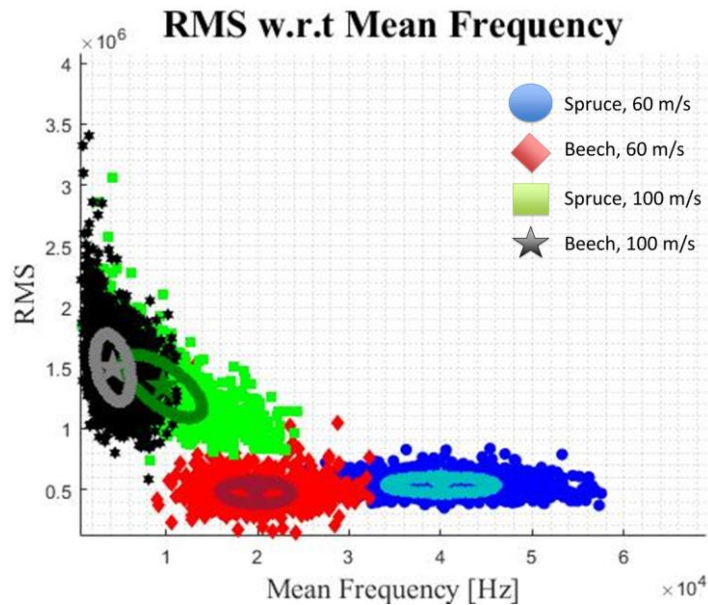


Figure 7: Root mean square value with respect to mean frequency [Hz]

A significant separation between the speeds that were tested can be observed. It follows that at low speeds, the two species of wood can be easily separated from each other by getting their mean frequency. This indicates the existence of a power significant frequency band where different kinds of wood can be distinguished from each other.

In the case of the higher cutting speed, the mean frequency clustered due to the presence of very strong spindle emissions. Despite these redundant influences, it can be seen that the separation occurred according to wood species as well, as seen in Fig. 8.

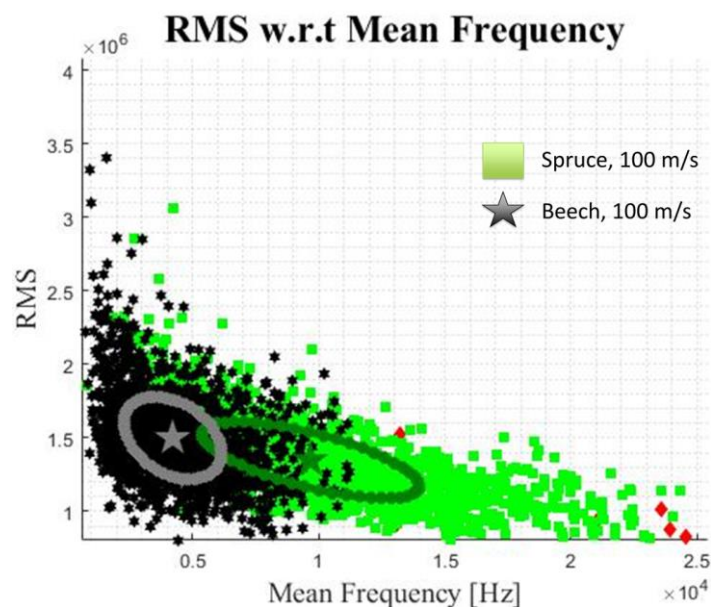


Figure 8: Root mean square value with respect to mean frequency [Hz], zoomed in at $V_c = 100$ m/s

Statistical Approach

A PCA algorithm was executed on the matrix shown in Fig. 1 by means of SVD. Two principal components were calculated since the first principal component had close to 90% of the total variance present (Fig. 9).

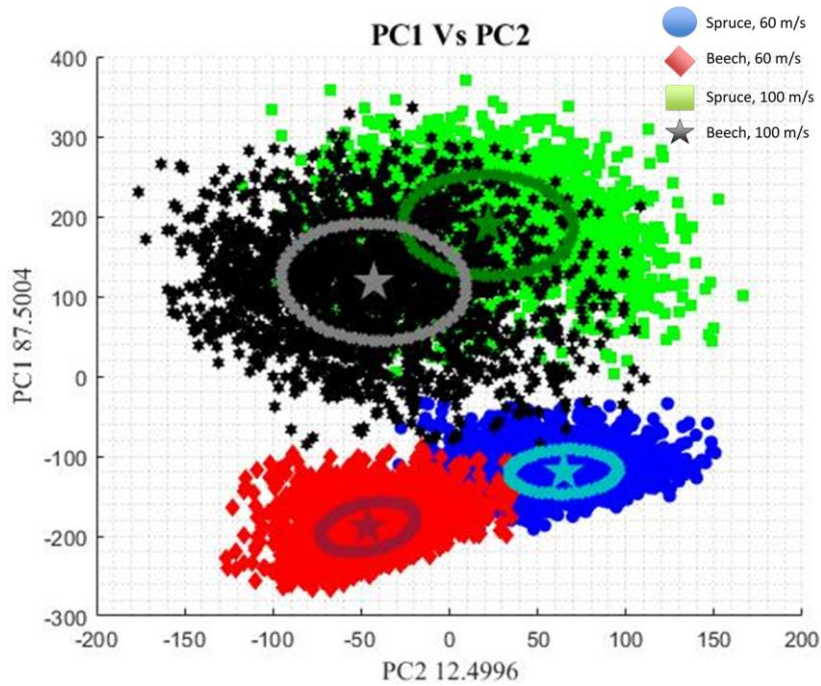


Figure 9: Eigenvectors of PC1 and PC2

The distinction between wood species and cutting speed is readily visible. Improvements can be made by first removing the spindle emissions and the consequent harmonics, and then locating and concentrating on frequency bands that are only relating to particular features of interest in the process.

In Fig. 10, the loadings vectors were plotted in order to visualize the significant frequency band.

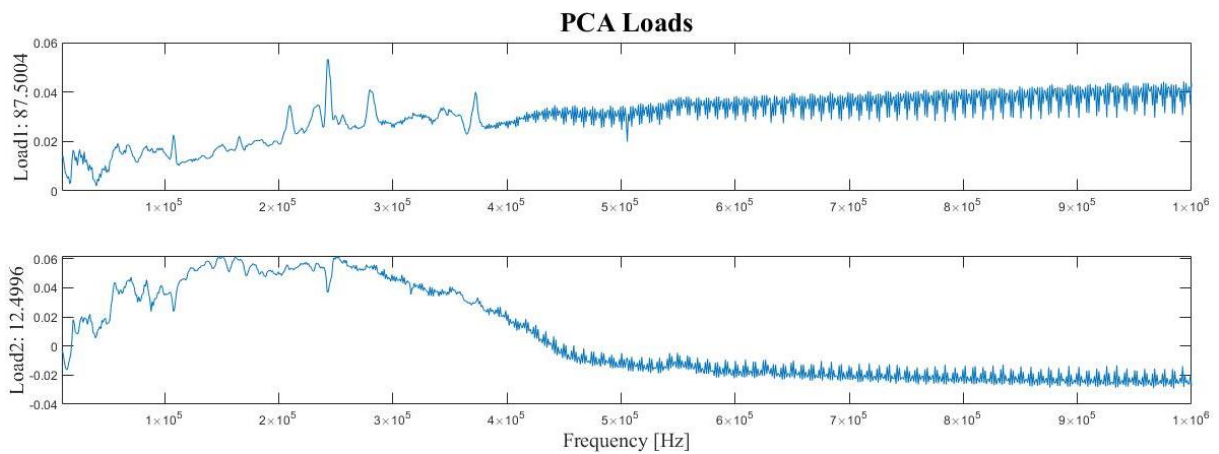


Figure 10: Loadings with respect to frequency [Hz]

It can be seen that there is significant information reaching up to 400 kHz. After 400 kHz the frequency spectrum exhibits noisy behaviour.

CONCLUSION

The use of an optical microphone to identify the effect of process parameters during wood machining was investigated in this paper. Two wood species and two cutting speeds were investigated.

The first analysis method relied on two signal features which represent the strength (RMS) and the tone (mean frequency) of the acoustic emissions. This analysis was very effective for the lower cutting speed at 60 m/s. The major component resulting from the spindle clustered the data in a small frequency range at a cutting speed of 100 m/s, although the difference between spruce and beech was still discernible.

The second analysis method relied on applying PCA on a feature matrix made out of the frequency response of each individual cut. This method was also deterministic in separating the clusters from each other. Some improvements were proposed for this method based on the loadings that showed the significant frequency band spanning from 10 Hz to almost 400 kHz.

REFERENCES

- Gottlöber, C. (2014) *Zerspannung von Holz und Holzwerkstoffen*. Fachbuchverlag Leipzig im Carl Hanser Verlag, pp. 30-33.
- Guthrie, W.F., Filliben, J., Heckert, A. (2012) *e-Handbook of Statistical Methods*. Chapter 4.3: Process Modelling Design.
- Lemaster, R.L., Kato, K. (1991) Generation of acoustic emission during chip formation. In: *Proceedings of the 10th IWMS*, October 21–23, Richmond, CA, pp. 146–150.
- Marchal, R., Mothe, F., Denau, L.E., Thibaut, B., Bleron, L. (2009) Cutting forces in wood machining – Basics and applications in industrial processes. A review. *Holzforschung*. **63**, 157-167.
- Mohring, H.C., Eschelbacher, S., Güzel, K., Kimmelmann, C., Schneider, M., Zizelmann, C., Häusler, A., Menze, C. (2019) En route to intelligent wood machining-current situation and future perspectives. *Journal of Machine Engineering*. **19**(4), 5-26.
- Vetrichelvan, G., Sundaram, S., Kumaran, S.S., Velmurugan, P. (2015) An investigation of tool wear using acoustic emission and genetic algorithm. *Journal of Vibration and Control*. **21**(15), 3061-3066. doi:10.1177/1077546314520835

Effect of specimen moisture content on wood degrading capability of *Fuscoporia contigua* in vitro testing

István Eső¹, Norbert Horváth²

¹ 4. Bajcsy-Zsilinszky str., 9400 Sopron, Hungary, University of Sopron, Simonyi Karoly Faculty, e-mail: eso.istvan@uni-sopron.hu

² 4. Bajcsy-Zsilinszky str., 9400 Sopron, Hungary, University of Sopron, Simonyi Karoly Faculty, e-mail: horvath.norbert@uni-sopron.hu

Keywords: Correlation, Mass Loss, Moisture Content, *Fuscoporia contigua*

ABSTRACT

Our research focuses on the in vitro wood degrading capabilities of *Fuscoporia contigua* on *Pinus sylvestris* and *Picea abies* specimen. Experiments were carried out using white rot fungi *Trametes versicolor* and *Pleurotus ostreatus* for comparison. Prerequisite tests show starting MC of specimen has no effect on the wood decaying capability of *Fuscoporia contigua*, however the fungi establish its preferred moisture conditions. The goal of this study is to better understand the correlation between moisture content and the wood decaying capabilities of the observed fungi.

INTRODUCTION

Several factors such as local climate and exposure conditions have an indirect effect on decay in outdoor conditions. Besides these factors, in particular the wood moisture content (MC) directly impacts the fungus and its ability to metabolize and degrade wood cell wall substance over time. The role of wood moisture content for wood decay has been addressed by many approaches to predict the service life of wooden materials and structures. Decay models frequently use wood MC as input variable and relationships have been established between climate conditions and the resulting risk for onset and progress of decay (Brischke and Thelandersson, 2014).

A wide range of field experiments have been undertaken by various researchers to quantify the effect of wood moisture on decay under varying climate conditions (Augusta, 2007; Van den Bulcke et al., 2009; Meyer et al., 2013). As a result very different models have been developed describing the effect of temperature, humidity and also rain events on decay (Brischke and Thelandersson, 2014).

Huckfeldt et al. (2005), Huckfeldt and Schmidt (2006) and Stienen et al. (2014) performed experiments with small, piled wood samples in wide mouth Erlenmeyer flasks. The bottoms of the piles were exposed to malt agar inoculated with fungal mycelium serving as nutrition and water source at the same time. The set up provided an MC gradient pile upwards and limit values for fungal growth. The wood decay samples were obtained from the experiments without additional conditioning.

EXPERIMENTAL METHOD

Specimens of 5 (longitudinal) x 40 x 40 mm³ were made from spruce (*Picea abies*) and scots pine sapwood (*Pinus sylvestris*) wood species were prepared where always 50 replicate specimens were axially matched. 3 parallel samples were prepared and tested.

Wood MC at the fiber saturation point (FSP) was determined for every material using 9 replicate samples. To determine the crucial points of wood MC for different fungi and wood species in terms of mycelial growth and decay activity a piling method was used. The tests were performed according to Meyer-Veltrup et al. (2015). In this study the pile direction was identical with the longitudinal direction of the wood specimens allowing easy water transport and mycelial growth through the wood pile upwards (Fig. 1).

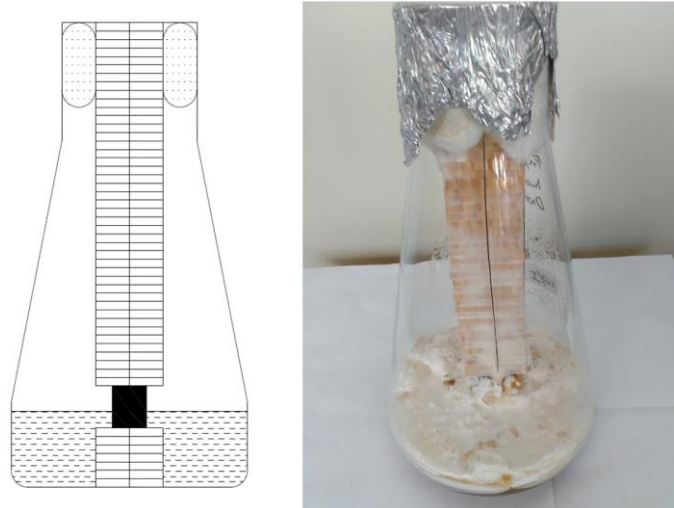


Figure 1: Pile test configuration

For each material/fungus combination 3 x 50 specimens were piled and a metal ring (\varnothing 28 mm, h = 25 mm) was placed between sample number 7 and 8 to avoid direct contact between malt agar and test specimens. Afterwards, the piles were tied up with thin wires, dipped in tap water for 60 s and put into wide mouthed 21-Erlenmeyer flasks, filled with 500 ml freshly prepared and still liquid malt agar. The flasks were then covered with a cotton plug and aluminum foil and sterilized in a steam oven at 120 °C for 30 min. The flasks were then stored in 20 °C/65%rH to generate a moisture gradient within the piles. After two weeks of storage 10 inoculated wood samples (\varnothing 10 mm, h = 10 mm) were placed on the agar next to the pile. The inoculation samples were pre-incubated in small Petri-dishes. In total 3 different fungi were used for the decay tests:

- *Trametes versicolor*
- *Pleurotus ostreatus*
- *Fuscoporia contigua*

During incubation the mycelium growth height was measured and marked on the flasks once a week. After 16 weeks of incubation at 20 °C/65%rH all specimens were cleaned from adhering mycelium, weighed, oven dried and weighed again to determine moisture content (MC) and mass loss (ML) by fungal decay.

RESULTS AND CONCLUSIONS

The relationship between MC and ML was determined for every single pile. For all piles a moisture gradient, increasing from bottom to top was found: within the 16 weeks of exposure a continuously mass loss (ML) decreased with decreasing moisture content (MC). Both wood species exposed to *Trametes versicolor* and *Pleurotus ostreatus* showed remarkably high MC in the bottom half of the pile. In case of *Trametes versicolor*, 14,5% MC is the necessary minimum for evincible ML (>2%), however elongated exposure to high level of MC is necessary for uninterrupted degradation.

Pleurotus ostreatus performed similar to *Trametes versicolor* on both wood species, however *Pleurotus ostreatus* has a steeper ML gradient as both scots pine and spruce lost more than 50% of its mass during the 16 week period in the lower third, but there were no decay in the upper third of the pile.

In all cases *Fuscoporia contigua* was unable to grow past the the metal rings during the 16 week test period (Fig. 3), therefore a new method of testing is necessary to determine the relationship between MC and ML. Additional exposure times could give more insight into the development of MC and ML.

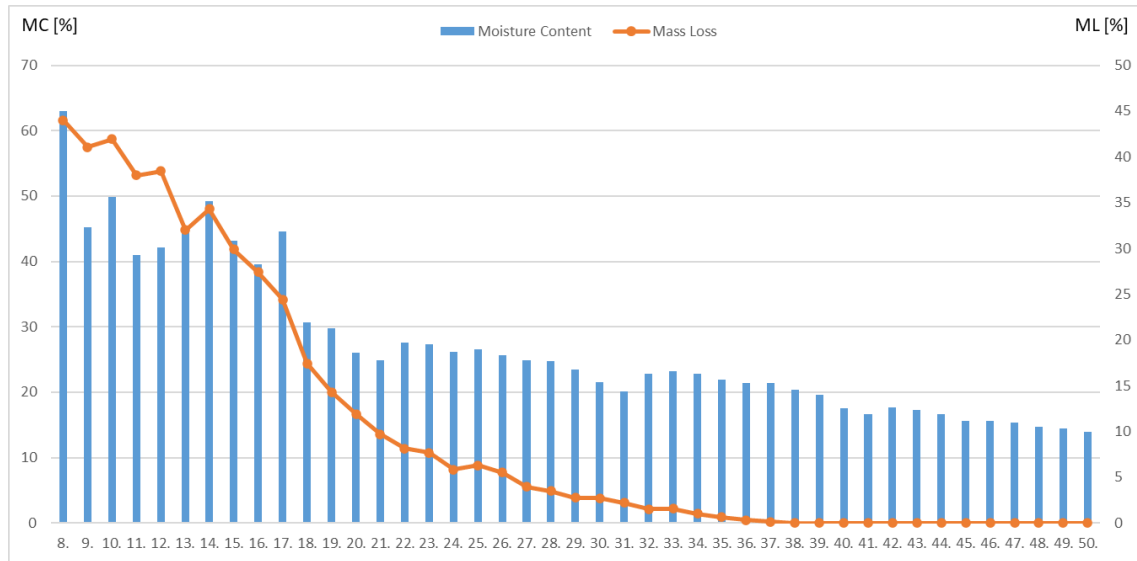


Figure 2: Moisture Content (MC) and Mass Loss (ML) of *Pinus sylvestris* sapwood of *Pleurotus ostreatus* after 16 weeks of incubation

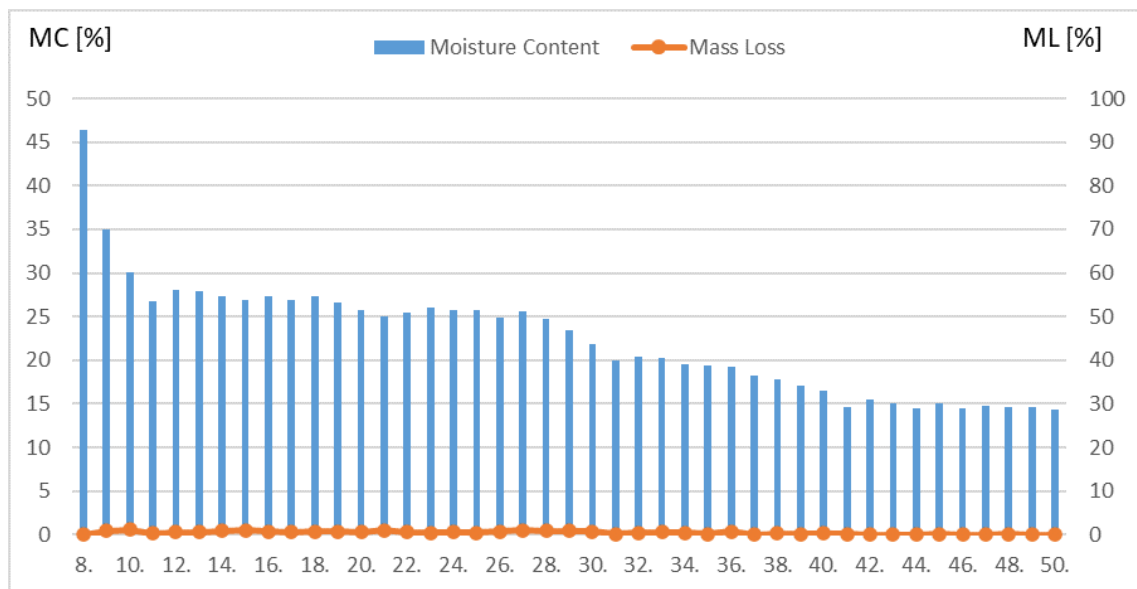


Figure 3: Moisture Content (MC) and Mass Loss (ML) of *Pinus sylvestris* sapwood of *Fuscoporia contigua* after 16 weeks of incubation

In some cases, rusting of the metal rings appeared which caused rust inhibiting the bottom 2-3 samples, altering the result of the end mass of these samples (results show higher moisture content and lower mass loss than real), therefore the MC and ML results of the bottom 3 samples (by visual confirmation) should be disregarded.

It should be considered that malt agar, an external moisture and nutrient source was available for the fungi. Therefore growth and decay limits might differ and are worth to examine separately, without an external moisture source. The physiological thresholds obtained in this study can be used for a more accurate modeling of wood decay by lignofil fungi. Additional studies on requirements for mycelium growth and decay without an external moisture source are necessary and are in progress.

REFERENCES

- Augusta, U. (2007). Untersuchung der natürlichen Dauerhaftigkeit wirtschaftlich bedeutender Holzarten bei verschiedener Beanspruchung im Außenbereich. *Dissertation*. University of Hamburg; Hamburg.
- Brischke, C., Thelandersson, S. (2014). Modelling the outdoor performance of wood products - a review on existing approaches. *Constr. Build. Mater*, **66**, 384-397.
- Huckfeldt, T., Schmidt, O., Quader, H. (2005). Ökologische Untersuchung am Echten Hausschwamm und weiteren Hausfäulepilzen. *Holz als Roh Werkst*, **63**, 209-219.
- Huckfeldt, T., Schmidt, O. (2006). Hausfäule-und Bauholzpilze. *Rudolf Müller*, Cologne.
- L. Meyer-Veltrup, C. Brischke, A. Treu, P. Larsson-Brelid (2015). Critical moisture conditions for fungal decay of modified wood by basidiomycetes as detected by pile tests. *Holzforschung*, **10**. doi: 1515/hf-2015-0046.
- Meyer, L., Brischke, C., Rieken, J. (2013). Testing Wood Durability in 27 Differently Severe Above-ground Exposure Conditions. *IRG/WP/13-20517*. The International Research Group on Wood Protection, Stockholm.
- Stienen, T., Schmidt, O., Huckfeldt, T. (2014). Wood decay by indoor basidiomycetes at different moisture and temperature. *Holzforschung*, **68**, 9-15.
- Van den Bulcke, J., Van Acker, J., De Smet, J. (2009). An experimental set-up for realtime continuous moisture measurements of plywood exposed to outdoor climate. *Build. Environ*, **44**, 2368-2377.

Novel test set-up for detailed analysis of wood cutting processes

Stephan Frömel-Frybort ^{1,2}

¹ Kompetenzzentrum Holz GmbH, Altenberger Straße 69, 4040 Linz, Austria, s.froemel-frybort@wood-kplus.at

² BOKU, UFT - Universitäts- und Forschungszentrum Tulln, Konrad-Lorenz-Straße 24, 3430 Tulln, Austria

Keywords:

ABSTRACT

Although mechanical disintegration of wood is a long-established technology, basic knowledge about correlations between wood and tool or process parameters, and mechanisms involved is still poor. Changes in raw material composition, i.e. from softwood to hardwood species, further complicates that matter. To bring new insights into analysis of wood cutting, a novel test method was developed. The newly developed test set-up enables detailed examinations of the linear cutting process of different raw materials, tools and process parameters. For data correction the inverse filter is applied. Thereby disturbing influences arising from the whole measurement chain can be eliminated, enabling highly reproducible cutting force measurements at various cutting speeds. Examinations were done for oak, where fibre angle, moisture content and cutting speed were varied.

A short background to hardwood resources and properties in Ghana

James Govina^{1,2}, Róbert Németh¹

¹ University of Sopron, Simonyi Karoly Faculty of Engineering, Wood Science and Applied Arts, Institute of Wood Science, Sopron, Hungary. nemeth.robert@uni-sopron.hu

² Council for Scientific and Industrial Research – Forestry Research Institute of Ghana, Kumasi, Ghana. ndvm36@uni-sopron.hu

Keywords: Ghana, plantation, forestry, hardwood, properties.

ABSTRACT

The High Forest Zone and the Savanna Woodland of Ghana is composed of a variety of hardwood species. Over the years, the natural forest cover has been phenomenally lost through over-exploitation of timber, illegal logging, wildfire, illegal mining, agricultural expansion, weak implementation of forest management policies etc. The challenges associated with the forests destruction in Ghana includes the shortage of raw materials for the wood industry which was once a pillar to the Ghanaian economy. Presently plantation forestry runs parallel to natural forest management as the guarantee for future wood supply. Considering other benefits derived from forests, Ghana developed its National Climate Change Policy which recognizes forest plantations development as one of the tools to combat climate change challenges. Reports from the National Forest Plantation Development Programme and the Ghana Forest Plantation Strategy suggests that close to 300, 000 hectares of forest plantation cover has been established between the year 2002 and 2019. Tree species used in forest plantations across the country are hardwoods, but predominantly (about 90%) *Tectona grandis* (Teak) which is an exotic species. The other species, covering the about 10% of plantations, include *Cedrela odorata* (Red Cedar), various Eucalyptus species, and *Gmelina arborea*. Some indigenous species successful in plantation establishment include, *Terminalia superba* and *T. ivorensis*, *Ceiba pentandra*, *Triplochiton scleroxylon*, *Khaya species*, and *Milicia excelsa*.

INTRODUCTION

Ghana covers 23.9 million hectares of land area, with about 34% being a forested area in the southern part of the country. Under Ghana's forest management practices, this area of forest is called the High Forest Zone (HFZ) with diverse hardwood species. The HFZ is further divided into nine forest types, which were designated into forest reserves. In addition, there are off-reserves areas within the HFZ (Hall and Swaine 1976). Forest reserves earmarked for timber production plus the off-reserve areas are the hubs where timbers are extracted to meet domestic and international demands (Hawthorne and Abu-Juam 1992, Norlan et al. 1992). Fig. 1 illustrates the location of Ghana on the African continent whereas Fig. 2 highlights its undulating topography.

Ghana remains a country with a strong history regarding timber industry development (Eshun et al. 2010). About two decades ago, the sector was the fourth largest foreign exchange earner to the nation (Owusu 2001). Admittedly, the timber industry sector is presently faced with shortage of the raw materials. The inadequacy is attributed to multi-faceted challenges: increased wood demand, unsustainable forest management practices, agricultural activities, illegal timber harvesting, wildfire, illegal mining, weak implementation of policies among other reasons (Asamoah et al. 2020, Appiah et al. 2009). Food and Agriculture Organisation (FAO) reported data for decades ago indicated that the current area of land for timber production in the HFZ of Ghana was about 1.5 million hectares (FAO 2010). However, whether this area of land can presently be allocated for timber production would be difficult to predict. A reduction would be a fair prediction to make as deforestation persist.

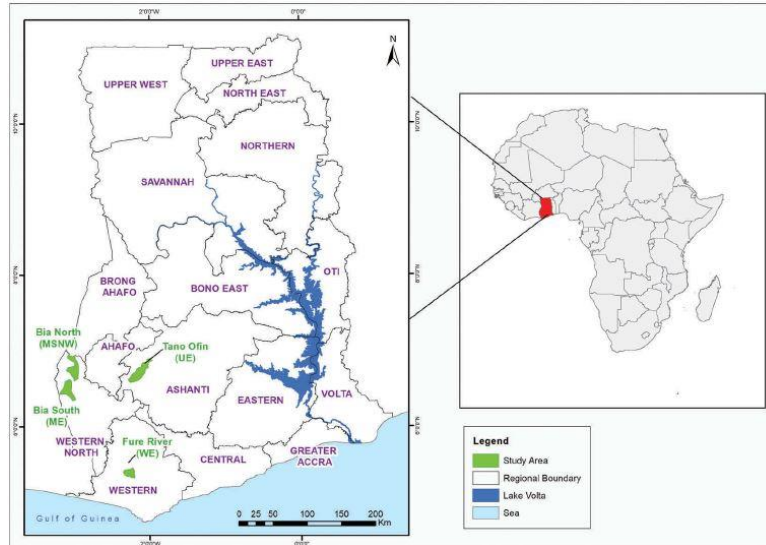


Figure 1: A map showing the location of Ghana (source: Ankomah et al. 2019)



Figure 9: A map showing the topography of Ghana (source: Philippe Rekacewicz, UNEP/GRID-Arendal)

Between 1990 and 2014, Ankomah et al. (2019) found mean annual rate of forest cover loss to be about 1% in the HFZ of Ghana. They authors observed that the rate of forest cover loss was more rapid between 1990 and 2000. Similarity, Tsai et al. (2019) reported of about 6% forest cover loss for selected forest reserves in the southern Ghana. Contrary, though unmatched, Oduro et al. 2015 reported annual reforestation compensate for about 13% of the annual deforested area. Yearly increment of plantation forests is presented in Fig. 3. Meanwhile, apart from wood, the forests provide other benefits including ecosystem services and mitigating the negative effects of climate change – a global environmental pandemic.

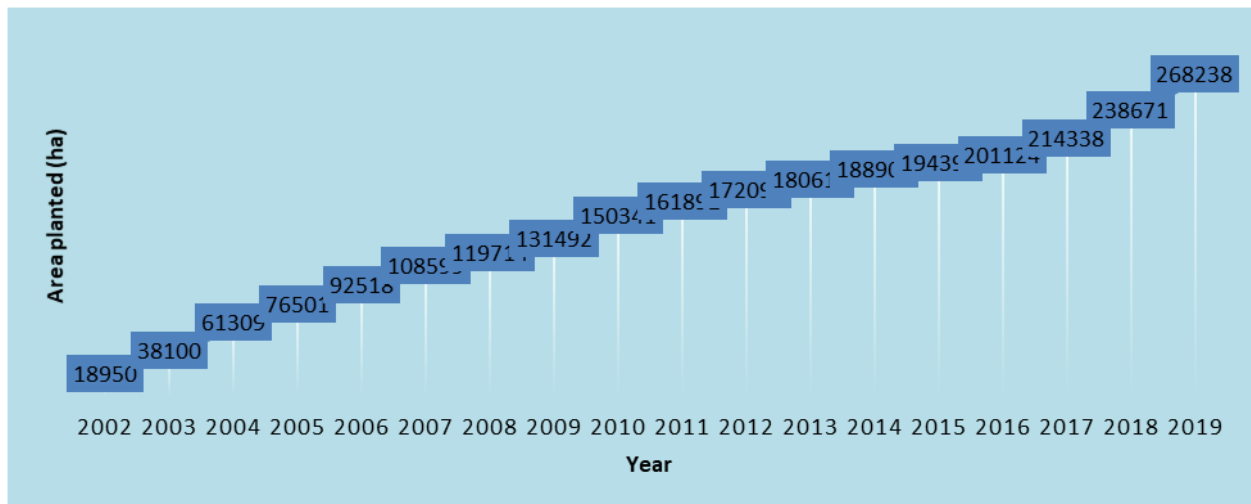


Figure 3: Cumulative forest plantations areas developed in Ghana since 2002. (Data source: Forestry Commission 2017, 2020)

Besides the closed forests, the remaining land for Ghana known is the Savanna woodland. The savanna has about 60% open canopy of smaller trees and shrubs resources (Hawthorne and Abu-Juam 1992). Trees in savanna are mainly harvested for bioenergy purposes (firewood and charcoal), and provide building poles for local building construction (Oduro et al. 2012).

HARDWOOD PLANTATION RESOURCES IN GHANA

In Ghana, efforts to augment the raw material base have resulted into initiatives for various reforestation programmes. The objectives of the reforestation programmes include establishing tree plantations on all deforested portions within forest and off-forest reserves (Insaideo et al. 2012). Tree planting to increase forest cover not only safeguarding the future supply of wood. It contributes to efforts to combat climate change challenges which include rainfall variability, increased temperatures, extreme drought. Ghana's greening initiatives for multiple reasons is factored into the development of the National Climate Change Policy (NCCP) (Ministry of Environment Science Technology and Innovation [MESTI] (2013). This affirms that the country recognises natural resources management like forestry a tool to combat climate change challenge. In relation forestry, the integrated Ghana's NCCP has two key programme areas out of ten. The two key areas are to target the increment of carbon sink and minimize greenhouse gas emission. The species composition for forest plantations in Ghana are from both domestic and exotic hardwood species. *Tectona grandis* (Teak) the world premier hardwood, is the most predominant plantation species covering about 90% of planted areas. Teak species success and acceptance is attributed to its shorter harvesting cycle and ability to withstand wildfires (Oteng-Amoako and Sarfo 2003). The other species, covering the about 10% of plantations, include *Cedrela odorata* (Red Cedar), various Eucalyptus species, and *Gmelina arborea*. Some indigenous species successful in plantation establishment include, *Terminalia superba* and *T. ivorensis*, *Ceiba pentandra*, *Triplochiton scleroxylon*, *Khaya species*, and *Milicia excelsa*. In reference to reports traced backed to 2002, the difference plantation development programmes in Ghana have successfully planted about 200,000 ha of degraded forest on on-reserve and off-reserve lands (Forestry Commission 2017, Forestry Commission 2020).

MACRO-STRUCTURE OF HARDWOODS

The identified uses of wood by human are all secondary benefits derived from trees. The wood found in a tree has a primary function of ensuring that the tree survives. It supports the leaves towards sunlight and transport water and minerals from the roots to the leaves (Butterfield 2006, Schweingruber 2007, Wiedenhoef and Miller 2005). Higher plants are phylogenetically grouped into angiosperms and

gymnosperms. Angiosperms are flower bearing (clothed seeded) plants, whereas gymnosperms (naked seeded) bear cones. Angiosperms are further divided into Monocotyledons and Dicotyledons, where hardwoods species belong (Campbell 2008).

Hardwood comprises of axial (vertical) and radial (horizontal) system of cells making them a complex and higher developed xylem. Typical with all plants, hardwoods have cambium which divides to produce cells into both xylem and phloem portions of the tree. The new daughter cells in the xylem portion further develop into specific woody cells to perform specific functions. In hardwoods, these tissue elements are vessels, axial and radial parenchyma, fibres, and in some cases gum ducts (Butterfield 2006). Generally, by proportion, vessel occupy between 6-55%, fibres 29-79%, axial parenchyma 0-23%, radial parenchyma 6-31% (Antwi-Boasiako and Atta-Obeng 2009, Fichtler and Worbes 2012, Morris et al. 2016a, Zobel and van Buijtenen 1989). The varied proportions and associations of these tissue elements coupled with other factors give unique characteristics to each wood species. Three advantages of the unique macro-structure of wood, in no special order, are:



1. It creates a unique pattern at the transverse surfaces of each wood. Patterns are very useful diagnostic feature for wood identification purpose. Inarguably, the advantages of correct wood identification cannot be over-emphasized. They include avoidance of price – transfers during trade, tax evasion leading to loss of revenue by timber producing country governments, inefficient use of wood, deforestation (Oteng 2006, Wiedenhoef and Miller 2005).
2. It influences all salient properties of wood needed before selecting some wood for an application. For instance, the proportion of fibre, how long fibres are and how thicker their walls are influences wood density. Parenchyma content influences natural durability because their starch content presents a weakness to the wood. It makes wood susceptible to bio-deterioration agents like insects. Vessels proportion and sizes influences impregnability of preservatives (Baar et al., 2016, Ocloo and Laing, 2003, Dadzie et al., 2018, Zobel and van Buijtenen, 1989)
3. It creates unique grain or figure at the tangential and radial surfaces when logs are sawn into boards. This occasionally influences the selection of wood for outdoor applications with an aesthetic objective.



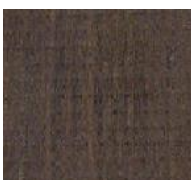

Vessels conduct water and minerals from the roots to other parts of the living tree, whereas fibres are for support and strength. Parenchyma are living cells for transport (vertically and horizontally) and storage of photosynthate, from the leaves to other parts of the tree (Baas et al 2004, McElrone et al., 2004, Myburg et al., 2013). They are also responsible for producing cells for repairs during injury and defence against pathogens when necessary (Morris et al., 2016b).

SELECTED PROPERTIES OF GHANA HARDWOODS

Wood can be efficiently used if its properties are known. The various applications demand that certain key properties are outstanding. Clearly, a denser wood can be an advantage in one application but a disadvantage in the other. Therefore, matching wood quality with desired application is recommended. This document only highlights selected properties (basic density, durability, and colour) that influences the utilization of Ghanaian hardwoods (Zobel and van Buijtenen, 1989). The selected properties (Table 1) have been considered because density relates with strength, durability relates to deterioration and colour and texture relates to aesthetic selection of solid wood. Again, these selected properties are likely to influence the promotion of lesser-used and lesser-known species predictably found in abundance. Examples of species provided in Table 1 are in the utilization category of lesser-used and lesser-known species. They are being promoted as substitutes for the premium and commercial species such as *Milicia excelsa* *Triplochiton scleroxylon* and *Pericopsis elata* (Afromosia – CITES App II).

Table 1: Basic density, durability and colour of Ghanaian hardwoods

Property	Classification	Example of tree species	Remarks
Basic density (g/cm ³)	Low (<0.5)	Bombax buonopozense, Ceiba pentandra, Cordia milleni, Hannoa klaineana, Lannea welwitschii, Pycnanthus angolensis, Ricinodendron heudelotii	Boat and canoe construction Interior joinery, frames and trims, boxes, crates and packing cases, panelings, claddings and mouldings, shingles, shakes and weather boards, rotary core veneer and plywood
	Medium (0.5 to 0.75)	Albizia ferruginea, Alstonia boonei, Aningeria altissima, Celtis species, Octoknema borealis, Parkia bicolor, Samanea dinklagei, Scottellia ldaineana, Sterculia species, Pachypodanthium staudtii	Roof trusses, joists and beams Joinery, frames and trims, floorings, steps and stairs, panelings, mouldings and claddings, luxury cabinet and furniture work. Most hardwoods species in Ghana have density within this range
	High (0.75 to 1+)	Afzelia species, Allanbiakia floribunda, Amphimas pterocarpoides, Anogeissus leiocarpus, Chrysophyllum species, Diospyros species, Erythrophleum species, Guibourtia ehie, Mammea Africana, Manilkara obovara, Petersianthus macrocarpus, Pseudocedrela kotschyi	Industrial beams, joists, frames and trusses, industrial floorings, steps and stairs, sleepers, bridges, piles and deckings, ship, boat building and truck bodies
Durability BS EN 350-1 (1994) BS EN 252 (1989)	Non-durable	Allanblakia floribunda, Alstonia boonei, Bombax buonopozense, Ceiba pentandra, Celtis species, Chrysophyllum species, Pycnanthus angolensis, Ricinodendron heudelotii, Scottellia klaineana	All the low-density woods are non-durable woods. However, there are medium and high-density wood species from genus Chrysophyllum that are equally non-durable. Preservative treatment or modification of such wood species is recommended to prolong service life.
	Moderately durable	Aningeria altissima, Petersianthus macrocarpus, Sterculia species	Species with wood density range of medium to high dominates this durability classification. Wood can be treated or modified to enhance their service life.
	Durable	Albizia ferruginea, Pseudocedrela kotschyi	
	Very durable	Afzelia species, Diospyros species, Erythrophleum species, Manilkara obovara, Mammea africana, Samanea dinklagei	Species with high wood density. Wood can be used without treatment.
Colour	Whitish	 Celtis adolfi-friderici	Heart and sapwood have same colour.
	Yellow	 Enantia polycarpa	Heart and sapwood have same colour.

	Brown	 Erythrophleum suaveolens	Heartwood demarcated from sapwood.
	Red	 Chrysophyllum subnudum	Heartwood demarcated from sapwood.
	Black	 Diospyros species	Heartwood demarcated form sapwood
	Pink	 Corynanthe pachyceras	Heart and sapwood have same colour.
			There are numerous species having shades of listed colours. However, the most common colour is the shades of brown.

(Bolza and Keating 1972, Opoku 2007, Oteng-Amoako 2006, Badejo 1988, Bourreau et al. 2013)

Over the years the durability of Ghanaian hardwood species has been determined by hardness and weight loss experiments, and these are complemented by visual durability ratings (Antwi-Boasiako and Allotey 2010). In most hardwood species, especially the non-whitish woods, heartwood colour is visibly differentiated from the sapwood. The heartwoods are darker because of their extractive contents, though this feature varies with factors including species, age of wood, site of growth (Zobel and van Buijtenen 1989).

CONCLUSION

Ghana is endowed with tropical forests which has numerous hardwood species composition. The natural forest keeps dwindling, resulting in the shortage of raw materials for the wood industry. Production under low capacity reduces the sector's support to the Ghanaian economy. Reforestation efforts have succeeded in establishing plantation with both indigenous and exotic hardwoods species (predominantly Teak) to augment the wood raw material base. The internal structure of hardwood makes it complex and uniquely characterize each species. The variability of wood quality for hardwoods in Ghana is considerably wide. Basic density ranges from very low (example *Ceiba pentandra*) to very high (example *Manilkara obovara*) with numerous species in each category. Likewise, durability ranges from non-durable (example *Pycnanthus angolensis*) to very durable (example *Mammea africana*). Wood colour ranges from creamy white (*Celtis* species), to golden yellow (*Albizia adianthifolia*), to black (*Diospyros* species).

REFERENCES

- Ankomah, F., Kyereh, B., Asante, W. and Ansong, M. (2019). Patterns of forest cover change and their association with forest management regimes of forest reserves in the high forest zone of Ghana. *Journal of Land Use Science*, **14**(3), 242-257.
- Antwi-Boasiako, C. and Allotey, A. (2010) The effect of stake dimension on the field performance of two hardwoods with different durability classes. *International Biodeterioration and Biodegradation*, **64**(4), 267-273.
- Antwi-Boasiako, C. and Atta-Obeng, E. (2009). Vessel-fibre ratio, specific gravity and durability of four Ghanaian hardwoods. *Journal of Science and Technology (Ghana)*, **29**(3).
- Appiah, M. (2012). Changes in plant species composition within a planted forest in a deciduous agroecosystem in Ghana. *Agroforestry systems*, **85**(1), 57-74.
- Appiah, M., Blay, D., Damnyag, L., Dwomoh, F.K., Pappinen, A. and Luukkanen, O. (2009). Dependence on forest resources and tropical deforestation in Ghana. *Environment, Development and Sustainability*, **11**(3), 471-487.
- Asamoah, O., Kuitinen, S., Abrefa Danquah, J., Quartey, E.T., Bamwesigye, D., Boateng, C.M. and Pappinen, A. (2020). Assessing Wood Waste by Timber Industry as a Contributing Factor to Deforestation in Ghana. *Forests*, **11**(9), 939.
- Baar, J., Tippner, J. and Gryc, V. (2016). Wood anatomy and acoustic properties of selected tropical hardwoods. *International Association of Wood Anatomy Journal*, **37**(1), 69-83.
- Baas, P., Ewers, F.W., Davis, S.D. and Wheeler, E.A. (2004). Evolution of xylem physiology. In *The evolution of plant physiology*, pp. 273-295. Academic Press.
- Badejo, S.O.O. (1988). Effect of flake geometry on properties of cement-bonded particleboard from mixed tropical hardwoods. *Wood Science and Technology*, **22**(4), 357-369.
- Bolza, E. and Keating, W.G. (1972). African timbers – the properties, uses and characteristics of 700 species.
- Bourreau, D., Aimene, Y., Beauchêne, J. and Thibaut, B. (2013). Feasibility of glued laminated timber beams with tropical hardwoods. *European Journal of Wood and Wood Products*, **71**(5), 653-662.
- Butterfield, B. (2006). The structure of wood: form and function. *Primary wood processing*, Springer, Dordrecht.
- BS EN 350-1 Durability of Wood and Wood-based Products – Natural Durability of Solid Wood. Part 1. Guide to the Principles of Testing and Classification of the Natural Durability of Wood European Committee for Standardization (CEN) (1994)
- Campbell, N.A., Urry, L.A., Cain, M., Wasserman, S.A. and Minorsky, P.V. (2017). *Biology* (Vol. 8). New York, USA. Pearson.
- Dadzie, P.K. and Amoah, M. (2015). Density, some anatomical properties and natural durability of stem and branch wood of two tropical hardwood species for ground applications. *European Journal of Wood Products*, **73**, 759-773.

- Dadzie, P. K., Amoah, M., Ebanyenle, E., and Frimpong-Mensah, K. (2018). Characterization of density and selected anatomical features of stemwood and branchwood of *E. cylindricum*, *E. angolense* and *K. ivorensis* from natural forests in Ghana. *European journal of wood and wood products*, **76**(2), 655-667.
- Eshun, J.F., Potting, J. and Leemans, R. (2010). Inventory analysis of the timber industry in Ghana. *The International Journal of Life Cycle Assessment*, **15**(7), 715-725.
- Food Agricultural Organisation (2010). Global Forest Resources Assessment. FAO Forestry Paper No. 163, Rome.
- Fichtler, E. and Worbes, M. (2012). Wood anatomical variables in tropical trees and their relation to site conditions and individual tree morphology. *International Association of Wood Anatomists Journal*, **33**(2), 119-140.
- Forestry Commission (2017). National Forest Plantation Development Programme. *Annual Report 2016*, Ministry of Land and Natural Resources, Forestry Commission – Ghana, Accra, pp. 46.
- Forestry Commission (2020). Ghana Forest Plantation Strategy. *Annual report 2019*, Ministry of Land and Natural Resources, Forestry Commission – Ghana, Accra, pp. 90.
- Hall, J.B. and Swaine, M. (1976). Classification and ecology of closed-canopy forest in Ghana. *The Journal of Ecology*, 913-951.
- Hawthorne, W. and Abu-Juam, M. (1992). Protected forest areas in Ghana. *FRMP, Kumasi*.
- Insaidoo, T.F., Ros-Tonen, M.A., Hoogenbosch, L. and Acheampong, E. (2012). Addressing forest degradation and timber deficits: Reforestation programmes in Ghana. *European Tropical Forest Research Network News*, **53**, 230-239.
- McElrone, A.J., Pockman, W.T., Martínez-Vilalta, J. and Jackson, R.B. (2004). Variation in xylem structure and function in stems and roots of trees to 20 m depth. *New Phytologist*, **163**, 507-517. <https://doi.org/10.1111/j.1469-8137.2004.01127.x>
- Ministry of Environment Science Technology and Innovation (2013). Ghana National Climate Change Policy, *Government document*, Accra, pp. 88.
- Morris, H., Plavcová, L., Cvecko, P., Fichtler, E., Gillingham, M.A.F., Martínez-Cabrera, H.I., McGlenn, D.J., Wheeler, E., Zheng, J., Ziemińska, K. and Jansen, S. (2016a). A global analysis of parenchyma tissue fractions in secondary xylem of seed plants. *New Phytologist*, **209**, 1553-1565. <https://doi.org/10.1111/nph.13737>.
- Morris, H., Brodersen, C., Schwarze, F.W. and Jansen, S. (2016b). The parenchyma of secondary xylem and its critical role in tree defense against fungal decay in relation to the CODIT model. *Frontiers in Plant Science*, **7**, 1665.
- Myburg, A.A., Lev-Yadun, S. and Sederoff, R.R. (2013). *Xylem Structure and Function*. John Wiley and Sons. <https://doi.org/10.1002/9780470015902.a0001302.pub2>.
- Nolan, T.M., Ghartey, K.K.F., Miller, F.R. and Adam, K. L. (1992). Management of the tropical high forest of Ghana – Wise management of tropical forests. In: *Proceedings of Oxford Conference on Tropical Forests 30 Oxford (RU)* (No. 333.750913063 W813 1992).

Oduro, K.A., Duah-Gyamfi, A., Acquah, S.B. and Agyeman, V.K. 2012. Ghana forest and wildlife handbook: a compendium of information about forest and wildlife resources, forestry related issues and wood processing in Ghana. Forestry Commission, Ghana, pp. 87.

Oduro, K.A., Mohren, G.M.J., Pena-Claros, M., Kyereh, B. and Arts, B. (2015). Tracing forest resource development in Ghana through forest transition pathways. *Land Use Policy*, **48**, 63-72.

Opoku, F. Y. (2007). *An investigation into the suitability of selected lesser utilised Ghanaian hardwoods for use as outdoor furniture and decking* (Unspecified Master of Philosophy thesis), Buckinghamshire, United Kingdom, pp. 159.

Oteng-Amoako, A., and Sarfo, D. (2005). Development of teak plantations in Ghana: propagation, processing, utilization, and marketing. In: *Proceedings of ITTO/Kerala Forest Research Institute International Conference on Quality Timber Products of Teak from Sustainable Forest Management*, Peechi, India.

Owusu, J.H. (2001). Determinants of export-oriented industrial output in Ghana: the case of formal wood processing in an era of economic recovery. *The Journal of Modern African Studies*, **39**, 51-80.

Schweingruber, F. H. (2007). *Wood structure and environment*. Springer Science and Business Media.

Timber Export Development Board (1994). *The Tropical Timbers of Ghana*, Takoradi, Ghana/London, UK, pp. 42.

Tsai, Y.H., Stow, D.A., López-Carr, D., Weeks, J.R., Clarke, K.C. and Mensah, F. (2019). Monitoring forest cover change within different reserve types in southern Ghana. *Environmental monitoring and assessment*, **191**(5), 1-15.

Wiedenhoef, A.C. and Miller, R.B. (2005). Structure and function of wood. *Handbook of wood chemistry and wood composites*, 9-33.

Ocloo, J.K. and Laing, E. (2003). Correlation of relative density and strength properties with anatomical properties of the wood of Ghanaian *Celtis* species. *Discovery and Innovation*, **15**(3/4), 186-196.

Zobel, B.J. and Van Buijtenen, J. P. (2012). *Wood variation: its causes and control*. Springer Science and Business Media.

An introduction of Ghana's hardwood products and market specialties

James Kudjo Govina^{1,2}, Róbert Németh¹

¹ University of Sopron, Simonyi Karoly Faculty of Engineering, Wood Science and Applied Arts, Institute of Wood Science, Sopron, Hungary. nemeth.robert@uni-sopron.hu

² Council for Scientific and Industrial Research – Forestry Research Institute of Ghana, Kumasi, Ghana. ndvm36@uni-sopron.hu

Keywords: Ghana, timber, hardwood, wood products.

ABSTRACT

Ghana has for decades been known as a major producer of tropical timber. The country's natural forest cover was endowed with a variety of hardwood species. Plantation forestry is dominated by *Tectona grandis* (Teak). The consumption of the timber was at both the domestic and international level. The early years of timber export to international markets outside Africa was characterized by shipment of round logs. The earlier known species, by their frequent demand and trade, were classified into utilization whereas their abundance guaranteed their classification into conservation status. Species such *Milicia excelsa*, *Terminalia ivorensis*, *Tieghemella heckelii*, *Pericopsis elata* were classified as premium species. Other utilization following Premium are Commercial, Lesser-used and Lesser-known. These premium and commercial species are mostly within the Endangered and Vulnerable conservation status. The Lesser-used and Lesser-known species are mostly within the Lower-Risk-Least-Concerns or Threatened. Presently, log export has been banned in Ghana. Logs are processed into 88% lumber, boule, veneer, plywood. Wood billets constitute about 9% whereas tertiary processing constitutes about 3%. *Tectona grandis* (Teak), *Triplochiton scleroxylon* (Obeche), *Ceiba pentandra* (Kapok), *Khaya species* (Mahogany), *Daniellia ogea* (Senya), *Azizia species* (Papao), *Cylicodiscus gabunensis* (Denya), *Aningeria species* (Asanfina), *Pterygota macrocarpa* (Koto). The major international markets for Ghanaian hardwood timber export are Asia, Europe, Africa, the Americas, and the Middle East.

INTRODUCTION

Over 300 hardwood tree species grow into timber size across the tropical forest in Ghana. The tropical West African nation, for decades, is known for export of hardwood timbers to overseas markets. In Ghana, the decline of the forest resources, hence the wood raw material base, cannot be over-emphasized (Acheampong et al. 2019, Agyarko 2001, Damnyag et al. 2012). Timber remains the most tangible resource obtained from the Ghanaian forests. In 2018, the forestry sector contributed 2.4% to Ghana's Gross Domestic Product (GSS 2020). The formal (registered Wood Processing Industry) and informal (illegal chainsaw operation) employed about 250,000 people – a contribution to employment (Agyarko 2001). The Timber Industry is the fourth largest foreign exchange earner (Domson 2008, FIP 2012). The wood raw material shortage has reduced the number of functional Timber Processing Industries by at least 25%, whereas the remaining ones operate at half of their previous capacity (Agyarko 2001, Daily Guide 2012).

GHANA'S HARDWOOD TIMBER TRADE

Hardwood timbers exported from Ghana since pre-independence were only limited to few premium species such *Milicia excelsa*, *Khaya species*, *Entandrophragma species*, *Pericopsis elata*. The concern of overexploitation of premium species resulted in Ghana government intervention to promote the other lesser-known and lesser-used species like *Manilkara obovata*, *Chrysophyllum species*, *Daniellia ogea*, *Ceiba pentandra* (Donkor et al. 2005). Even with the alarming shortage of the wood raw material base, log processing recovery is still below 40%. Additionally, tertiary, or value-added processed wood products (mouldings, doors, dowels, furniture parts) are only 3% of volume exported, secondary (lumber, boule,

vener, plywood etc) and primary (wood billet) processing are 88% and 9% respectively. The billets are mainly plantation hardwood species (Teak) (TIDD 2019). These findings highlight the potential for increasing the percentage of tertiary processed products through research, technology, product development, standardize testing, education, and policy implementation.

SOME ANOMALIES

Presently, the operations of Ghanaian wood industry are still associated with both old and new anomalies. Among the old anomalies, in no special order, are:

- Low recovery rate during log processing.
- Wood misidentification.
- Wood value transfers.
- Resources Tax evasion.

Some of the new anomalies, in no special order, are:

- Leading species exported fluctuates.
- Introduction of unknown timbers into the local market.
- Sustainable and guaranteed raw materials.
- Comparatively smaller sizes of logs from natural forests.

REFERENCES

Acheampong, E.O., Macgregor, C.J., Sloan, S. and Sayer, J. (2019). Deforestation is driven by agricultural expansion in Ghana's forest reserves. *Scientific African*, **5**, 00146.

Agyarko, T. (2001). Forestry Outlook Study for Africa (FOSA). *FOSA Country Report, Ghana Ministry of Lands and Forestry, Accra*. <http://www.fao.org/3/ab567e/AB567E00.htm#TOC> (accessed 15.01.2021).

Damnyag, L., Saastamoinen, O., Appiah, M. and Pappinen, A. (2012). Role of tenure insecurity in deforestation in Ghana's high forest zone. *Forest Policy and Economics*, **14**(1), 90-98.

Daily Guide. (2012). 60 Timber companies collapse, 30,000 jobs lost. <http://www.viasat1.com.gh/v1/vnews/business.php?postId=398> (accessed 29.05.2014).

Donkor, B.N., Vlosky, R.P. and Attah, A. (2005). Appraisal of Government Interventions for Diversification of Species Utilization in Forest Product Exports: Lessons from Ghana. *Journal of the Institute of Wood Science*, **17**(1), 1-10.

Domson, O. (2008). *Strategic analysis of Ghana's wood export sector*. Master's Thesis, Louisiana State University, United States of America. https://digitalcommons.lsu.edu/gradschool_theses/3489

Forest Investment Plan. (2012). *Ghana Investment Plan for the Forest Investment Program (FIP)*. Ministry of Lands and Natural Resources, Accra, Ghana.

Ghana Statistical Service (2020). Annual Gross Domestic Product by production. *Quarterly Report*, 4th, Accra, Ghana: Ghana Statistical Service.

Timber Industry Development Division (2018). Report on export of timber and wood products. *Monthly report*, Accra, Ghana. Forestry Commission, Ghana, pp. 31.

Timber Industry Development Division (2017). Report on export of timber and wood products. *Monthly report*, Accra, Ghana. Forestry Commission, Ghana, pp. 35.

Timber Industry Development Division (2019). Report on export of timber and wood products. *Monthly report*, Accra, Ghana. Forestry Commission, Ghana, pp. 24.

Conduction of heat in the high temperature modified oak wood

Richard Hrčka¹, Barbora Slováčková¹

¹ Department of Wood Science, Faculty of Wood Sciences and Technology, Technical University in Zvolen, T. G. Masaryka 24, 96001 Zvolen, Slovak Republic, hrcka@tuzvo.sk, xslovackova@is.tuzvo.sk

Keywords: oak wood, specific heat, thermal conductivity, thermal diffusivity, emissivity

ABSTRACT

The group of oaks (english or sessile, *Quercus* sp.) is the second most abundant broadleaved tree genus of species in Slovakia. Oak wood was found as shortage goods. The optimization of oak wood heating requires the knowledge of thermal properties values. The optimization of heat conduction in wood mainly consists of answers to three questions. How much heat do we need to change the temperature? How much heat will pass through the wall? How fast two different temperatures will equilibrate? All three questions are solved by using the results of transient measurement of oak wood thermal properties simultaneously. The method is based on solution of heat conduction equation. Wood is treated as continuum. The factors influencing the oak wood thermal properties are direction of flow, density of wood at moisture content, temperature and others. Mass specific heat capacity was measured at range of 1.2-1.4 kJ·kg⁻¹·K⁻¹, thermal conductivity of 0.11-0.50 W·m⁻¹·K⁻¹, thermal diffusivity of 1.4·10⁻⁷-5.9·10⁻⁷ m²·s⁻¹, emissivity of 0.65-0.78 at longitudinal, radial and tangential directions, density of 607-698 kg·m⁻³ at moisture content of 4.7-12.9%, temperature of 20°C and treatment temperature of 20-180-220°C. The larger treatment temperatures of oak wood resulted to lower density at moisture content. The moisture content was measured at temperature of 20°C and relative humidity 65% assuming its equilibrium value. Moreover, density at moisture content affected the most of the thermal properties significantly.

INTRODUCTION

Compared to the year 2000, the average age of oak increased by 14.2 years in Slovakia (MARD 2017). There is a lack of facilities for processing one of the highest quality softwood/hardwood roundwood. On the other hand, the production of products with added value is needed to support competitiveness of the timber processing industry. The competitiveness is qualified with production of products with added value. Wood properties need to be understood prior and after processing in order to be able to add a value to the final product. Oak wood properties are widely and undoubtedly appreciated. The utilization of oak wood has been known since ancient times as documented in contribution of Sinković et al. (2009). Oak wood heartwood is considered as impermeable to liquids (Požgaj et al. 1993). Also, oak wood was utilized as construction material of waterlogged piles (Welling et al. 2018). The various manners of oak wood utilization from ancient times to present are described in publication of Makovíny (2010). Heat passes through wood boundaries spontaneously according to difference of temperature between wood and surroundings during wood processing. Drying of oak wood is a difficult and time consuming process, plasticizing of oak wood is inevitable before bending to a small radius of curvature, heating the oak logs is required before the production of veneers. Oak wood parquets are usually in contact with elevated temperatures during heating the interior or in contact to human skin. Most of the problems which are related to heat and wood are solved by answers to three questions. How much heat do we need to change the temperature? How much heat will pass through the wall? How fast will two different temperatures equilibrate? The first question is related to specific heat capacity, the second one to thermal conductivity and last one to thermal diffusivity. In general, mass specific heat capacity of wood does not depend on wood species oven dry density and anatomical direction, but it depends on moisture content and temperature (Kanter 1957, Radmanovič 2014). Thermal conductivity and thermal diffusivity of wood are symmetric tensors of the second order, which eigenvalues depend on oven dry density, anatomical direction, moisture content and temperature (Regináč and Babiak 1977, Požgaj et al. 1993, Malujda et al. 2014, Deliskii and Tumbarkova 2017, Vay et al. 2015). The dominant transport of heat through impermeable oak wood is conduction. The solutions of heat conduction equation are used for computing the transient temperature

fields. Wood is often considered as continuum. However, if wood is in contact with fluids, the convection and also radiation occur on boundaries. Then, boundary condition of the third kind is used in solutions of heat conduction equation (Lykov 1968). The boundary condition of the third kind introduces the heat transfer coefficient. The contact temperature between wood and solid is described by the solution with the equality of fluxes and temperature on the both surfaces. The equilibrated value of temperature is influenced by the ratio of wood and solid effusivities (Obata et al. 2005). All mentioned properties together with heat transfer coefficient are useful in description of the heat transport phenomena in wood because they play a key role in answering the three above mentioned questions properly. The optimization of heat transport processes through valuable oak wood is desired. The results of measurement in the form of data of oak wood heat transport characteristics are the aim of this contribution. The results will serve as the bases for computing the temperature fields in oak wood specimens using solutions of heat conduction equation; mainly in the specimens of large dimensions.

EXPERIMENTAL METHODS

Oak wood (*Quercus sp.*) was obtained from locality Vlčí jarok (Budča, Central Slovakia). The logs were cut into slabs of 110cm x 11cm x 2cm (L x R x T) dimensions. A final moisture content of 10% for flat sawn lumber was achieved by the kiln drying method at the Technical University in Zvolen. The three slabs were stored at the temperature of 10°C. Two of them were thermally modified at the temperatures of 180 and 220°C and one sample remained unmodified. The hydrothermal treatment was performed at the Arboretum of FLD (CZU in Prague) in Kostelec nad Černými lesy (Czech Republic) using heating technology in the LAC S 400/03 chamber KATRES s.r.o. (Koleda et al. 2019). A temperature of 60°C or lower was recorded on the slabs after removing them from the chamber. Two slabs were thermally treated according to the following procedure (Table 1):

- the 1st period: the lumber was heated to reach target temperature.
- the 2nd period: the lumber was heated at different treatment temperatures (180 and 220 °C) for 4 h.
- the 3rd period: the lumber was cooled to an ambient temperature of 60 °C and the target moisture content was reached up to the desired value by the water spraying method.

Table 1: The schedule of the thermal treatment.

Temperature (°C)	1 st Period (h)	2 nd Period (h)	3 rd Period (h)
180	12	4	4
220	16	4	6

The parts of treated oak timber were equilibrated in humid air in a climatic chamber Binder KBF 720 (Tuttlingen, Germany). The controlled parameters of humid air were at a relative humidity of 65% and a temperature of 20 °C for half year. The specimens' final dimensions of 100mm x 50mm x 8mm (L x R x T) were cut off from the slabs and radial surfaces were sanded on wide belt sander (P80). The total number of used different specimens was 60. The equilibrium was detected according to the constant mass of the moisture specimen using the technical scales Kern KB 1000-2 (Balingen, Germany).

The principle of thermal properties method measurement is described in the publication of Hrčka and Slováčková (2019). The difference between described method of Hrčka and Slováčková (2019) and used method in this contribution is in the utilization of two heating foils (NiCr - Vacronium, thickness of 0.01mm) symmetrically placed inside of four specimens block (Fig. 1).

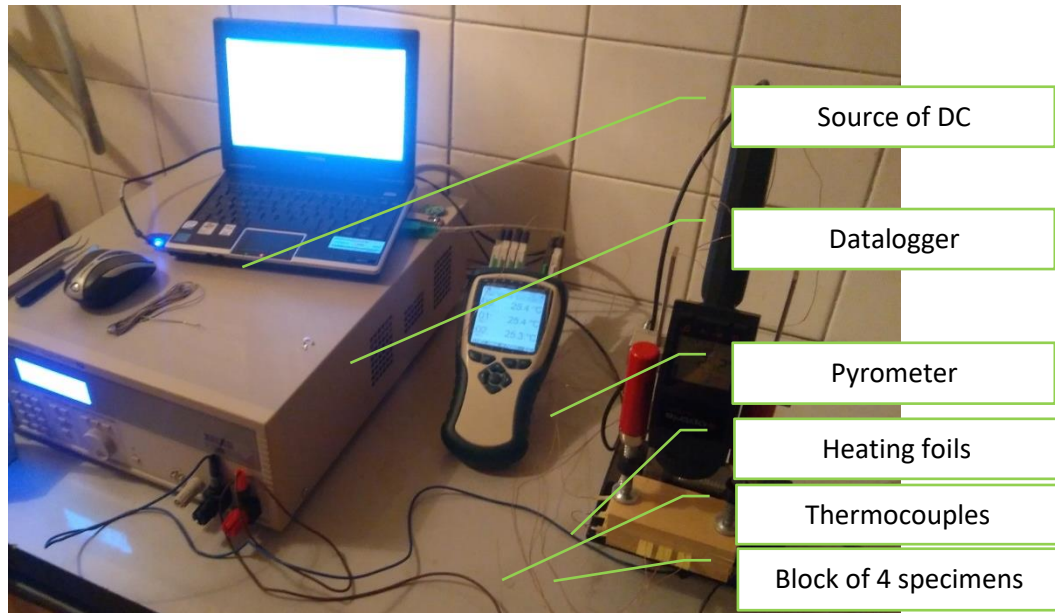


Figure 1: Arrangement of apparatus

Then, the position of three thermocouples of type K (Omega, USA) is shown in Fig. 2.

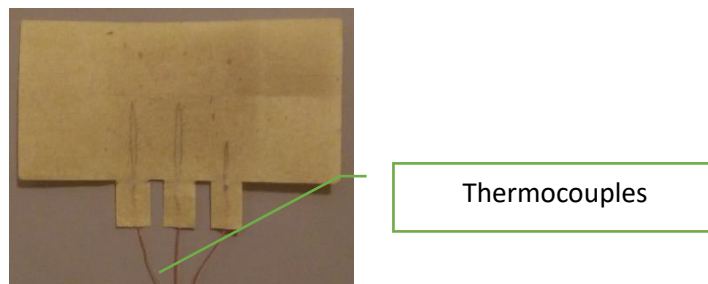


Figure 2: Position of thermocouples

The fourth thermocouple is placed in the position of one heating foil. The form of the heating foil is structured source which consists in thin strips as is shown in Fig. 3.

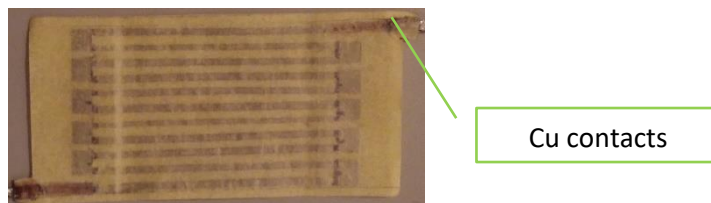


Figure 3: Structured heating foil

The set current was 0.12mA (QPX1200SP, TTI, UK) and expected maximum temperature rise was 20°C at the position of the heating foil.

RESULTS AND DISCUSSION

The oak wood density at given moisture content significantly decreased with decreasing moisture content, because oven dry density of oak wood is below density of water. The moisture content significantly decreased with increasing treatment temperature, Table 2. These facts are known from the other experiments (for example Babiak and Németh 1998, Hrčka et al. 2018), also.

Table 2: Equilibrium moisture content and average input parameters of oak wood thermal properties measurement (below standard deviations; t modifying temperature; T , R , L – dimensions in principal anatomic directions; ρ – density at given moisture content; w – equilibrium at relative humidity of 65% and initial temperature of 20 °C)

t °C	T m	R m	L m	ρ kg.m ⁻³	w
20	0.01514	0.04977	0.09489	697.8 (7.8)	0.129 (0.002)
180	0.01526	0.04991	0.096094	669.1 (24.0)	0.056 (0.004)
220	0.01554	0.05008	0.096112	606.5 (34.3)	0.047 (0.008)

(below in parenthesis: standard deviations)

Mass specific heat capacity is a scalar quantity. Thermal conductivity and thermal diffusivity are symmetric tensors of the second order. The heat transfer coefficient may depend on orientation of the surface. Therefore, the measurement of wood thermal quantities requires at least seven degrees of freedom. The measurement of temperature at different position of specimens proved the lateral heat transfer from the specimens, because the measurement temperatures do not overlap, Fig. 4.

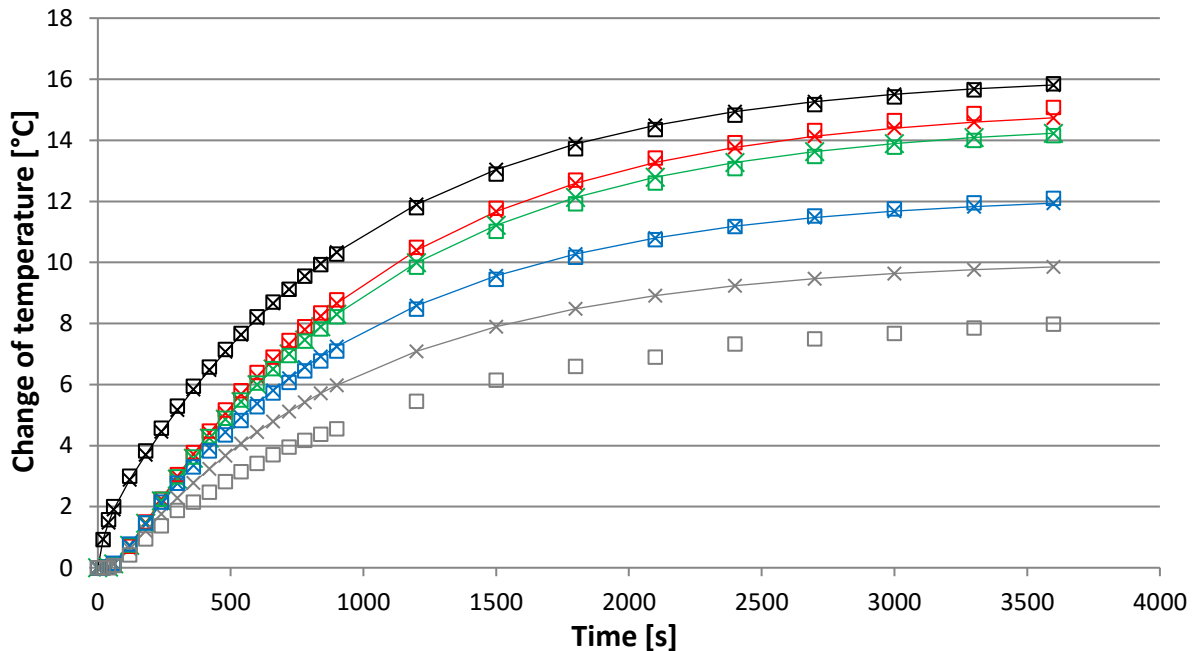


Figure 4: Temperature increase in different thermocouples (squares) and fitted temperatures (crosses). Black curve depicts the measurement of temperature at heating foil position, red curve depicts the position of the 1st thermocouple, green the position of the 2nd thermocouple, blue the position of the 3rd thermocouple and grey curve belongs to surface temperature which was measured by pyrometer (squares) with set emissivity to 1.000, computed surface temperature is indicated with grey crosses

Mass specific heat of oak wood depends significantly on moisture content and so does on treatment temperature. The larger mass specific heat capacity was measured by Hřčka et al. (2018). This fact can be attributed to the structure of heating foil, Fig. 3, instead of non-structured heating foil used in previous experiments. The significant decrease of thermal conductivity with decreasing moisture content and density was measured for all anatomical directions. The most constant oak wood thermal property is thermal diffusivity, if the factor is moisture content. Thermal conductivity and thermal diffusivity depends on anatomical direction, Table 3. Wood is orthogonal anisotropic construction material.

Table 3: Thermal diffusivities (a), thermal conductivities (λ) in principal anatomical directions and mass specific heat capacity (c) of oak wood and its modification form by heat at elevated temperatures (t)

t °C	λ_R W.(m.K) ⁻¹	λ_T W.(m.K) ⁻¹	λ_L W.(m.K) ⁻¹	c J.(kg.K) ⁻¹	a_R m ² .s ⁻¹	a_T m ² .s ⁻¹	a_L m ² .s ⁻¹
20	0.17 (0.02)	0.14 (0.01)	0.50 (0.06)	1470 (36)	$1.7 \cdot 10^{-7}$ ($2.0 \cdot 10^{-8}$)	$1.4 \cdot 10^{-7}$ ($0.9 \cdot 10^{-8}$)	$5.0 \cdot 10^{-7}$ ($6.7 \cdot 10^{-8}$)
180	0.15 (0.01)	0.14 (0.01)	0.49 (0.01)	1220 (27)	$1.8 \cdot 10^{-7}$ ($1.1 \cdot 10^{-8}$)	$1.7 \cdot 10^{-7}$ ($0.7 \cdot 10^{-8}$)	$5.9 \cdot 10^{-7}$ ($1.4 \cdot 10^{-8}$)
220	0.13 (0.01)	0.11 (0.01)	0.40 (0.03)	1190 (21)	$1.8 \cdot 10^{-7}$ ($1.3 \cdot 10^{-8}$)	$1.6 \cdot 10^{-7}$ ($0.7 \cdot 10^{-8}$)	$5.5 \cdot 10^{-7}$ ($3.8 \cdot 10^{-8}$)

(below in parenthesis: standard deviations)

The method utilizes the independence of radiative heat flux on temperature, which is measured with pyrometer. The emissivity is set to 1.000 during the experiment. Then, radiative flux is computed with adjusted emissivity according to computed surface temperature. And finally, computed radiative flux is compared to measured radiative flux according to adjusted emissivity, Fig. 5.

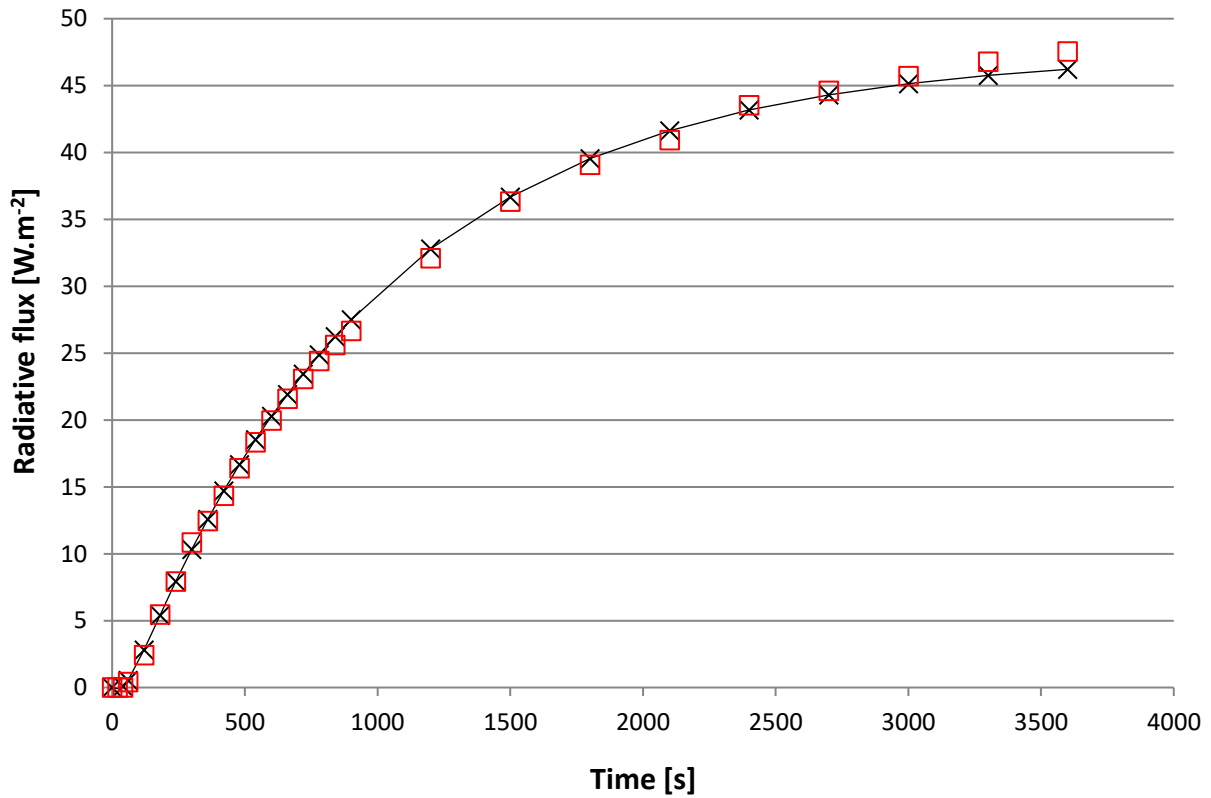


Figure 5: Radiative flux increase in time as measured by pyrometer (red squares) and computed using adjusted emissivity (grey crosses)

The measured Biot number and computed heat transfer coefficient are shown in Table 4. The Biot number determines the surface temperature. Its value is not infinity. Therefore, surface temperature differs from ambient temperature of surroundings (20°C).

Table 4: Emissivity, Biot number, heat transfer coefficient and effusivity on oak wood radial surfaces.

T °C	ϵ	Bi _T	α_T W.m ⁻² .K ⁻¹	e_T W.m ⁻² .K ⁻¹ .s ^{0.5}
20	0.77 (0.03)	1.4 (0.09)	13	381
180	0.76 (0.04)	1.7 (0.07)	15	333
220	0.65 (0.02)	1.6 (0.07)	11	284

(below in parenthesis: standard deviations)

The effusivity value decreases with decreasing moisture content and density. From the point of view of higher temperature of solid, the lowest temperature on the surface will be set at the contact with solid and oak wood treated at the highest treated temperature (in this experiment 220°C).

CONCLUSIONS

1. Mass specific heat capacity depends significantly on moisture content. The arrangement of apparatus significantly influences its values, even the physical principle is the same.
2. Oak wood is orthogonal anisotropic construction material, because thermal conductivity is regarded as second order symmetric tensor, with its eigenvalues being different. The oak wood tangential eigenvalue is smaller than radial one. The oak wood density at given moisture content significantly influences eigenvalues of thermal conductivity.
3. Thermal diffusivity is a property which insignificantly depends on treatment temperature.
4. Biot number and heat transfer coefficient finite values indicate a difference in surface temperature and temperature of the surroundings. Emissivity values significantly differ only on samples treated at 220°C temperature. Also, effusivity of oak wood treated at 220°C indicates pleasurable contact with human skin.

ACKNOWLEDGMENTS

This work was supported by the Slovak Research and Development Agency under contract No. APVV-16-0177 and the Internal Project Agency under contract 17/2020.

REFERENCES

- Babiak, M. and Németh, R. (1998) Effect of steaming on the sorption isotherms of black locust wood. *Acta facultatis Ligniensis*, Sopron, pp. 64-68.
- Deliskii, N. and Tumbarkova, N. (2017) An approach and algorithm for computation of the unsteady icing degrees of logs subjected to freezing. *Acta Facultatis Xylogiae Zvolen*, **59**(2), 91-104. doi: 10.17423/afx.2017.59.2.09
- Hrčka, R., Kučerová V. and Hýrošová, T. (2018) The Correlations between Oak Wood Properties. *Bioresources*, **13**(4), 8885-8898.

Hrčka, R. and Slováčková, B. (2019) The method of wood emissivity measurement. *Acta facultatis xylologiae Zvolen*, **61**(2), 17-24. doi: 10.17423/afx.2019.61.2.02

Kanter, K.R. (1957) О тепловых свойствах древесины. (Thermal properties of wood) *Деревообрабатывающая промышленность*, **7**, 17-18.

Koleda, P., Barčík, Š., Korčok, M. and Jamberová, Z. (2019) Effect of temperature of heat treatment of oak wood on energetic efficiency when planar milling. In: *XXI International Conference of Young Scientists*, 11th – 12th June 2019, Nitra, Slovakia

Makovíny, I. (2010) *Úžitkové vlastnosti a použitie rôznych druhov dreva (The Utility Properties and Use of Various Wood Species)*, TU Zvolen, Zvolen, Slovakia. ISBN 978-80-228-2127-8 (in Slovak)

Malujda, I., Talaška, K., Dudziak, M. (2014) The Thermal Conductivity - Experimental Studies of Thermal Processes in Woodworking. *Machine Dynamics Research*, **38**(1), 121-128.

Ministry of Agriculture and Rural Development of the Slovak Republic (MARD) (2017) *Report on the Forest Sector of the Slovak Republic*. <http://www.mpsr.sk/en/index.php?navID=1&id=67>. (accessed: 21 June 2018).

Obata, Y., Takeuchi, K., Furuta, Y. and Kanayama, K. (2005) Research on better use of wood for sustainable development: Quantitative evaluation of good tactile warmth of wood. *Energy* **30**, 1317–1328. doi:10.1016/j.energy.2004.02.001

Požgaj, A., Chovanec, D., Kurjatko, S., and Babiak, M. (1993) *Štruktúra a vlastnosti dreva (Wood Structure and Properties)*, Príroda, Bratislava. ISBN 80-07-00600-1 (in Slovak)

Radmanovič, K., Đukić, I. and Pervan, S. (2014) Specific Heat Capacity of Wood. *Drvna Industrija*, **65**(2), 151-157.

Regináč, L. and Babiak, M. (1977) Základné tepelnofyzikálne charakteristiky smrekového dreva pri normálnych podmienkach (Basic thermo-physical characteristics of spruce wood under normal conditions), *Drevársky Výskum* **22**(3), 165-174. (in Slovak)

Sinković, T., Govorčin S., Roth, W., and Sedlar, T. (2009) Usporedba tehničkih svojstava abonosa i recentnog drva hrasta lužnjaka (*Quercus robur* L.) (Comparison some physical and mechanical properties of abonos and recent oak (*Quercus robur* L.)). *Šumarški List* **133**(11-12), 605-611. (in Croatian)

Vay, O., De Borst, K., Hansmann, C., Teischinger, A., and Müller, U. (2015) Thermal conductivity of wood at angles to the principal anatomical directions, *Wood Sci. Technol.* **49**, 577-589. doi: 10.1007/s00226-015-0716-x

Welling, J., Schwarz, T., and Bauch, J. (2018) Biological, chemical and technological characteristics of waterlogged archaeological piles (*Quercus petraea* (Matt.) Liebl. of a medieval bridge foundation in Bavaria, *Eur. J. Wood Prod.* (accepted for publication). doi: 10.1007/s00107-017-1168-9

Selected elastic properties of thermally treated beech wood

Rastislav Lagaňa¹, Andrej Janeka², Tomáš Andor³

¹ Technical University in Zvolen, T. G. Masaryka 24, Zvolen, Slovakia, lagana@tuzvo.sk

² Technical University in Zvolen, T. G. Masaryka 24, Zvolen, Slovakia, xjaneka@is.tuzvo.sk

³ Kronospan, s.r.o., Lučenecká cesta 21, Zvolen, tandor6829@gmail.com

Keywords: beech wood, high-temperature treatment, elastic properties, Poisson's ratio

ABSTRACT

The study aimed to evaluate the effect of high-temperature modification on sorption and elastic properties focusing on Poisson's ratio. The European beech wood was treated at 160 °C, 180 °C, and 200 °C for 1,5 hours and 3 hours. The effects of time and temperature on equilibrium moisture content, compression modulus parallel to the grain, and Poisson's ratio (μ_{RL} and μ_{TL}) were determined. Results showed that the changes in properties started after 160 °C treatment. The temperature of the treatment was a significant factor affecting all selected properties. Time of treatment affected the EMC only. Poisson's ratio proportionally decreased with increasing treatment temperature within the temperature range from 160 °C to 200 °C. This result confirmed the stiffening process during the high-temperature treatment.

INTRODUCTION

High-temperature modification is a common treatment method for improving selected properties of wood. A positive aspect is low equilibrium moisture content that improves dimensional stability and consequently, in some reported cases, enhances stiffness or strength of wood (Andor, Lagana 2016). Elastic modulus behavior varies for different wood species. Romagnoli et al. (2015) observed the mechanical properties of several wood species. While bending modulus decreased in Douglas fir wood, the same temperature treatment riced modulus of Corsica pine wood. This increase is limited and occurred between 180 °C and 200 °C based on wood species and type of heat treatment (Boruvka et al. 2015, Molinski et al. 2016, Zawadzki et al. 2013). Volkmer et al. (2014) tested Poisson's ratio of beech wood treated in the heat pressure steam and the result showed a varied effect of the heat treatment.

This study aims to evaluate the effect of the temperature and duration of the high-temperature modification in the oxidizing atmosphere on the elastic properties of beech wood and determine the changes in the selected properties.

EXPERIMENTAL METHODS

Materials and the thermal treatment

The tested samples (35x35x120 mm, R x T x L) were cut and carefully sorted getting specimens free of defects. The samples were divided into six treated groups and one reference group. Each group consisted of 16 samples.

Before the treatment, the samples were oven-dried at the temperature of 103 °C ± 2 °C. A treatment was realized in the high-temperature oven in an oxidizing atmosphere. Three different temperature levels 160 °C, 180 °C, and 200 °C during two different treatment times (1,5 and 3 hours) were used to thermally modified groups of treated samples. After the treatment, the samples were cooled. The oven-dried weight and dimensions were measured. The samples were placed into a climate chamber which was set to the relative humidity 75 % and the temperature 20 °C. Equilibrium moisture content (EMC) was determined after reaching the equilibrium.

Elastic properties

Before testing in compression parallel to the grain, the surface of the samples was painted creating a random pattern for strain field measurements using ARAMIS 3D system. Active and passive deformations were measured in longitudinal and transverse directions on the RL surface and TL surface. The Poisson's ratios were calculated according to the equations:

$$\mu_{TL} = \frac{\varepsilon_T}{\varepsilon_L} [-] \text{ and } \mu_{RL} = \frac{\varepsilon_R}{\varepsilon_L} [-] \quad (1)$$

where ε_T is an average passive deformation (out of four measured reference length) in the tangential direction, ε_R is an average passive deformation (out of four measured reference length) in the radial direction, and ε_L is an average active deformation (out of four measured reference length) in the longitudinal direction (Fig. 1). Modulus of elasticity E was calculated from the linear relationship between compression stress and strain at the reference length.

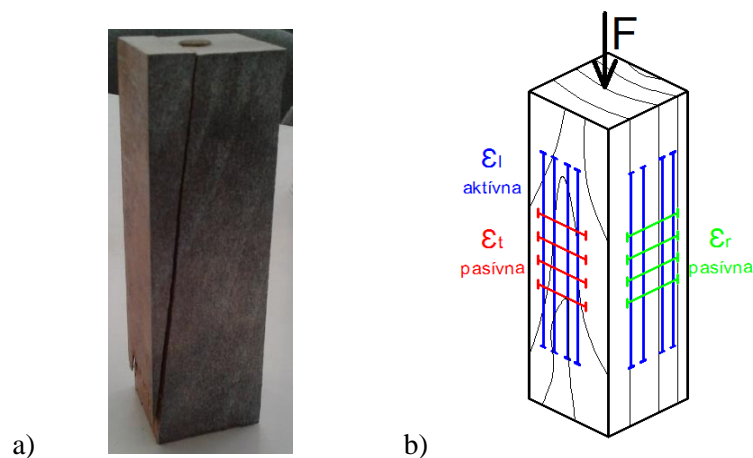


Figure 1: a) A sample with a random surface pattern, b) reference lengths for determination of active (blue) and passive (red, green) deformations

RESULTS AND DISCUSSION

Equilibrium moisture content

Results of ANOVA confirmed a significant decrease in EMC (Fig. 2). Both factors, the factor of the temperature and the factor of treatment time led to significant EMC changes. Higher temperature and longer duration of the thermal treatment caused lower EMC. Similar changes reported Gereke et al (2009) when EMC reached 10.9% at the standard conditions (RH = 65 %, T = 20 °C).

The 180 °C treatment showed the first significant change in EMC (8% of untreated EMC). The highest EMC drop (34% of untreated EMC) was observed after 3 hours of treatment at 200 °C reaching EMC 8,4 %. Baar et al. (2021) used very similar treatment conditions resulting in EMC 9,5 % after 3 hours of 200 °C beech wood treatment.

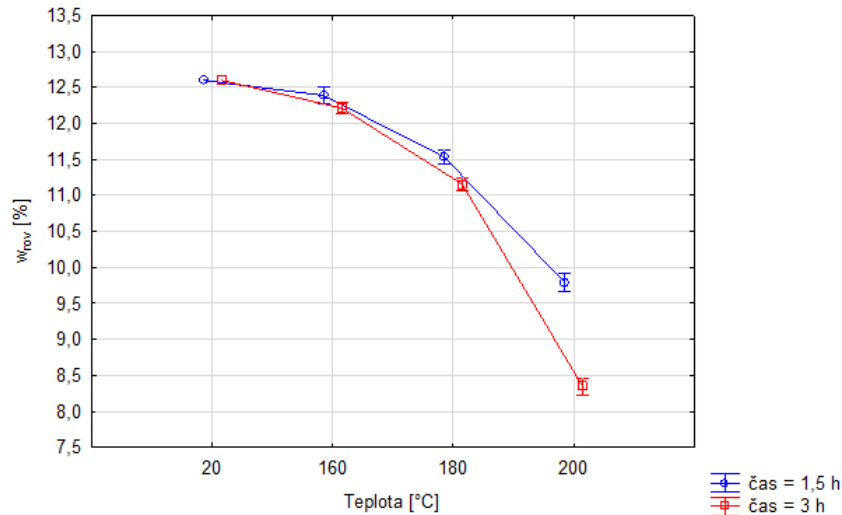


Figure 2: An effect of the thermal treatment on the equilibrium moisture content

Modulus of elasticity

The ANOVA confirmed the significant factor of the temperature (Fig. 3). The factor of the treatment time was statistically insignificant. The average elastic modulus of untreated beech wood was 14,4 GPa. The temperature treatment at 160 °C did not change the modulus. The significant changes occurred after that temperature level. Again, the highest elastic modulus drop was observed after a 3-hour treatment at 200 °C when the modulus reached 11,6 GPa (20 % change of the initial modulus), very close to the reported 11,4 GPa (Baar at al. 2021). A similar reduction of beech wood elasticity was reported by Percin et al. (2016). Some authors described an increase of MOE after the high-temperature treatment due to lignin-cellulose complex cross-linking. Rautkari et al. (2014) showed an increase of elastic modulus of pine wood (2,3 GPa increase after a 150 °C treatment) and the same study reported a 0,2 GPa decrease after a 180 °C treatment. A question for future research is the leading cause of elasticity changes caused by the lower hygroscopicity, the thermal degradation, or interaction of both factors, respectively.

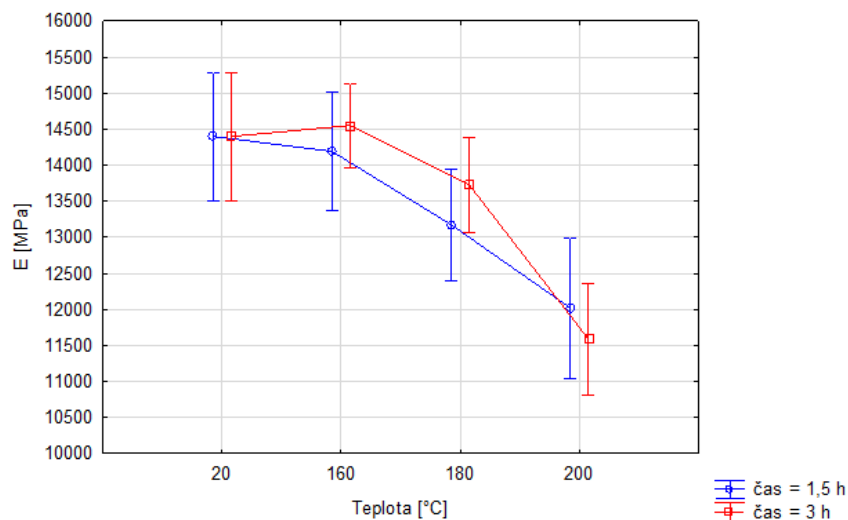


Figure 3: A change of elastic modulus in compression parallel to the grain after the thermal treatment

Poisson's ratio

The average values of the Poisson's ratio of untreated wood were $\mu_{RL} = -0,489$ and $\mu_{TL} = -0,504$. Hering et al. (2011) reported beech wood Poisson's ratio at $\mu_{RL} = -0,27$ and $\mu_{TL} = -0,24$. When they compared beech wood value with studies of several authors, Poisson's ratio was in the range between 0,24 and 0,51 for μ_{RL} and 0,27 to 0,45 for μ_{TL} . The high-temperature treatment affected the values of Poisson's ratio. Absolute values decreased and this change was linear within the temperature range 160 °C – 200 °C for both surfaces (Fig. 4 and Fig. 5). Beech wood became stiffer after the treatment, and this affected lateral deformations too. Volkmer et al. (2014) tested Poisson's ratio of treated wood in saturated vapor at 120 °C for 50 hours. The results were different for each surface. The radial surface Poisson's ratio decreased 10 % while the tangential surface Poisson's ratio increased 9,8 %. Our results pointed to the stiffening of wood that occurred in both transverse directions. The time of treatment effect was insignificant while the temperature was a significant factor.

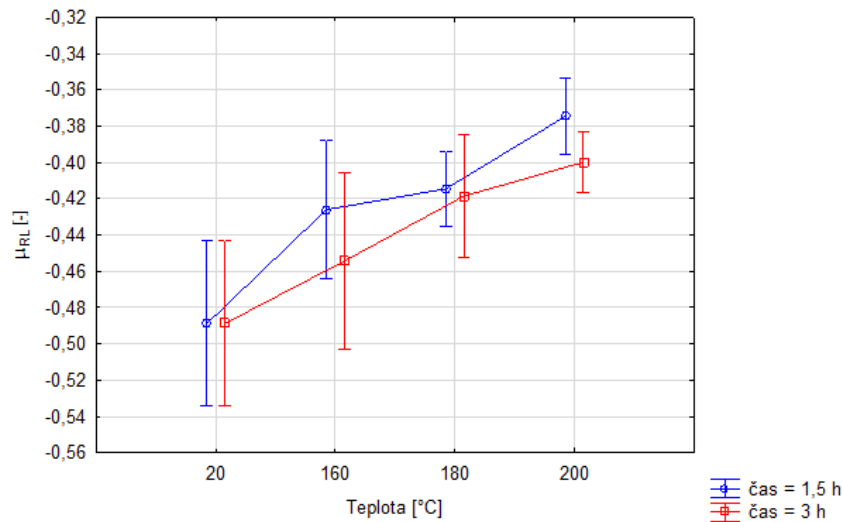


Figure 4: An effect of the thermal treatment on Poisson's ratio measured on the radial section

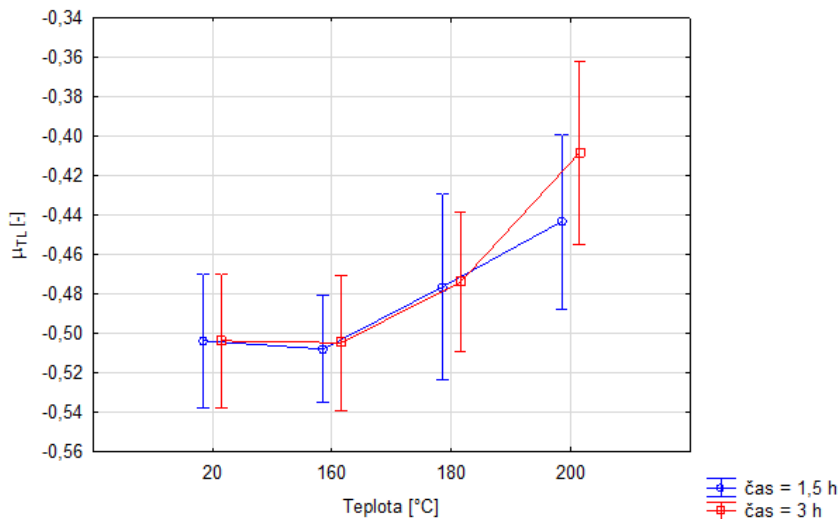


Figure 5: Effect of the thermal treatment on Poisson's ratio measured on the tangential section

CONCLUSIONS

The selected properties of beech wood changed after the thermal treatment in an oxidizing atmosphere. We have confirmed a drop of EMC, compression strength, and modulus of elasticity values after the treatment. The study showed that beech wood became stiffer resulting in lowering the Poisson's ratio.

ACKNOWLEDGMENTS

This work was supported by the Slovak Research and Development Agency under contract No. APVV-16-0177.

REFERENCES

- Andor, T. Lagaña, R. (2016) An effect of the thermal treatment on selected properties of ash wood. *Proceedings of the "Eco-Efficient Resource Wood with Special Focus on Hardwoods" in conjunction with the "Conference of Climate protection through forestry, renewable materials, smart technologies and environmental education" and with the "COST Action FP1407 Workshop"*. Sopron, Hungary, pp. 98-99.
- Baar, J., Brabec, M., Slávik, R., Čermák, P. (2021) Effect of hemp oil impregnation and thermal modification on European beech wood properties. *European Journal of Wood and Wood Products*, **79**, 161–175.
- Borůvka, V Zeidler, A., Holeček, T. (2015) Comparison of stiffness and strength properties of untreated and heat-treated wood of douglas fir and Alder. *BioResources* **10**(4), 8281-8294.
- Gereke, T., Schnider, T., Hurst, A., Niemz, P. (2009) Identification of moisture-induced stresses in cross-laminated wood panels from beech wood (*Fagus sylvatica* L.). *Wood Science and Technology*, **43**, 301.
- Hering, S., Keunecke, D. & Niemz, P. (2012) Moisture-dependent orthotropic elasticity of beech wood. *Wood Science and Technology*, **46**, 927–938.
- Molinski, W., Roszyk, E., Jablonski, A., Puszynski, J., Cegiela, J. (2016) Mechanical parameters of thermally modified ash wood determined by compression in radial direction, *Maderas. Ciencia y tecnología*, **18**(4), 577-586.
- Percin, O., Peker, H., Atilgan, A. (2016) The effect of heat treatment on some physical and mechanical properties of beech (*Fagus orientalis* lipsky) wood. *Wood Research*, **61**, 443-456.
- Rautkari, L., Honkanen, J., Hill, C. A. S., Ridley-Ellis, D., Hughes, M. (2014) Mechanical and physical properties of thermally modified Scots pine wood in high pressure reactor under saturated steam at 120, 150 and 180 °C. *European Journal of Wood and Wood Products*, **72**, 33–41.
- Romagnoli, M., Cavalli, D., Pernarella, R., Zanuttini, R. Togni, M. (2015) Physical and Mechanical Characteristics of Poor-Quality Wood After Heat Treatment. *IForest: Biogeosciences and Forestry*, **8**(1), 884-891.
- Zawadzki, J., Radomski, A., Gawron, J. (2013) The effect of thermal modification on selected physical properties of wood of Scots pine (*Pinus sylvestris* L.). *Wood Research*, **58**(2), 243–250.

A study of the surface properties of a solid wood coating system with self-healing microcapsules

Rastislav Lagaňa¹, Ján Svocák², Jozef Kúdela³

¹ Technical University in Zvolen, T. G. Masaryka 24, Zvolen, Slovakia, lagana@tuzvo.sk

² Technical University in Zvolen, T. G. Masaryka 24, Zvolen, Slovakia, xsvocak@is.tuzvo.sk

³ Technical University in Zvolen, T. G. Masaryka 24, Zvolen, Slovakia, kudela@tuzvo.sk

Keywords: self-repairing wood coatings, microcapsules, adhesion, roughness, dissipation energy, AFM

ABSTRACT

This study was a part of the research covering stability of pigment coating system for wood with a special middle layer that contains microcapsules with self-healing action. The main purpose of this layer is to close damaged upper layers (cracks, scratches, etc.). To better understand the mechanisms of the middle layer containing microcapsules, the properties of the middle layer were determined using an atomic force microscope (AFM). Moreover, the surface characteristics (color, roughness, waviness) of spruce wood coated with this special middle layer and sustained to 600-hour artificial aging were studied on the coating system. A free film containing microcapsules and 3-layer and 2-layer coated samples were made for this purpose. We evaluated the surface roughness, dissipative energy, and the adhesion force between the silicon tip and the surface of the solid coating in the spot above the microcapsule as well as of the microcapsule position. Results showed that the highest differences were observed in the surface roughness and ability to absorb mechanical energy. Lower values were found above the microcapsule position in both cases. The low dissipative energy at the microcapsule is explained by a liquid or gel-like state of the microcapsule. The microcapsules help in spreading the coating at the surface, which was a reason for decreasing the roughness of the solid coating at the capsule location. The adhesive force between the middle layer coating and the AFM tip was lower in the presence of the microcapsules suggesting the low local adherence between the coating layers. The research on surface aging showed that the coating system with the self-healing middle layer was more stable than without one. Proposed reasons dwelled in the viscoelastic properties of the middle layer and in the fact that microcapsules were able to fill artificially made cracks in the coating and to avoid water transport into the wood surface. The color changes were independent of the special middle layer presence.

INTRODUCTION

Mechanical damage of coatings and cracks are serious defects of the wood surface finishing. Defects break the integrity of a coating film. The damaged areas initiated the spreading of other defects in the surface finishing. A coating film gradually loses a protective function against external impacts. The broken areas of coatings are often a reason for the transport of humid air into the wood surface. Consequently, the surface layers of wood swell. The swelling at the face interphase between wood and a solid coating causes stresses that lead to more cracks and cracks propagation in the coating. The adhesion of a coating to the substrate gradually diminishes and the coating peels off. For that reason, the surface finishing requires routine renovation that is time and financially demanding. New ways of protection are developed to maximize protection against these unwanted features.

Recently, the use of wood coatings with a self-healing action that contain special microcapsules. Studies of microcapsules showed practical assets limiting the problem of crack propagation in materials such as concrete, asphalt, or fiber-reinforced polymer (Giannaros et al. 2016, Garcia et al. 2009, Tan et al. 2020, Moll et al. 2010). This type of coatings is interesting for wood surface finishing applications. The special fillings for microcapsules are developed. They are based on low viscosity polymers covered in various microcapsules (Rule et al. 2005, Yuan et al. 2006, Yuan et al. 2008) that must sustain the shear stress during coating mixing (Zhao et al. 2012). After curing the coating and creating a crack, the microcapsule

shell is broken, and the low viscosity polymer flows out of the microcapsule to the crack. After curing the polymer, the crack is closed.

This is a reason for research of how the microcapsules added into the film-forming coating affect properties of the coating. The layer containing microcapsules is usually in the middle of the three-layer coating system where it is expected to be broken. The knowledge about this layer, its behavior, and interactions with a sublayer or the final layer will optimize the setting of the coating system applied to wood.

This research aimed to study the properties of free coating film with microcapsules as well as research the stability of three-layered coatings with the middle layer containing the microcapsules for healing cracks.

MATERIALS AND METHODS

Experiment 1

A pigmented, water-soluble coating filler was used for the study of a free coating film. It was an acrylate dispersion with added microcapsules filled with liquid that provides closing cracks when coating integrity damage occurs (for example after a hailstorm).

The filler was spread on the Teflon substrate using a spreading ruler. After curing the layer in the laboratory conditions (temperature 20 °C and relative humidity of air 40-50 %), the solid coating film had a thickness of 100 µm. The film was peel off the Teflon substrate and dried as a free film for three days in laboratory conditions. The film was cut to 5 x 5 mm samples and glued to a metal plate using a double side adhesive tape. Two types of samples were prepared. One sample faced up the teflon side and the other sample faced up the opposite side, the upper side of the free film. The surface properties of both samples were measured at the reference area 10 × 10 µm² and 1 × 1 µm². The areas were located above a visible microcapsule and out of the microcapsule location. Atomic force microscope (Multimode 8, Bruker with Nanoscope V controller, Bruker Nano Surfaces, Santa Barbara, CA, USA) in PeakForce QNM mode was used for measuring the surface properties. We used a ScanAsyst Air tip with a 2 nm tip radius and spring constant 0,4 N/m. The cantilever was calibrated in the frequency method (Tune mode). The exact radius of the tip was calibrated using a TGT calibration sample. The measurements were performed in the temperature-controlled laboratory conditions (temperature 23 °C and relative humidity of air 40 – 50 %). Three surface properties were determined: the surface roughness given by the surface parameters R_a and R_q , dissipation energy, and adhesion force between the silicone tip and the solid coating surface.

Experiment 2

We used two coating systems for the second experiment. The first one is a three-layered coating system consisting of the basic layer, the middle layer with special microcapsules with a self-repairing action, and the top layer. The second one, the reference system, is a two-layered coating system without the middle layer. Both surface finishers are white water-soluble pigments. These coating systems were applied on the tangential surface of spruce wood. The samples have dimensions 100 mm × 50 mm × 15 mm (L × T × R). These coated samples were fast aged.

The accelerated aging was simulated in a Xenotest Q-SUN Xe-3-HS (Q-Lab, USA). The aging conditions in the xenon test chamber followed the standard ASTM G 155. The “wet” aging mode simulated wood exposition to both UV and rain (Table 1). The radiation intensity was 0.35 W·m⁻² with a radiation wavelength of 340 nm, following the Standard. This value corresponds to the mean annual value for the temperate zone. The accelerated aging cycle consisted of two steps, covering altogether 120 min. The aging process represented 300 cycles which is 600 hours in total.

Table 1: The aging parameters set according to the Standard [10] „wet mode”

Step	Mode	Radiation intensity (W/m ²)	Black panel temperature (°C)	Air temperature (°C)	Relative air humidity (%)	Time (min.)
1	Radiation	0.35	63	48	30	102
2	Radiation + water spraying	0.35	63	48	90	18

During the accelerated aging process, the color stability and the overall stability of the system were observed. Part of the samples was intentionally damaged with a razor (Fig. 3) to observe a coating sealing effect of the self-repairing layer with microcapsules.

The color space of all samples was measured and expressed in CIE $L^*a^*b^*$ coordinate system before and during the aging process. For that purpose, we used a spectrophotometer Spectro-guide 45/0 gloss (BYK – GARDNER GmbH). The discoloration was expressed as the total color difference ΔE , calculated according to the equation:

$$\Delta E = \sqrt{\Delta L^2 + \Delta a^2 + \Delta b^2} \quad (1)$$

$$\text{Where } \Delta L^* = L_2 - L_1 \quad (2)$$

$$\Delta a^* = a_2 - a_1 \quad (3)$$

$$\Delta b^* = b_2 - b_1 \quad (4)$$

Note: the index “1” denotes the referential value measured on the wood surface before the aging process and the “2” means the color value after wood surface irradiation,

Morphology changes of wood surface finishing after the aging process were expressed by measured roughness and waviness parameters. The roughness was measured by profilometer Surfcom 130A (Carl Zeiss, Germany). The reference length of the profile was assembled from the driveaway length, five characteristics lengths l_r (cutoff λ_c), and the stopway length. Based on preliminary results of parameters R_a and R_z , the basic length was set to 2.5 mm (measuring length 12 mm).

RESULTS AND DISCUSSION

Experiment 1

When applying the coating, we observed harder spreading of the film due to a microcapsule content. Observation of both surface sides of the solid film showed uniformly distributed microcapsules over the entire area of the film. The microcapsule size was between the range of 10 to 50 μm (Fig. 1). The microcapsules were more visible from the teflon side of the film. We assumed that the embedded capsule had a higher density than the coating. Consequently, the microcapsules sunk to the bottom of the coating before the coating cured. The average values of physical properties of the free surface films are in Table 2 and Table 3.

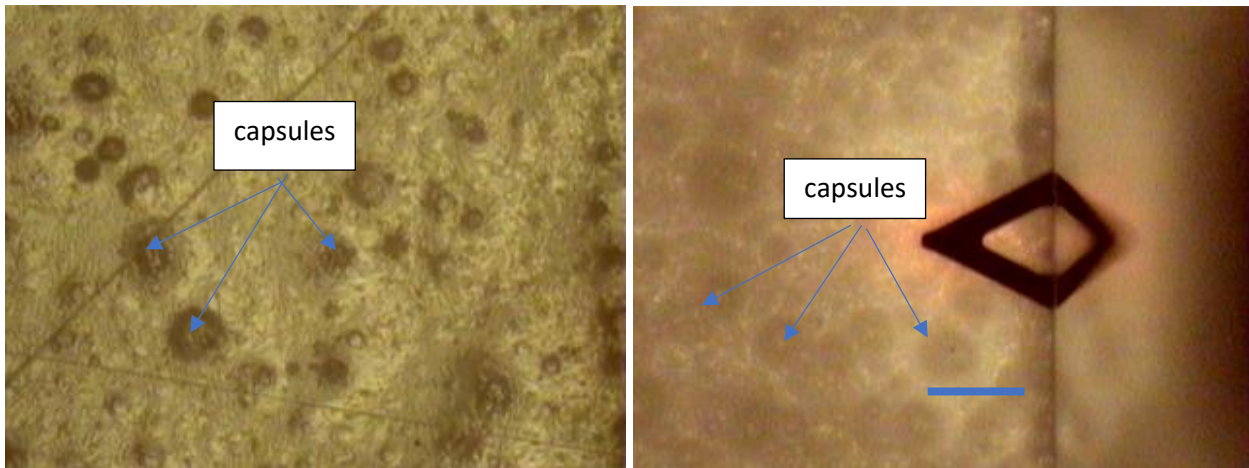


Figure 1: Images from a positioning optical microscope within AFM. The right image is the teflon side, the left image is the upper side. The dark V shape is a cantilever of the AFM tip. A sidebar stands for 100 μm

Table 2: Average surface characteristics of the 10 x 10 μm^2 area of interest

Surface side	Capsule position	Ra, nm	Rq, nm	Fa, nN	Diss, eV
Teflon side	Out of a capsule	26	34.9	3.67	209
	Above a capsule	54.8	70.1	3.34	152
Upper side	Out of a capsule	67.9	88.2	1.10	455
	Above a capsule	58.8	79.3	4.16	158

Table 3: Average surface characteristics of the 1 x 1 μm^2 area of interest

Surface side	Capsule position	Ra, nm	Rq, nm	Fa, nN	Diss, eV
Teflon side	Out of a capsule	11.1	14.2	3.30	163
	Above a capsule	22.4	29.7	2.97	162
Upper side	Out of a capsule	50.3	62.2	3.98	271
	Above a capsule	6.4	9.45	3.50	209

Experimental results confirmed that the lower roughness was observed on the teflon side of the film. This roughness was given by the roughness of the teflon substrate. The roughness depended on the measured position (above a capsule or out of a capsule). In the case of the bottom side of the film (teflon side), the roughness of the film was smaller out of the microcapsule position. Roughness above the microcapsule showed higher parameter values. We assume that the coating above the microcapsule had a different distribution of cohesion forces and different contraction of the coating. This could cause an increase in the roughness due to higher deformations. On the upper side, the coating was stretched above the microcapsule during shrinking and this locally decreased the roughness of the coating. At the same time, the roughness out of the microcapsule increased.

The indentation of the AFM tip to the surface required higher dissipation energy out of the microcapsule location. It was more noticeable on the upper side of the film. Above the capsule, the dissipation energy was lower. This points to the liquid or gel type of uncured capsule filling that is easily deformable.

The adhesion force between the coating and AFM tip was mostly higher out of the capsule position (the anomaly adhesion force was observed in the case of the upper side measured for the area $10 \times 10 \mu\text{m}$). We proposed that a higher concentration of the capsules in the coating or their large diameter compared to the coating thickness could decrease the adhesion between the middle layer and the neighboring layers. Together with lowering of cohesion forces in the coating due to the high concentration of the microcapsules, this could lead to a decrease of overall adhesion between the coating system and wood substrate (Yan and Peng 2021).

Experiment 2

Results of the observed properties during the process of accelerated aging of the surface coated samples with two-layer and three-layer coating systems are summarized in Table 4 and Table 5. The color change of the top layer during accelerated aging was not significantly affected by the coating type.

Practically, the color changes are invisible to the naked eye. The value of the total color difference ΔE did not cross the threshold 1,5 (Fig. 2) which is the boundary for the second level (small change) in the six-scale grade (Allegretti et al. 2009). The color difference of both coating systems was graded to the first level (the invisible change) according to the six-scale grade. The surface finishing of the spruce wood was very good color stable, and the color changes depended mostly on the color stability of the top layer.

Roughness results (Table 5) showed that significant changes were not observed in any coating system after aging. On contrary, the waviness W_a was higher after the aging than before the aging process. The higher waviness was observed in the 3-layer coating system.

No defects in coating finishing (cracks, breaks) were shown after the aging process. Therefore, the effectivity of the tested middle layer could not be confirmed. By observing the intentionally created cracks with a razor (Fig. 3), we validated that the coating system with a self-repairing middle layer was more stable in creating no additional cracks. We ascribed this result to the viscoelastic properties of the middle layer, as well as the fact that microcapsules partially filled the artificial crack in the coating and protected water transport into the substrate. Cracks close to the artificial crack were observed in the 2-layer coating system (Fig. 3).

Table 4: The basic statistic of the characteristic color coordinates L^* , a^* , and b^* in different stages of the aging

Coating system	Color characteristics	Average \bar{x} , standard deviation s	Aging time [hours]						
			0	100	200	300	400	500	600
3-layer	L^*	\bar{x}	97.46	96.56	96.59	96.42	96.42	96.26	96.11
		s	0.17	0.17	0.21	0.14	0.14	0.16	0.21
	a^*	\bar{x}	-0.68	-0.74	-0.71	-0.74	-0.77	-0.80	-0.82
		s	0.02	0.04	0.04	0.04	0.03	0.04	0.04
	b^*	\bar{x}	1.76	2.17	2.08	2.13	2.13	2.24	2.30
		s	0.06	0.09	0.10	0.11	0.09	0.11	0.11
2-layer	L^*	\bar{x}	96.67	96.08	96.14	95.96	95.89	95.81	95.70
		s	0.34	0.23	0.26	0.24	0.14	0.19	0.17
	a^*	\bar{x}	-0.52	-0.67	-0.67	-0.73	-0.75	-0.75	-0.77
		s	0.08	0.07	0.08	0.07	0.06	0.20	0.08
	b^*	\bar{x}	1.35	1.83	1.78	1.81	1.83	1.79	1.81
		s	0.13	0.17	0.17	0.20	0.14	0.20	0.17

Table 5: The basic statistic of the surface characteristic parameters before and after testing of coating systems

Coating system	Average \bar{x} , standard deviation, s	Roughness and waviness parameters [μm]							
		before aging				after 600 hours of aging			
		R_a	R_z	R_{Sm}	W_a	R_a	R_z	R_{Sm}	W_a
3-layer	\bar{x}	1.08	6.82	266.78	1.47	0.93	6.04	251.45	3.01
	s	0.46	6.11	129.62	0.32	0.33	4.04	137.59	1.95
	n	120	120	120	24	120	120	120	24
2-layer	\bar{x}	0.92	5.97	246.23	1.55	1.05	6.99	250.04	2.39
	s	0.29	3.10	134.79	0.83	0.36	4.15	124.93	1.64
	n	120	120	120	24	120	120	120	24

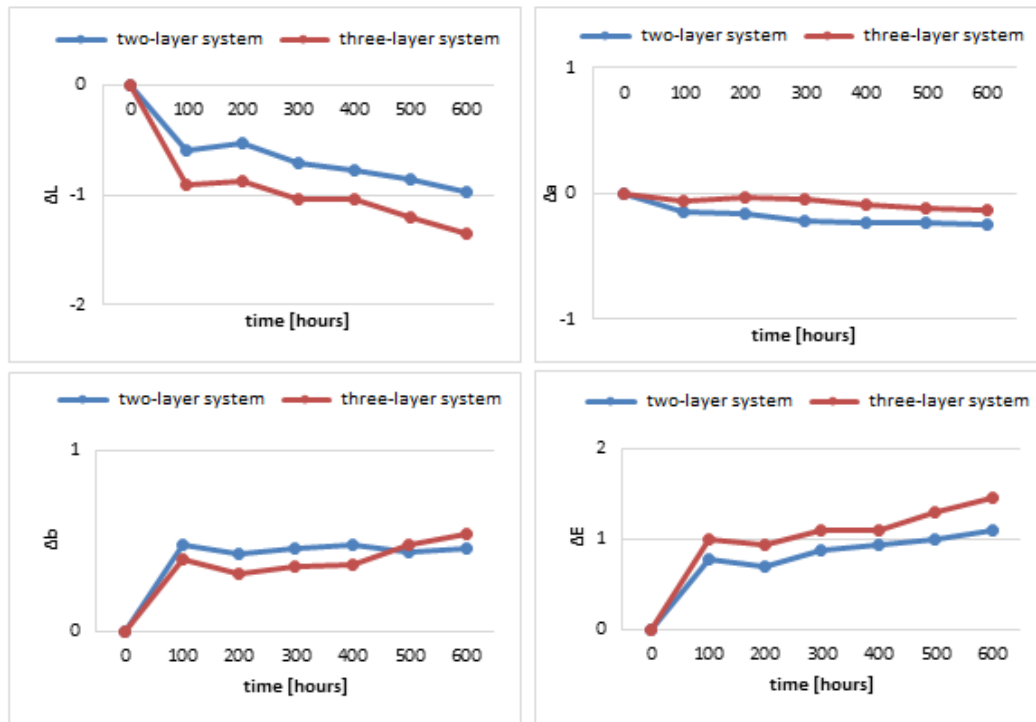


Figure 2: A change in the color coordinates L^* , a^* and b^* and the total color difference ΔE

Study of Slabejová et al. (2020) tested the durability of the same coating systems after natural aging. Authors claimed that the coating system with the middle layer after 1 year of natural aging showed good mechanical properties (hardness, flexibility, abrasion resistance). Insignificant changes in adherence were found between these two systems. In both cases, 2-layer or 3-layer system, respectively, the coatings broke at the interface between wood and the coating. The important fact is that the failure did not occur in an inner coating layer.

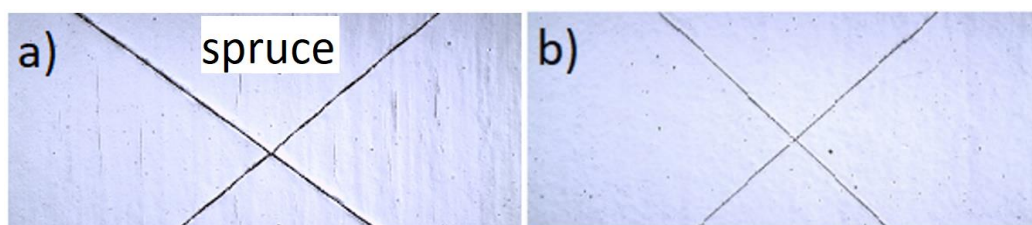


Figure 3: The surface of samples after a 600-hour artificial aging in Xenotest (an exterior schedule with the rain simulation), a) 2-layer coating system, b) 3-layer coating system

CONCLUSIONS

A study of properties of free films that contain special microcapsules with the self-repairing action and a study of coating stability in the process of artificial aging led us to the following conclusions.

The observation of the surface properties of the free film in the locations of microcapsules as well as at the locations out of capsules showed the biggest differences in the roughness and an ability to absorb mechanical energy (dissipation energy). Both properties showed lower values above a microcapsule. Low dissipation energy explained the liquid (gel) state of microcapsule fillings. At the position of the microcapsules, the adhesion force between coating and AFM tip was lower and this could affect the overall adhesion.

The observation of the surface properties of coated spruce wood with the system containing the middle self-repairing microcapsule layer showed that the coating system after 600 hours of accelerated aging was kept in very good color stability and overall structural stability. The middle layer did not affect the color change after aging. The color changes were depended mostly on the color stability of the top layer. Visco-elastic properties of the middle layer and a microcapsule ability to partially fill artificial defects shielded water transfer into the substrate. The 3-layer coating system was more flexible and stable than the system without the special capsulated middle layer.

ACKNOWLEDGMENTS

This work was supported by the Slovak Research and Development Agency under contract No. APVV-16-0177.

REFERENCES

- Allegretti, O., Travan, L., Cividini, R. (2009) Drying techniques to obtain white Beech. In: Wood EDG Conference, 23rd April 2009, Bled, Slovenia. <http://timberdry.net>
- ASTM G155 (2005) Standard Practice for Operating Xenon Arc Light Exposure of Non-Metallic Materials.
- Garcia, A., Schlangen, E., Van de Ven, M. (2009). Two Ways of Closing Cracks on Asphalt Concrete Pavements: Microcapsules and Induction Heating. *Key Engineering Materials*, 417–418, 573–576.
- Giannaros, P., Kanellopoulos, A., Al-Tabbaa, A. (2016). Sealing of cracks in cement using microencapsulated sodium silicate. *Smart Mater. Struct.*, **25**, 084005 (12pp).

- Moll, J. L., White, S. R., & Sottos, N. R. (2010). A Self-sealing Fiber-reinforced Composite. *Journal of Composite Materials*, **44**(22), 2573–2585.
- Rule, J.D., Brown, E.N., Sottos, N.R., White, S.R., Moore, J.S. (2005). Wax-protected catalyst microspheres for efficient self-healing materials. *Adv. Mater*, **17**, 205-208.
- Slabejová, G., Šmidriaková, M., Svocák, J. (2020) Interlayer with microcapsules and its influence on the surface finish quality. *Acta Facultatis Xylologiae Zvolen*, **62**(2), 61-74.
- Tan, X., Zhang, J., Guo, D., Sun, G., Zhou, Y., Zhang, W., Guan, Y. (2020). Preparation, characterization and repeated repair ability evaluation of asphalt-based crack sealant containing microencapsulated epoxy resin and curing agent. *Construction and Building Materials*, **256**, 119433.
- Yan X, Peng W. (2021). Effect of Microcapsules of a Waterborne Core Material on the Properties of a Waterborne Primer Coating on a Wooden Surface. *Coatings*, **11**(6), 657.
- Yuan, L., Liang, G., Xie, J.Q., Li, L., Guo, J. (2006). Preparation and characterization of poly(urea-formaldehyde) microcapsules filled with epoxy resins. *Polymer*, **47**, 5338-5349.
- Yuan, Y.C., Rong, M.Z., Zhang, M.Q. (2008). Preparation and characterization of microencapsulated polythiol. *Polymer*, **49**, 2531-2541.
- Zhao, J., Zhang, W., Liao, L., Wang, S., Li, W. (2012) Self-healing coatings containing microcapsule. *Applied Surface Science*, **258**(6), 1915-1918.

Oriented investigations on the application of NIR spectroscopy for the evaluation of the bonding quality of glued laminated timber from hardwood

Peter Niemz¹, Jakub Sandak², Juana Mai³, Andreas Hänsel³

¹ Berner Fachhochschule, Solothurnstrasse 102, CH 2500 Biel 6 and Umeå University Campus Skellefteå, 931 87 Skellefteå, Sweden, niemzp@retired.ethz.ch

² InnoRenew CoE, Livade 6, 6310 Izola, Slovenia and University of Primorska

³ Berufsakademie Sachsen, Staatliche Studienakademie Hans-Grundig Strasse13, D-01067 Dresden

Keywords: wood gluing, ash wood, delamination, NIR spectroscopy, Micro-NIR, hyperspectral imaging, quality control

ABSTRACT

The method is intended for the predetermination of the bonding properties (delamination according to EN 302-2) and is to be used step by step for quality control of the bonding under industrial conditions. The method can be used to test wood moisture, surface properties, density, grain angle and other important factors of the wood (e.g. extracts) that affect the delamination resistance. The surface property parameters determined by NIR sensors are correlated with the results of the delamination test using multivariate statistics. The aim is to optimize the pressing times and to gradually take into account fluctuations in wood quality and also ambient climate (air humidity, temperature) when controlling the press. Tests were carried out in an industrial plant (gluing of ash wood) and in the laboratory (under variation of wood moisture, density, condition of the cutting edges (sharp and dull), comparison of sanding and planing. Fig. 1 show an example.

The method is intended for the predetermination of the bonding properties (delamination according to EN 302-2) and is to be used step by step for quality control of the bonding under industrial conditions. The method can be used to test wood moisture, surface properties, density, grain angle and other important factors of the wood (e.g. extracts) that affect the delamination resistance. The surface property parameters determined by NIR sensors are correlated with the results of the delamination test using multivariate statistics. The aim is to optimize the pressing times and to gradually take into account variations in wood quality and also ambient climate (air humidity, temperature) when controlling the press. Tests were carried out in an industrial plant (gluing of ash wood) and in the laboratory (under variation of wood moisture, density, condition of the cutting edges (sharp and dull), comparison of sanding and planing.

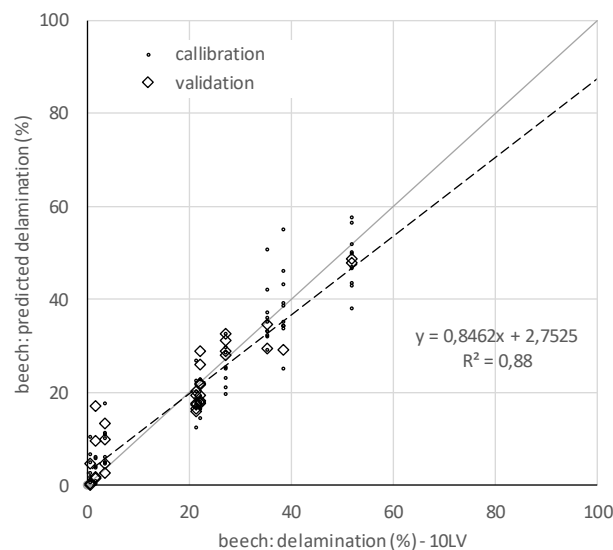


Figure 1: Correlation between experimental tested (EN 302-2) and estimated with NIR for ash wood

Develop an app to quickly identify popular timber species traded in Hanoi, Vietnam

Le Xuan Phuong¹, Vu Manh Tuong², Nguyen Thi Loan³, Dong Thanh Hai⁴, Le Minh Tuyen⁵

¹ Xuanmai town, Hanoi, Vietnam, Vietnam National University of Forestry, phuonglx@vnuf.edu.vn

² Trang Bom, Dong Nai, Vietnam, Vietnam National University of Forestry, tuongvm@vnuf.edu.vn

³ Xuanmai town, Hanoi, Vietnam, Vietnam National University of Forestry, loannt@vnuf.edu.vn

⁴ Xuanmai town, Hanoi, Vietnam, Vietnam National University of Forestry, haidt@vnuf.edu.vn

⁵ Ba La, Hanoi, Vietnam, Hanoi Forest Protection Department, leminhtuyen_sonnptnt@hanoi.gov.vn

Keywords: A.I., wood anatomy, wood identification, imported hardwood, native species, smartphone, Vietnam

ABSTRACT

Vietnam is a leading wooden product exporting country with its fast annual growth rate of 12-15% over the past ten years. The export turnover of Vietnamese wooden products in 2020 exceeds 12 billion USD, the biggest in South East Asia. Hanoi is the capital of Vietnam and the second-largest city that significantly contribute to the development of the wood industry in Vietnam. Therefore, there are many timber species traded and processed in Hanoi including native species and imported ones from around the globe. This study investigates the possibility of applying A.I. (Artificial Intelligent) to quickly identify popular timber species traded in Hanoi using a smartphone. 50 popular timber species were selected for this study. A collection of 1500 color photos per species were prepared by firstly cross-cut the air-dried timber specimen by knife, then taken a photo using a smartphone camera (iPhone 4 above) with aid of a macro lens (x15) to obtain an image (dimensions 1920x2560). Then 1,200 photos will be trained by machine learning and the remain 300 photos will be used for testing the model. Fundamental steps of supervised machine learning for image-based species identification (Waldchen et. al. 2018) using deep learning convolutional neural networks (CNNs). The selected model can real-time detect the image and species identification decided with an accuracy rate above 80%. A database of useful information of the timber is also integrated into the app such as Name, Classifications, Anatomical characteristics, Distribution, Properties, Usages, Threats.

INTRODUCTION

Vietnam is a leading wooden product exporting country in South East Asia with its export turnover in 2020 exceed 12 billion USD and import about 2.5 billion USD of timber materials (Phuc et. al. 2021). To sustainably develop this wood industry, one of the main tasks is to control illegal logging to fulfill the requirements of its important markets such as the EU (FLEGT) or the US (Lacey Act), or Japan (Clean wood act). The most common way of identifying wood species is by microscopic observation (Abe 2016). The nature of this identification is based on wood anatomical features observation and comparing these features with known species from a recognized database (IAWS 1989, IAWS 2004, Tinh 1998). This time-consuming work requires skillful wood anatomists of preparing good anatomical images and experience in observing the features. Some recent reviews on automated plant species identification (Wäldchen and Mäder 2017, Waldchen et. al. 2018) or wood identification (Khalid et. al. 2008, Abe 2016, Hwang and Sugiyama 2021) suggests the important role of using A.I. (Artificial Intelligent). Thanks to the new image recognition technology, now we have specialized software and applications that can decipher visual information. In this study, we want to try to use TensorFlow, an end-to-end open-source platform for machine learning to quickly identify 50 popular timber species traded in Hanoi using a smartphone. This tool is hoped to help Hanoi forest rangers to quickly identify timber species in the inspection and effective supervision of timber traded in Hanoi city as regulated in Circular 27, 2018, ensuring the use of legal timber and has a clear origin.

EXPERIMENTAL METHODS

Wood samples

The group of the 50 most common wood species (Table 1) was selected based on the actual survey results at the wood processing and trading enterprises in Hanoi in 2019.

Table 1: List of 50 timber species popularly traded in Hanoi in the database

No.	Vietnamese timber name	Commercial name	Scientific name
1	Anh đào	Cherry	<i>Prunus avium</i>
2	Bạch đàn nhập khẩu	Rose gum	<i>Eucalyptus grandis</i>
3	Bồ đề		<i>Styrax tonkinensis</i>
4	Cẩm lai		<i>Dalbergia oliveri</i>
5	Cắm xe		<i>Xylia xylocarpa</i>
6	Cao su	Rubber wood	<i>Hevea brasiliensis</i>
7	Chiêu liêu		<i>Terminalia chebula</i>
8	Chò chỉ		<i>Parashorea chinensis</i>
9	Curupau	Curupau	<i>Anadenanthera colubrina</i>
10	Dáng hương		<i>Pterocarpus macrocarpus</i>
11	Dáng hương châu Phi - Padouk	Padouk	<i>Pterocarpus soyauxii</i>
12	Dương - Poplar	Poplar	<i>Populus alba</i>
13	Dẻ gai	Beech	<i>Fagus sylvatica</i>
14	Đinh hương		<i>Dysoxylum cauliflorum</i>
15	Đinh thối		<i>Fernandoa brilletii</i>
16	Giổi lưa		<i>Magnolia odora</i>
17	Gỗ đỏ châu Phi - Doussie	Doussie	<i>Afzelia africana</i>
18	Gụ lau		<i>Sindora tonkinensis</i>
19	Iroko	Iroko	<i>Milicia excelsa</i>
20	Jatoba	Jatoba	<i>Hymenaea courbaril</i>
21	Keo lai	Acacia hybrid	<i>A. mangium x A. auriculiformis</i>
22	Lát hoa		<i>Chukrasia tabularis</i>
23	Lim nhập khẩu - Tali	Tali	<i>Erythrophleum ivorense</i>
24	Lim xanh		<i>Erythrophleum fordii</i>
25	Mít mật		<i>Artocarpus heterophyllus</i>
26	Mỡ		<i>Magnolia conifera</i>
27	Mun sọc		<i>Diospyros salletii</i>
28	Muồng đen		<i>Senna siamea</i>
29	Nghiến		<i>Burretiodendron hsienmu</i>
30	Óc chó - Walnut	Walnut	<i>Juglans regia</i>
31	Phong vàng	Yellow birch	<i>Betula alleghaniensis</i>
32	Quế		<i>Cinnamomum cassia</i>
33	Robinia	Black locust	<i>Robinia pseudoacacia</i>
34	Sapelli	Sapelli	<i>Entandrophragma cylindricum</i>
35	Sến mật		<i>Madhuca pasquieri</i>
36	Sồi đỏ	Red oak	<i>Quercus rubra</i>
37	Sồi trắng	White oak	<i>Quercus alba</i>
38	Sưa		<i>Dalbergia tonkinensis</i>
39	Tần bì	Ash	<i>Fraxinus excelsior</i>
40	Táu mật		<i>Vatica odorata</i>
41	Tếch	Teak	<i>Tectona grandis</i>
42	Trắc		<i>Dalbergia cochinchinensis</i>
43	Trái lý		<i>Garcinia fagraeoides</i>
44	Trám hồng		<i>Canarium bengalense</i>
45	Xà cừ		<i>Khaya senegalensis</i>
46	Xoan đào		<i>Prunus arborea</i>
47	Xoan ta		<i>Melia azedarach</i>
48	Xoay		<i>Dialium cochinchinense</i>
49	Pơ mu	Fokienia (Fujian cypress)	<i>Fokienia hodginsii</i>
50	Thông đuôi ngựa	Masson's pine	<i>Pinus massoniana</i>

All wooden samples (30 samples for each species of the size of at least: 15 (R) x 100 (T) x 150 (L) mm) collected from the survey were air-dried at a conditioned room of 20 °C and 65% RH to reach a moisture content of 12%.

Before taking a photo, all samples were checked the species using its anatomical features by our experts. The cross-section (both ends of the sample) was carefully cut using a paper-cutting knife (Fig. 1).

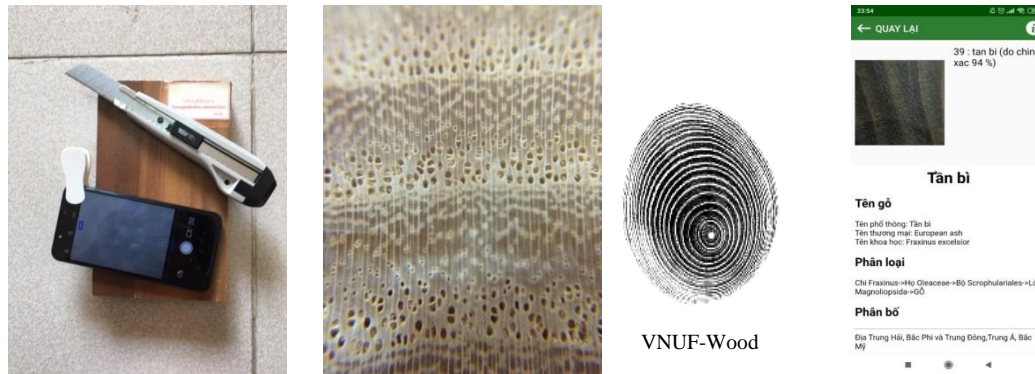


Figure 1: Tool, image obtained by a smartphone camera, app icon, and the result appearance

Image preparation

With the aid of a macro lens (15 times magnify) attached to the smartphone camera (iPhone 4 or above – Fig. 1), a collection of about 1,500 good images (dimensions 1920x2560) of each species were taken from the cross-section of the samples (both ends). Then 1,200 randomly selected photos (dataset) will be trained by machine learning and the remain 300 photos will be used for testing the model.

Database of the 50 selected wood species

Information on wood species includes wood image, names (common, commercial, and scientific names), classification, distribution, anatomical characteristics, properties, use, density, and conservation status. Specifically:

- Anatomical characteristics: includes brief information about the macro anatomical characteristics of the species, including sapwood/heartwood; annual ring; wood vessels distribution and aggregation; parenchyma cell distribution and aggregation; wood rays; resin canals; the color on the cross-section of wood (cut by paper-knife).
- Properties: information about density, radial shrinkage, tangent shrinkage, static bending strength, static bending elastic modulus, the longitudinal compressive strength of each species will be given in this section.
- Uses: main applications of these woods
- Conservation status: Conservation status based on IUCN Red List of threatened species (IUCN, 2017), Vietnam Red Data Book (2007), Convention on International trade in Endangered Species of Wild Fauna and Flora - CITES (2019), Decree 06/2019/ CP of the Vietnamese Government.

The last part is a list of references that includes all the documents cited by the research team.

The database is built on the web interface to facilitate the update of new data as well as search by information fields such as name and the density of the wood. The information in the database is designed to be user-friendly, concise, and easy to use for users, allowing quick and unmistakable access.

App development

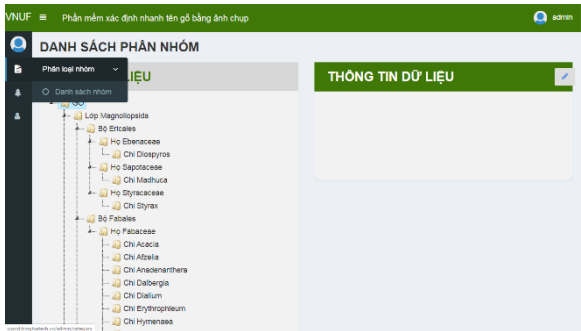
The 1,200 selected images were firstly resized to 224 x 224 images then trained. Fundamental steps of supervised machine learning for image-based species identification (Waldchen et. al. 2018) using deep learning convolutional neural networks (CNNs) are as follows: (1) Extract features; (2) Select the training model; (3) Training and assess the model; (4) Export the result; (5) Data sync (Database information on the server) with mobile devices (smartphone); (6) Identifying.

There are 2 options of inputting data (image) for identifying the species using the app: image from the field taken by forest ranger or using real-time images captured by the smartphone with the aid of macro-lens. In any case, the requirement for deciding the species is that the accuracy must be higher than 80%. For the real-time assessment: the species decision is made after the 3 consecutively identifying the same species with an accuracy is 80% or higher. This approach produces a faster result with higher confidence than a single image.

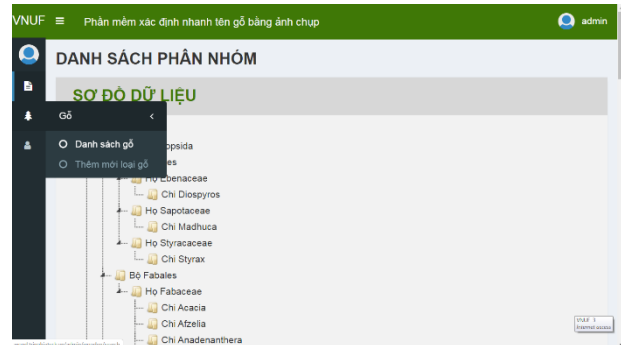
RESULTS AND DISCUSSION

Database of the 50 selected wood species

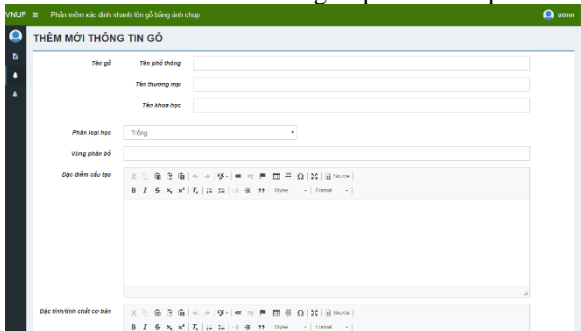
The database on the selected 50 species was prepared on a web platform to assist the searching task and manage the database easily. This also helps to update/ edit the information on wood species and add more species easily and the updating process of the app on the smartphone is easy too.



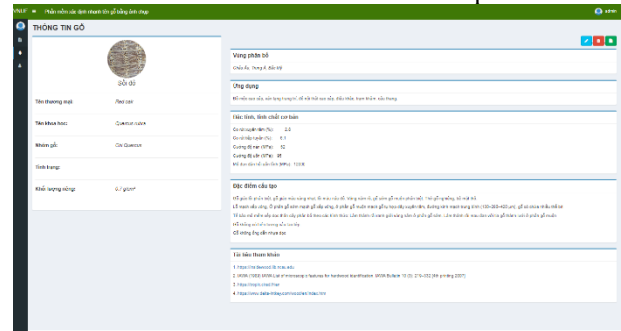
Module of insert/ edit the group of wood species



Module of insert/ edit each wood species



Information format of each wood specie



The appearance of Red oak species description

Figure 2: Database of 50 wood species on the web

The app “VNUF-Wood”

The app is built on apk file for a smartphone. The database of the 50 species is automatically updated when first installing the app. Both versions for Android and IOs are developed to fit with popular smartphones. There are several versions of the app of different accuracy levels that have been tested. The lower the accuracy level we use for the training model; the faster the recognition result could be obtained but more mistakes among similar species (with similar features) or take longer time to detect for the species with less significant features (difficult to detect). Therefore, after several trials, we decided to use an accuracy level of 80% or higher for this app. For some species with clear unique features such as ash, Robina, red oak, iroko..., the app can easier/ faster detect the species. A similar approach developed by experts from Forest products lab, USDA (Ravindran et. al. 2020) named XyloTron to use a good and clear image obtained from a special tool require more work to prepare the wood surface. In our case, we use a normal knife cutter with free direction (not proper (Radial-Tangential) direction of each image with the larger area) and the wood identification task can be done by an unskilful person (just a little train). With the dataset of 50 species, this app works quite well and uses an only popular smartphone regardless of the chip limit on data processing capacity.

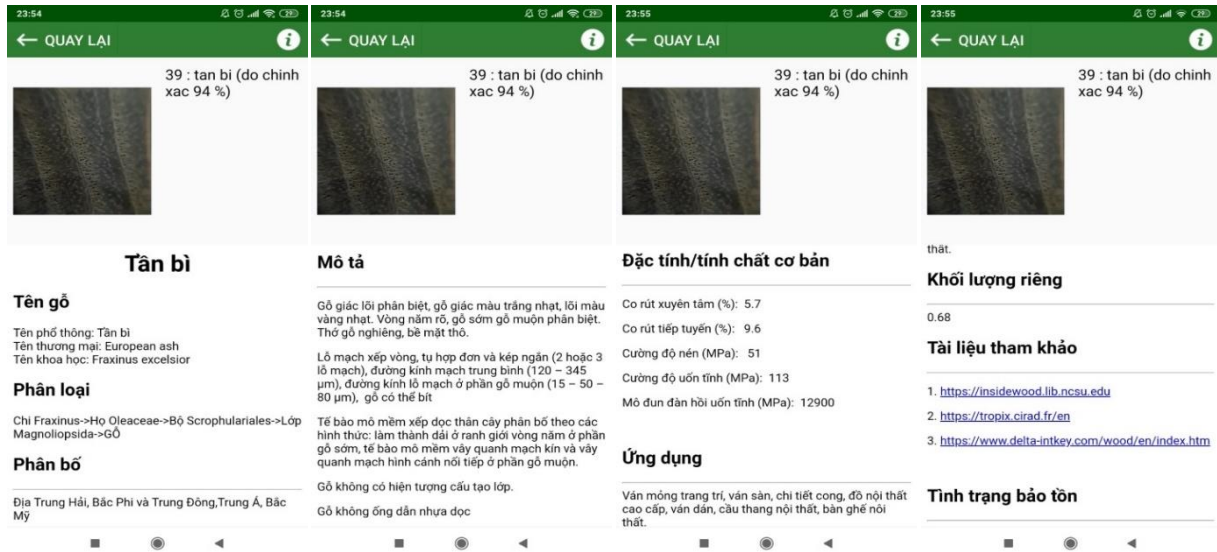


Figure 3 : Software interface for rapid identification of Ash on a smartphone

CONCLUSIONS

VNUF-Wood is an application (app) that can rapidly and accurately identify 50 common wood species popularly traded in Hanoi. With simple manipulation and tools, forest rangers can fully identify the 50 species mentioned above objectively and provide on-time solutions when handling administrative violations. This is an effective tool to support forest rangers as well as other forest products management forces in controlling and preventing the illegal trade and transportation of wood species, contributing to law enforcement, laws and compliance with international commitments that Vietnam has signed such as VPA / FLEGT when Vietnam's wood products entered the EU market or Lacey Act when entering the US market.

ACKNOWLEDGEMENT

The financial support from the Hanoi forest ranger department is gratefully acknowledged.

REFERENCES

- Circular 27 (2018) by MARD on management and tracing of forest products.
- Decree 06 (2019) by the government of Vietnam on the management of endangered, rare, and precious species of forest fauna and flora and observation of the Convention on International Trade in Endangered Species of Wild Fauna and Flora.
- Sung-Wook Hwang and Junji Sugiyama (2021) Computer vision-based wood identification and its expansion and contribution potentials in wood science: A review. *Plant Methods*, **17**, 47.
- IAWA (1989) IAWA list of microscopic features for hardwood identification. *IAWA Journal*, **10**, 219-332.
- IAWA (2004) IAWA list of microscopic features for softwood identification. *IAWA Journal*, **25**, 1-70.
- IUCN (2017) IUCN Red List of Threatened Species (Version 3, May 2017). www.iucnredlist.org.
- Khalid, M. et. al. (2008) Design of intelligent wood species recognition system. *USSST*, **9**(3), 9-19.

To Xuan Phuc et. al. (2021) [Vietnamese import-export of wood and wooden products. Situation in 2020 and Trends in 2021](#)

Ravindran P et. al. (2020) The XyloTron: Flexible, OpenSource, Image-Based Macroscopic Field Identification of Wood Products. *Frontiers in Plant Science*, **11**, 1015.

Le Xuan Tinh (1998) *Wood Science*. Agriculture Publishing House, Hanoi, Vietnam.

Waldchen, J. et. al. (2018) Automated plant species identification - Trends and future directions. *PLoS Computational Biology*, **14**(4), e1005993.

UNEP-WCMC (2019) Checklist of CITES species. <http://checklist.cites.org/#/en>.

Jane Wäldchen and Patrick Mäder (2017) Plant Species Identification Using Computer Vision Techniques: A Systematic Literature Review. *Archives of Computational Methods in Engineering*, **25**(2), 507–543.

Substitution of softwood by hardwood species in the MDF process

Pinkl Stephan¹, Bugelnig N², Drexler F², Fitzthum R², Führer J², Höchtl S², Kolbitsch L²,
Loike C², Malzl L², Meixner R², Pilz N², Rudolf K², Schnepps J², Vasovic D²,
Vennemann J², Yang Y², Gindl-Altmutter W², Konnerth J², Martin Riegler¹

¹ Wood K plus - Competence Center for Wood Composites & Wood Chemistry, Kompetenzzentrum Holz GmbH, Linz, Austria, s.pinkl@wood-kplus.at

² University of Natural Resources and Life Sciences, Vienna, Austria

Keywords: MDF, hardwood, wood fibres

ABSTRACT

In Austria, softwoods (spruce and pine) are primarily used for the production of fibreboards. In the course of forest alteration, deciduous tree species will become more important for industrial producers in the future. Therefore, three hardwood species (*Populus sp. L.*, *Fagus sylvatica L.*, *Tilia sp. L.*) and the Austrian main tree species *Picea abies (L.) H. KARST* were investigated for the production of medium density fibreboards (MDF). The laboratory tests include thermomechanical defibration, MDF production and characterization of fibres and boards. The morphological examination was carried out with an automated fiber analyzer (MorFi) and a manual fibre scan. Furthermore, thickness swelling, internal bond strength and bending properties were determined. Despite the constant thermomechanical pulping conditions, different fibre morphologies and effects on the bond quality were observed, which allow conclusions about different mechanical board properties.

Electric guitar neck from densified poplar? Experimental and numerical analysis

Sebera Václav^{1,3}, Mikuljan Marica¹, Niemelä J. Aarne¹, Prislan Rok¹, Mrissa Michael^{1,2},
Kutnar Andreja^{1,2}, Pečnik G. Jaka^{1,2}

¹ InnoRenew CoE, Livade 6, 6310 Izola, Slovenia, vaclav.sebera@innorenew.eu

² University of Primorska, Titov trg 4, 6000 Koper, Slovenia

³ Mendel University in Brno, Zemědělská 3, Brno, Czech Republic

Keywords: densified poplar, orthotropic material model, finite element analysis, electric guitar, acoustics

ABSTRACT

Electric guitar necks (EGNs) and parts are usually made of hardwoods (i.e., maple, ash, etc.), including protected exotic species coming from overseas (mahogany, etc.), due to their aesthetics, high stiffness and density. Additionally, EGNs typically include a truss rod – a metal bar stiffening the neck against bending caused by string tension. In order to reduce the environmental impact of guitar production, we believe that EGNs can be made from local and fast grown plantation wood modified using a thermo-hydro-mechanical (THM) process. In this paper, we analyze the potential of using THM densified poplar wood as a substitute material for EGN. We believe our approach for EGN production may be (i) more convenient due to higher mechanical properties of densified wood while preserving similar vibrational performance; (ii) more economical due to local and cheap resources use and absence of a truss rod; (iii) more environmentally friendly due to reduced logistics and energy costs. To analyze the hypothesis resulting from (i), we performed both experimental tests and numerical analyses. Experiments consisted of poplar wood densification (dens. ratio 2) to obtain the elastic orthotropic material model of densified poplar suitable for finite element analyses (FEA). We carried out compression tests accompanied with digital image correlation which provided a set of elastic material coefficients – 3x normal elastic moduli (E_L , E_R , E_T), 3x Poisson's ratios (μ_{LR} , μ_{RT} , μ_{LT}); 3x shear elastic moduli (G_{LR} , G_{RT} , G_{LT}) were calculated from measured values. Developed material models were employed in FEA of (i) guitar neck deflection induced by string tension and (ii) modal analysis of a neck including sensitivity study for the role of density and elastic moduli on eigenfrequencies. FEA showed the highest 1st principal stress (PS1) is located on the bottom of the neck. Further, PS1 changes with change of E_L – deflection decreased 40 % and PS1 increased ~ 11 % as E_L increased from 12.4 GPa to 22 GPa. Eigenfrequencies decrease with density but increase as E_L increases (1st freq 17.4 %, 2nd freq. 21.4 % and 3rd about 27 %).

INTRODUCTION

A broad range of wood types are used in the production of musical instruments. In case of many instruments, such as strings or guitars, the selection of wood has been defined through centuries of craftsmanship leading to the evolution of musical instruments as we know today. Depending on the part of the instruments, very diverse mechanical and dynamical properties are favored for the wood used. A large amount of research has been devoted to the understanding of the relation between the wood properties and the performance of the instrument in sense of structural requirements, playability and acoustic character.

Parts like guitar fretboard or violin pegs are built from very durable woods, such as ebony or rosewood. Those wood species are endangered meaning that suitable alternatives with similar mechanical properties are needed. Furthermore, in many instrument components the wooden part must be reinforced by other materials to achieve the desired strength. An example of this is the truss rod in the electric guitar's neck which is required to sustain the high torque produced by the strings. Could the truss rod be avoided if the neck would be built from densified wood with a higher MOE?

The mentioned cases are just some examples where modified wood could be a suitable alternative or building improvement for producing musical instruments. Our hypothesis is, that many more exist. Some pioneering work and research have been already performed to support this idea, but the full potential of using modified wood in musical instruments still has to be studied to a greater extent.

MATERIALS AND METHODS

Our work aimed on a comparison of native and densified poplar wood (*Populus* Sp.) originated from poplar plantation in Serbia. The comparison was based on mechanical properties of both materials and their performance in numerical modal analysis of EGN. The work consisted of the following steps: (i) densification; (ii) compressive tests coupled with visual data acquisition; (iii) experimental data evaluation and (iv) numerical static structural and modal analysis of EGN with use of experimental data.

Densification

Densification was carried out at the hot press (Langzauner LZT-UK-30-L) with heated plates. The sawn timber (Fig. 1 left) of 60 mm thickness was planned to final 53 mm. The planned boards were densified to a thickness of 27 mm, which give a general densification ratio (ρ ratio) about 2 (Fig. 1 right). The densification process was conducted under the following steps: wood specimens were put in the press at room temperature. Heating plates were heated to 60°C with 5°C/min heating rate and held pressed for 10 minutes. After that, heating was increased to 170 °C with a 5°C/min heating rate with addition of 300 kN force for 3 minutes. This step was followed by increasing the temperature to 200 °C with 20 °C/min heating rate for 2 additional minutes. The process was completed by cooling the press to 40°C, holding the temperature for 30 minutes and releasing the press.

The densification process on thick boards caused different density profiles, where middle parts got densified more than boundaries. The specimens for testing were cut out from the boards, so the parts with the highest density were used. This explains why the ρ ratio in the Table 1 is higher than 2.



Figure 1: Poplar wood in raw material (left) and in boards before and after densification (right)

Compression testing

Compression tests were performed using the Universal Testing Machine – UTM (Zwick Roell Z100, Zwick Germany) equipped with a 100 kN load cell. Preload was set to 10 N and speed of loading was controlled by a displacement rate of 5 mm/min. Compression specimens were loaded in longitudinal (L), radial (R) and tangential (T) direction and, at the same time, they were filmed using a 1 Mpx camera (Logitech) with a 30 fps acquisition rate synchronized with the UTM. 2D digital image correlation (2D-DIC) implemented in Mercury software (Sobriety Ltd., Czech Republic) was used to track markers on three planes of deformation to obtain active and passive strains and, consequently, three Poisson's ratios (ν_{LR} , ν_{RT} , ν_{TL}) from an elastic range of deformation (see Fig. 2). DIC algorithm assumed full-affine transformation, subset size was set to 35 px with a step of 5.

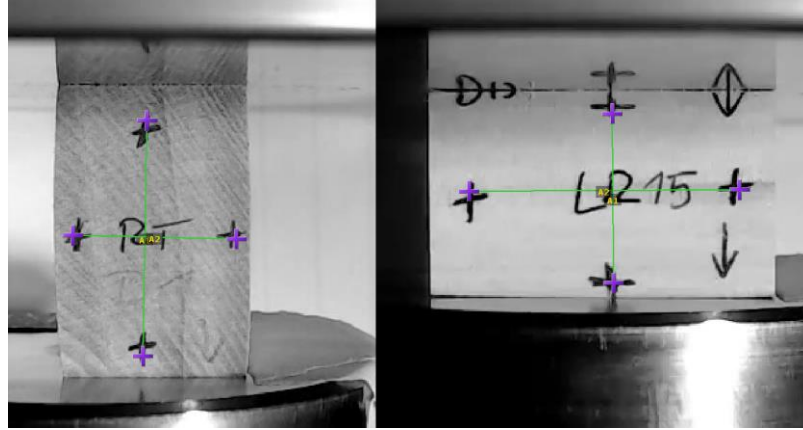


Figure 2: Specimens in compression tests of densified wood in tangential (left) and radial (right) directions with virtual strain gauges for obtaining strains and Poisson's ratios

Other three Poisson's ratios were derived from Hooke's law for orthotropic material, which can be written using Voigt's notation as follows:

$$\begin{matrix} \varepsilon_{LL} \\ \varepsilon_{RR} \\ \varepsilon_{TT} \\ 2\varepsilon_{RT} \\ 2\varepsilon_{TL} \\ 2\varepsilon_{LR} \end{matrix} = \begin{bmatrix} \frac{1}{E_L} & \frac{-\nu_{LR}}{E_R} & \frac{-\nu_{LT}}{E_T} & 0 & 0 & 0 \\ \frac{-\nu_{RL}}{E_L} & \frac{1}{E_R} & \frac{-\nu_{RT}}{E_T} & 0 & 0 & 0 \\ \frac{-\nu_{TL}}{E_L} & \frac{-\nu_{TR}}{E_R} & \frac{1}{E_T} & 0 & 0 & 0 \\ 0 & 0 & 0 & \frac{1}{G_{RT}} & 0 & 0 \\ 0 & 0 & 0 & 0 & \frac{1}{G_{TL}} & 0 \\ 0 & 0 & 0 & 0 & 0 & \frac{1}{G_{LR}} \end{bmatrix} = \begin{bmatrix} \sigma_{LL} \\ \sigma_{RR} \\ \sigma_{TT} \\ \sigma_{RT} \\ \sigma_{TL} \\ \sigma_{LR} \end{bmatrix} \quad (1)$$

where E_i is elastic modulus, G_{ij} is shear modulus, ε_{ij} is strain and ν_{ij} is Poisson's ratio. Indices i and j may be L , R and T that stand for longitudinal, radial and tangential anatomical directions, respectively. Because of the assumed material symmetry in compliance matrix (Eq. 1), we can derive following $\nu_{LR}/E_R = \nu_{RL}/E_L$, $\nu_{LT}/E_T = \nu_{TL}/E_L$, and $\nu_{TR}/E_R = \nu_{RT}/E_T$. These relationships were used to calculate Poisson's ratios complementary to those measured ones and these were used to calculate shear elastic moduli at three shear planes. Shear elastic moduli were calculated using approach given by Saint-Venant (1863), its successful use and analysis was demonstrated on walnut wood in Bachtiar et al. (2017), the calculation is as follows:

$$G_{ij} = \left[\frac{\nu_{ji}+1}{E_i} + \frac{\nu_{ij}+1}{E_j} \right]^{-1} \quad (2)$$

where i, j can be L, R, T , and $i \neq j$.

Finite element model

Geometrical and finite element model of the EGN was obtained from a publicly accessible database (<https://cockrum.net/lutherie.html>) and is depicted in Fig. 3. The numerical model was developed in Ansys 2019 R2 (Ansys Inc., USA). The numerical model considered pretension simulating pulling strings and in total, force equal of 306 N was used and applied on head of neck (red area in Fig. 3) in a direction of a nut where strings are bent. For all computations, a free mesh created by 3D quadratic finite element SOLID186 was used. FE model was used for both static structural evaluating bending of a neck due to strings pulling and modal analysis evaluating eigenfrequencies and modal shapes of EGN in dependence on elastic parameters and density.

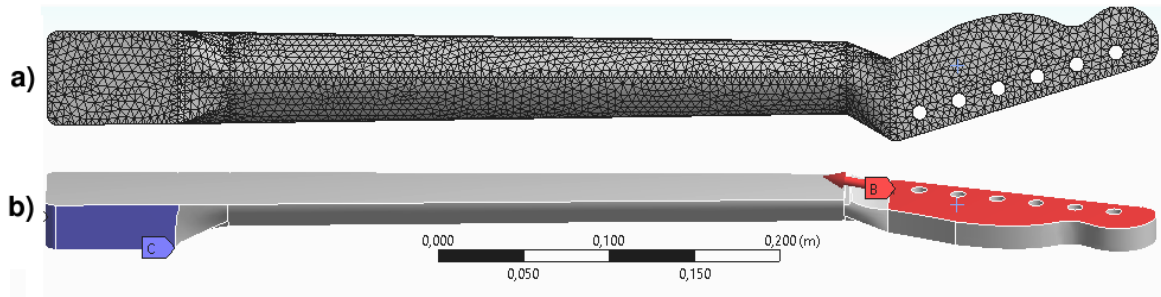


Figure 3: Numerical model of EGN, a) finite element mesh; b) geometrical model with boundary conditions where blue color denotes full constraint, red color denotes pretension simulating pulled strings

RESULTS

Results from the compression testing in a form of stress-strain diagrams for all tested groups are depicted in Fig. 4. By comparing diagrams of groups before and after the modification, it is clear that the densification substantially modified stress-strain response of wood, mostly by increasing strength and elastic modulus, but also by a global character of the stress-strain curve.

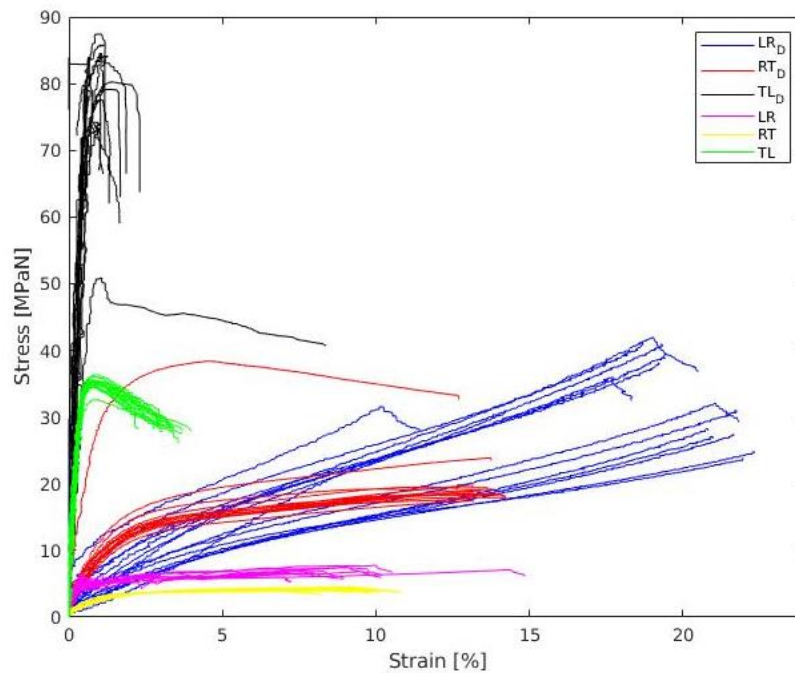


Figure 4: Stress-strain diagrams for native and densified wood (index "D"), the second letter denotes the force direction, strain is obtained from the marker tracking.

The descriptive statistics with removed outliers of obtained stress-strain diagrams is showed in Table 1. It shows that densification ratio (ρ ratio) for all tested specimen ranges between 2.32 and 2.45, but individual mechanical parameters have very different DP/NP ratios, the lowest for Poisson's numbers (0.06-0.28) and the highest for G_{LT} and E_T (3.55-3.6). The ratio of DP/NP with respect to longitudinal strength (σ_L) is very alike to ρ ratio (2.3 vs. 2.45). Elastic moduli in longitudinal and tangential direction increased substantially, except the radial one that decreased 3times. The shear moduli that were calculated using eq. 2 also show interesting change because G_{LR} decreased 66%, but G_{LT} increased 3.55times due to change of normal elastic moduli (E_T and E_R). In general, the presented DP/NP ratios show that the poplar densification has very different impact on its each individual parameter, so the coefficients of anisotropy might be modified too. This could impact a global behavior of wood not only in acoustic applications such as EGN.

Table 1: Descriptive statistics of material data for native (NP) and densified (DP) poplar, * denotes computed values

	E_L [MPa]	E_R [MPa]	E_T [MPa]	G_{LR} [MPa]	G_{LT} [MPa]	G_{RT} [MPa]	ν_{TR} [-]	ν_{TL} [-]	ν_{LR} [-]	σ_L [MPa]
NP mean	6408	1052	147	612*	139*	85*	0.29	0.63	0.18	35.1
CoV	20	43	11				4	41	215	2
n	15	13	15				15	13	11	15
DP mean	12479	278	524	266*	496*	178*	0.048	0.17	0.011	81.4
CoV	11	38	13				6	38	126	5.2
n	13	14	14				9	13	14	13
DP/NP	1.9	0.34	3.6	0.44*	3.55*	2.1*	0.16	0.28	0.06	2.3
ρ ratio	2.45	2.32	2.35	-	-	-	2.35	2.45	2.32	2.45

Finite element model

First, static structural FEA was performed to investigate location of stress allocation due to bending caused by pulled strings. The result of this analysis can be presented as total deformation which expresses bending (Fig. 4a). From legends in Fig. 4 it is clear that EGN made with densified poplar has 1.8x lower deflection due to 1.95x higher longitudinal elastic modulus (E_L) which is the main contributing material parameter in bending problems. The maximal 1st principal stress (PS1), which represents the tensile stress (Fig. 4b and c) is 1.14x higher for densified EGN compared to one from native, and it is also due to higher E_L .

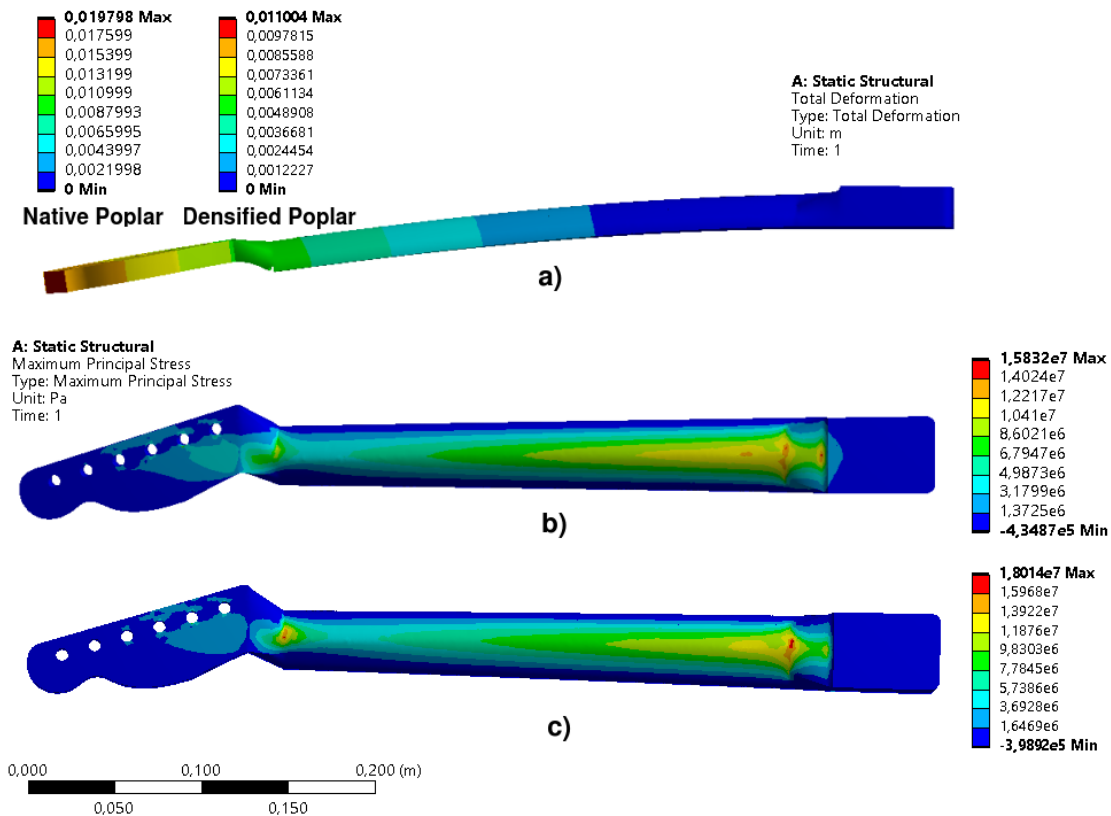


Figure 4: a) Bending of the EGN due to string pretension where NP and DP differs only by legend; b) 1st principal stress of NP and c) 1st principal stress of DP

The result of numerical modal analysis of both variants of EGN is showed in Table 2 that lists first twenty eigenfrequencies including their ratios. It says that densification changed all eigenfrequencies in different manner in a range of 2-18%. Every frequency is influenced by all material properties, but each of them has

a different participation to the obtained frequencies which explains the differences between them. Because the model has simplified geometry by not considering frets, tuning pets and truss rod, the frequencies will not match real guitar. Instead, the analysis aims only on an investigation of EGN behavior when material is changed.

Table 2: Eigenfrequencies of EGN made of native (NP) and densified (DP) poplar and ratios

Mode shape #	1	2	3	4	5	6	7	8	9	10
NP – freq [Hz]	39.7	80.6	163.3	250.2	328.7	516.7	662.9	726.7	919.5	1092.9
DP – freq [Hz]	36.5	76.5	151.2	223.2	335.0	423.5	617.1	766.4	792.4	985.4
DP/NP	0.92	0.95	0.93	0.89	1.02	0.82	0.93	1.05	0.86	0.90
Mode shape #	11	12	13	14	15	16	17	18	19	20
NP – freq [Hz]	1265.1	1416.4	1589.0	1635.6	1868.7	2045.2	2227.7	2330.9	2352.2	2796.7
DP – freq [Hz]	1146.2	1328.0	1403.9	1570.6	1638.4	1787.1	2061.8	2110.1	2142.7	2438.5
DP/NP	0.91	0.94	0.88	0.96	0.88	0.87	0.93	0.91	0.91	0.87

Then, we performed the sensitivity analysis to investigate an effect of increased longitudinal stiffness (E_L) on a deflection and PS1 without changing other material properties. This analysis showed in Fig. 5 left tells that increased E_L causes substantial lowering of deflection and increase of PS1. The impact of density increase on first three eigenfrequencies for two E_L (12 GPa and 20 GPa) is showed in Fig. 5 right. It shows that increase of density lowers eigenfrequencies, meanwhile E_L higher it and the higher the frequency is, the higher the impact.

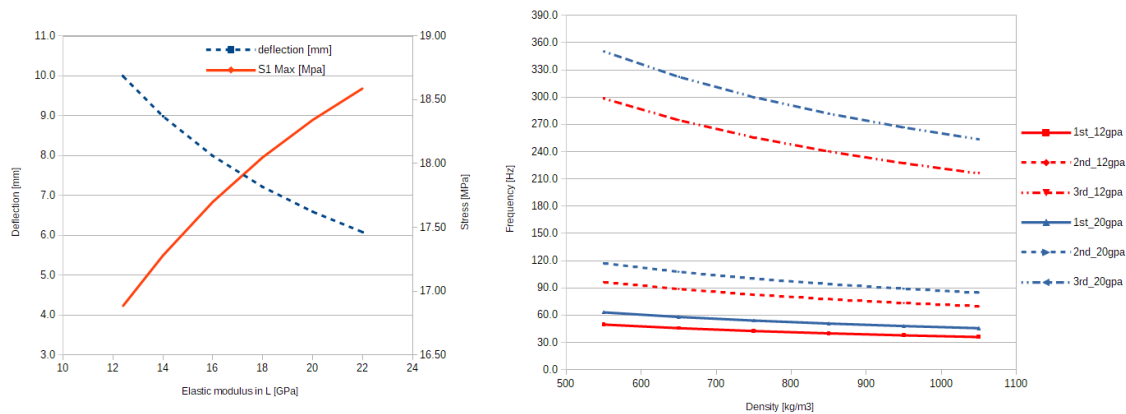


Figure 5: left – Principal stress and deflection depending on E_L , right – dependency of the first three eigenfrequencies on density for $E_L = 12.4$ GPa and 22 GPa

CONCLUSIONS

In this paper, we analyze the potential of using THM densified poplar wood as a substitute material for electric guitar necks. Such substitution contributes to the preservation of endangered exotic wood species and reduces the financial and environmental production costs, while preserving similar vibrational performance. Our experimental tests and numerical analyses show that in general, the increase of density due to densification has higher impact on vibrational properties than the increase of elastic parameters. Through FE modal analysis, we also show that orthotropic mechanical properties of densified poplar wood exhibit substantial increase in most of elastic parameters as well as in mutual ratios, and that most of eigenfrequencies decrease by using densified wood compared to native poplar.

As future work, we deem appropriate to explore how particular elastic properties participate on individual eigenfrequencies; how and what wolf tones to avoid in this EGN design; how the fully equipped EGN (frets, pegs etc.) differs in its response to currently simulated version; and what is our simulation error with respect to experimental modal analysis.

ACKNOWLEDGMENT

The authors acknowledge the European Commission for funding the InnoRenew project (grant agreement 739574) under the Horizon2020 Widespread-Teaming program and the Republic of Slovenia (investment funding from the Republic of Slovenia and the European Union's European Regional Development Fund).

REFERENCES

Bachtiar, E.V. Rugeberg, M., Hering, S., Kaliske, M., Niemz, P. (2017) Estimating shear properties of walnut wood: a combined experimental and theoretical approach. *Materials and Structures*, **50**, 248.

Cockrum, C. (2021) Guitar Building web page. <https://cockrum.net/lutherie.html>

Saint-Venant, B. (1863) Mémoire sur la distribution d'élasticité. *Journal de Mathématiques Pures et Appliquées* (Liouville), **2**, 8.

Influence of soil in oak root system on its response to bending

Sebera Václav^{1,3}, Tippner Jan¹, Paulic Vinko², Praus Luděk¹, Vojáčková Barbora¹,
Brabec Martin¹, Milch Jaromír¹

¹ Mendel University in Brno, Zemědělská 1, 613 00 Brno, Czech Republic

² University of Zagreb, Faculty of Forestry, Department of Forest Ecology and Silviculture, Svetošimunska
25, 10002, Zagreb, Croatia

³ InnoRenew CoE, Livade 6, 6310 Izola, Slovenia

Keywords: root system, tree mechanics, pulling test, digital image correlation, ultrasonic air stream method

ABSTRACT

Tree root system belongs to a key factor of the tree stability because it provides the anchorage point to the ground/soil, beside its physiological purpose. Therefore, to assess the tree stability with a certainty, it is needed to have information about tree root-plate, ie. to know roots health state, its geometrical distribution in a space with respect to a tree and surrounding objects, to know properties of the ground (soil) and to know material properties of roots. This work assessed 10 oak trees in terms of their reaction to bending induced by a standard pulling test accompanied with optical technique based on digital image correlation to obtain displacement at various locations of tree. Trees were tested in both intact state and with soil removed from the surface of the root plate. Results showed that performed soil removal did not have statistically significant effect on apparent tree stiffness. The same conclusions were found based on data provided by both inclinometers and digital camera.

INTRODUCTION

Trees are valuable part of urban environment, providing many positive functions, but also pose a risk of harm to inhabitants and adjacent structures, if failure occurs. The most severe consequences arise from failure of whole tree – uprooting or breakage in a stem. Simultaneously, root system damage is difficult to be identified, as the visual inspection is not possible or only indirect signs of damage can be used. Gibbs and Greig (1990) reported root failure in 52 % of *Fagus sylvatica*, 72 % of *Tilia vulgaris* and 73 % *Tilia platyphyllos* trees failed after 1987 storm, from population of 3954 parkland trees in Southern England, while only small portion of *Quercus robur* and *Aesculus hippocastanum* failed in this way. Koeser et al. (2020) reported 1% whole tree failures from 2069 trees after 2016 Hurricane Matthew in Charleston, South Carolina and Savannah, Georgia, US, while Klein (2020) reported 15 % of whole-tree failures from 4034 evaluated trees in Naples, Florida, US, after Hurricane Irma.

Both soil and roots are considered significant part of the tree mechanical resistance against uprooting (Coutts 1983). The influence of root system morphology alters according to the site soil properties (Dupuy et al. 2005, Dupuy et al. 2007, Fourcaud 2008), with more pronounced influence of roots in sandy soils and smaller effect in clay soils, where the outer structural roots were of major importance. The strength of the root system is affected by root geometry, root system morphology and by the soil properties (Rahardjo et al., 2009). Crook and Ennos (1996) reported high significance of the taproot and windward sinker roots to overturning resistance. Rahardjo et al. (2016) modelled effect of structural cells to uprooting resistance and found 2.5 – 3.3 increase in load resistance. Moore (2014) found significantly lower uprooting moments on *Pinus radiata* trees growing on yellow-brown pumice soils (sandy or gravelly soils) then on more clay soils. Danquechin et al. (2016) found the large main taproot, guyed by a large volume of deep roots, the major component of tree stability, as well as the greater shallow root flexural stiffness mainly at the end of the zone of rapid taper on the windward side.

Root system evaluation is difficult due to the impossibility to access it for visual assessment without certain level of damage. Indirect method are employed to investigate spatial and physiological parameters of the root system (Mancuso 2012, Čermák et al. 2015). Results of these methods is difficult to transfer into probability

of mechanical failure. For evaluation of tree uprooting probability, the pulling test method has been employed in various studies (e.g. Fraser 1962, Peltola et al. 2000, Ghani et al. 2009, James et al. 2013, Detter et al. 2014, Buza & Divos 2016). The so called general tipping curve has been established by Sinn and Wessolly (1989) for evaluation of uprooting resistance (Brudi & Van Wassanaer 2001) and the technology is widely used, despite some critics (Vanomsen 2006), both in research and practical arboriculture (Detter et al. 2014). Similar function for uprooting resistance evaluation has been introduced by Buza and Divos (2016).

Newly, optical methods are employed to allow more complex and harmless in situ measurement of trees (Sebera et al. 2014, Dahle 2017, Tippner et al. 2019). The Digital Image Correlation (DIC) methods allow easier comparison of results with numerical models and, thus, more effective analysis of tree behaviour. DIC is based on tracking of markers movement during deformation of an object. Two basic form of DIC are used, 2D-DIC and 3D-DIC. In 2D-DIC analyses of trees the stem inflections, strains, root-soil plate inclination and rotation can be measured. 3D-DIC is the stereoscopic form of DIC suitable for capturing displacements and strains on the curved surfaces as stem (Peters and Ranson, 1982; Sutton et al. 2009, Tippner et al. 2019).

MATERIAL AND METHODS

In our work, 10 oak trees (*Quercus pubescens* L.) were tested using pulling test in following regimes: (i) with soil untouched (Ref), and (ii) with soil removed (NoSoil). The trees were located in broadleaved forest, east from Zagreb city. During the test, both mechanical and optical techniques were employed to measure displacements and rotations on a tree stem, soil and roots after soil removal (see Fig. 1). The pulling force was induced using Yaletrac cable puller Y32 with nominal force 32 kN. The force was measured using forcemeter with measuring range 0 to 40 kN and accuracy of 300 N. The pulling test was controlled by a stem base rotation that was allowed up to 0.2° (Fig. 2 left) to obtain results in the non-destructive part of measurement (Sinn and Wessolly 1989) similarly to standard pulling-test examination. Stem base inclination was monitored using two inclinometers with measuring range ± 15 degrees and accuracy 0.005° . Devices are part of the Tree Qinetic system (Argus Electronic GmbH). The data were collected by communication and charger unit and controlled by Tree Qinetic system software with acquisition frequency 10 Hz.



Figure 1: a) root-soil system covered with optical markers, b) oak root system with soil removed

After each tree was measured in reference scenario (*Ref*), the soil from main root/plate was removed using air-spade to create the second scenario (*NoSoil*). The soil was removed using AirSpade 2000 powered by a diesel compressor. After soil removal (Fig. 1b), several metallic markers were inserted into the root system for optical measurement. Optical measurement employed a standard camera (Canon, 19 Mpx) with automatic acquisition with constant time step of 0.2 Hz. The image acquisition and pulling test were synchronized. Data from optical measurement were processed using digital image correlation (DIC) implemented in Mercury software (Sobriety Ltd., Czech Republic).

Each tree in both scenarios (Ref and NoSoil) was pulled by three cycles (see Fig. 2 left) and end of cycle was determined by an angle of $\sim 0.2^\circ$ measured at the tree base using inclinometer. Then a bending moment (M) was calculated using the height of rope bind at pulled tree (h), measured angle of rope (α) at maximal force (F_{max}), the moment was calculated using formula: $M = F \cdot \cos(\alpha) \cdot h$. This way we obtained M vs. angle (β) data (see Fig. 2 right) that were further used to calculate stiffness (S in kN/m). The angle β was calculated as resultant from x- and y- axis components using $\beta = \sqrt{x^2 + y^2}$. The S was calculated from M/β data from the second cycle in a range between 25% and 75% of (F_{max}) since this range represent somewhat linear relationship between bending moment and angle at the tree base (dashed lines in Fig. 2). The S was obtained through the linear regression of the filtered ranges and is expressed as slope in equation $y = a + Sx$, where a is an intercept with y-axis and S is the slope – stiffness. The linear regression were carried out using Matlab 2019b (Mathworks Inc., USA). The second cycle was chosen for the analysis because the first cycle is prone to adjustment of rope due to loading and also tree root system is compacting within an interaction with a soil. The second comparison for both scenarios was made based on optical data – horizontal displacements – from white markers created on a tree stem using chalk spray. In this study, we compared both scenarios based on three markers only – bottom, middle and top one.

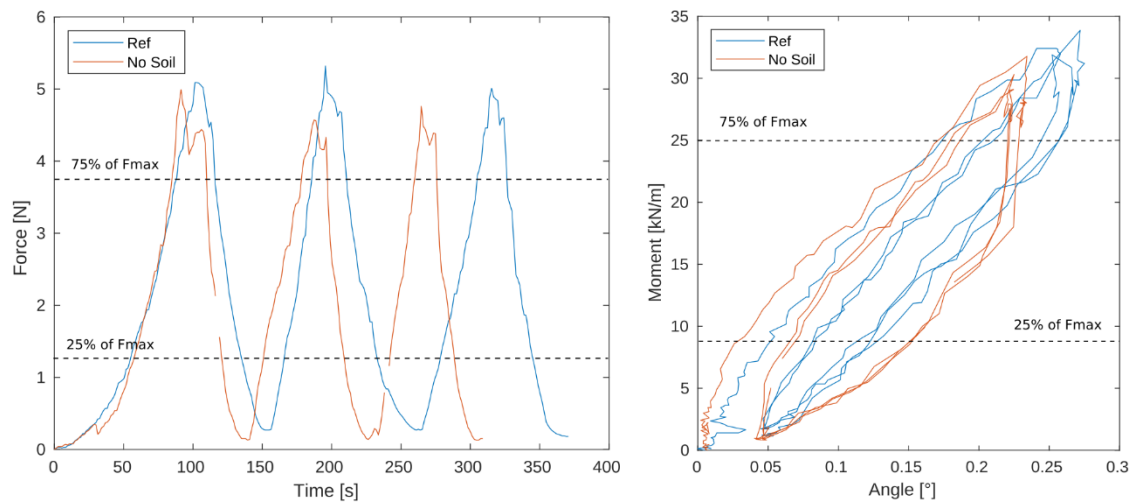


Figure 2: Example of field pulling test of three cycles, left - force vs. time data for Ref and No Soil scenarios, right – corresponding moment vs. angle data for both scenarios, line plots keep notion of cycles. Dashed lines show the range between 25-75% of F_{max} that were used to calculate stiffness.

RESULTS

The moment vs. angle data from the measurement before (Ref) and after soil removal (NoSoil) are depicted in the Fig. 3. This figure shows that each tree was loaded by three cycles that create an envelopes. The initial stage of the envelopes illustrate apparent stiffness of a tree that is examined further.

The range of moment vs. resultant angle (β) between 25% and 75% of F_{max} was fitted by a linear function and this result, for Tree no. 10, for all four mounted inclinometers is depicted in Fig. 4. It shows that slope of the fit decreased due to removing soil for three out of four inclinometers (Fig. 4b, c, d), but one inclinometer shows the opposite (Fig. 4a). These contradictory results between individual inclinometers are quite common and show how difficult it is to make convincing conclusions even for one single tree. To overcome this issue, the two inclinometers mounted at assumed neutral tree axis (at tree side) were joined and their combined slope was calculated and further analyzed.

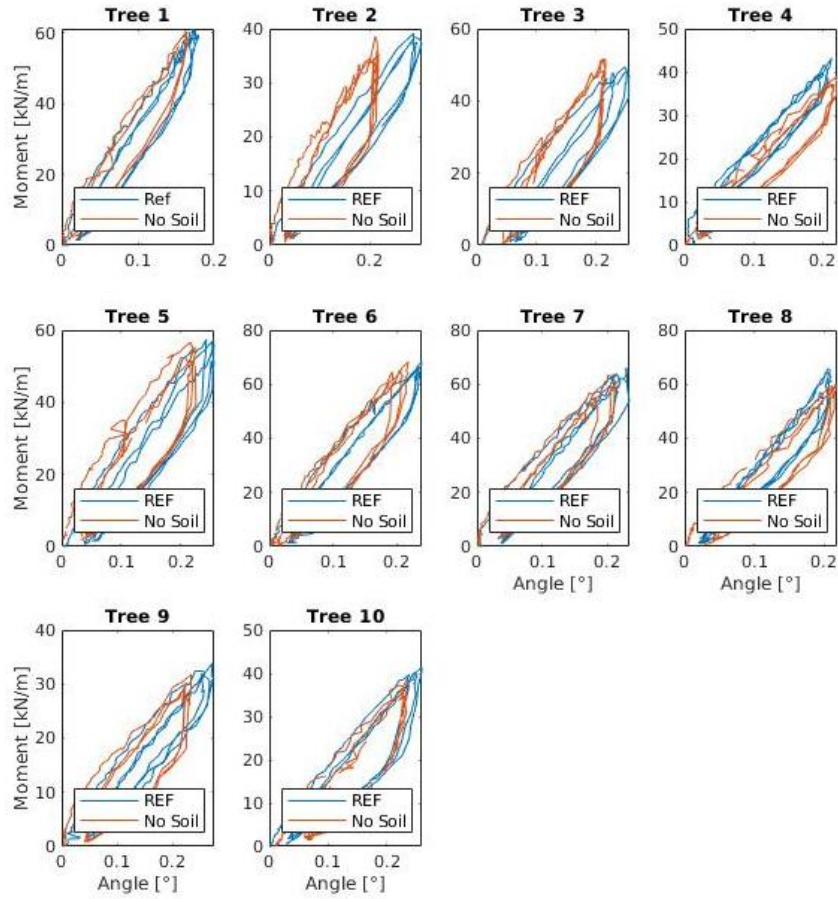


Figure 3: Moment vs. angle at the base for all tested trees with (REF) and without soil (No Soil)

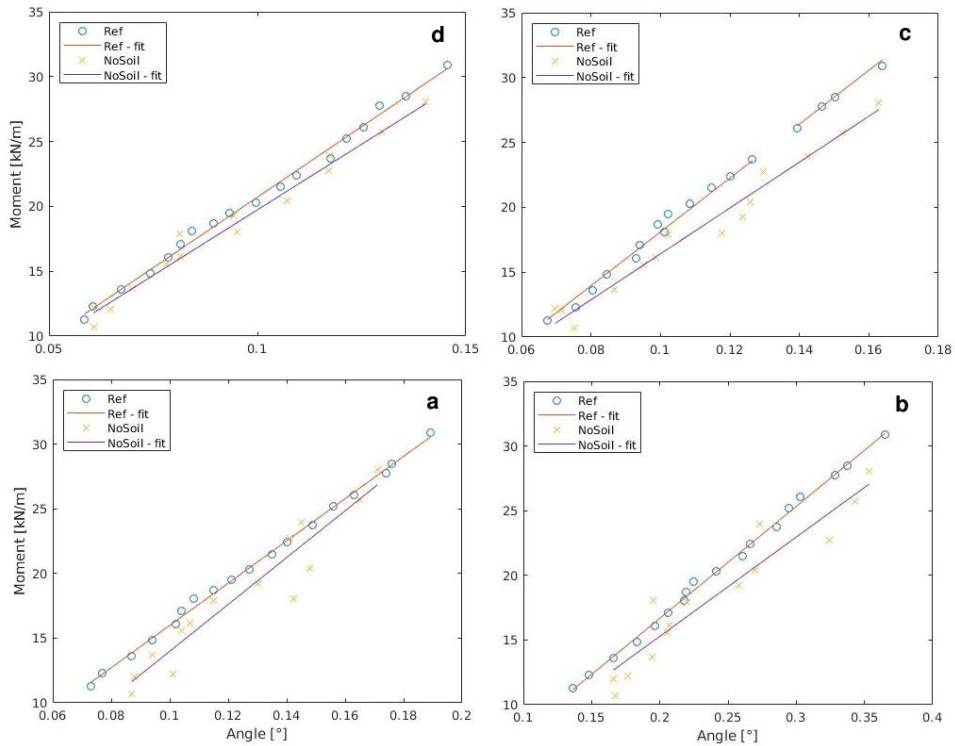


Figure 4: Moment vs. angle for Ref and NoSoil groups between 25% and 75% of F_{max} fitted by linear function for Tree no. 10

Combined slopes for each tree before and after removing soil produces two paired data sets (Table 1) that can be examined by t-test. Table 1. shows that slopes of NoSoil are sometimes lower and sometimes higher than Ref group, but these differences are within the variability of data given by slightly different conditions, different time of measurement and measurement error. T-test on a significance level $\alpha = 0.05$ showed the groups are not statistically different ($p = 0.543$).

Table 1: Slopes of linear fit for Ref and NoSoil groups

Tree no.	Slopes [kN/m.°]										<i>p</i>
	1	2	3	4	5	6	7	8	9	10	
Ref	281	122	189	207	235	306	308	253	131	150	0.543
NoSoil	265	165	251	160	253	277	335	269	133	141	

Optical data analysis

Evaluation of optical data acquired by the camera was done primarily for the markers along a tree stem (Fig. 5 left). Because there is no need to compare both groups using all the markers along the tree stem, only three markers were chosen (bottom, middle and top). For these, slopes of moment vs. displacement in horizontal direction was calculated. These three sets of paired data were analyzed using t-test as for the data from inclinometer. Tree no. 8 was not included in analysis of optical data since the light conditions at site during this measurement – changing of clear and cloudy sky – caused severe changes in image brightness and it did not allow successful tracking of markers. Fig. 5 right shows these slopes and it is clear that all the examined trees have similar responses before and after soil removal (except bottom marker at tree 6). T-test provided probability (p) and showed that slopes are not statistically different, it was $p = 0.40, 0.98,$ and 0.94 for bottom, middle and top marker, respectively. In other words, and similarly to data obtained from inclinometers, the optical analysis did not prove that soil removal statistically changed apparent stiffness of tested trees in the 2nd cycle.

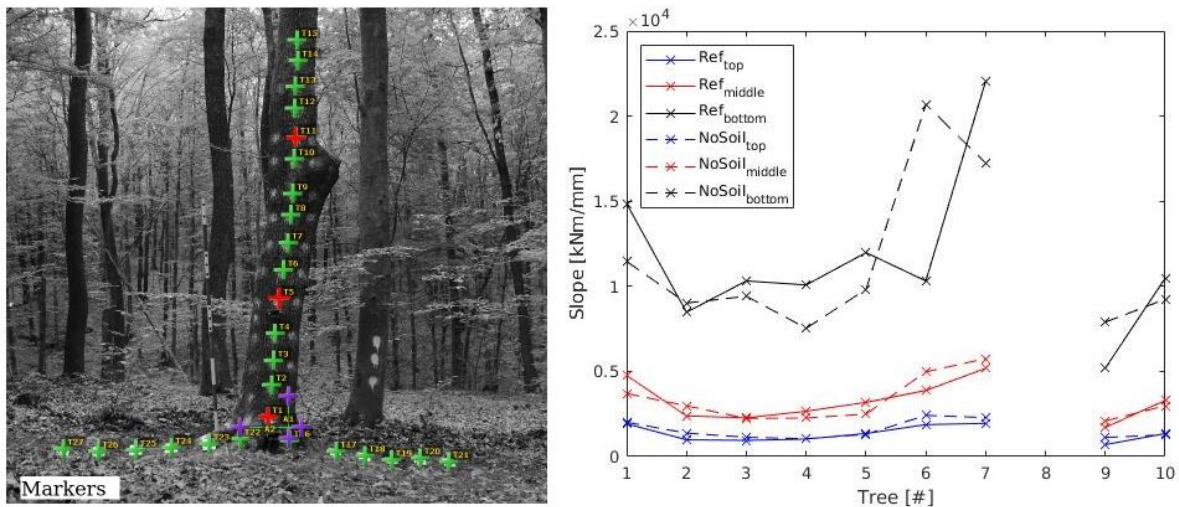


Figure 5: left – tree with three analyzed optical markers (bottom, middle, top) denoted in red; Right – slopes before (Ref) and after soil removal (NoSoil) taken from three markers for each tree (except tree no. 8).

CONCLUSIONS

From the presented work, we can draw following conclusion: i) paired t-test of measured data showed no statistical differences between tested slopes in moment vs. angle/displacement in a range of 25% and 75% of F_{max} , where the same outcome of statistical tests resulted from both inclinometers and digital camera data, ii) the variability of results corresponds with general trees mechanical behavior as complicated structure and requires further work with higher number of samples, iii) soil significance in different location within root system (in radius and depth) should be investigated.

ACKNOWLEDGMENTS

European Commission for funding the InnoRenew project (Grant Agreement #739574) under the Horizon 2020 Widespread-Teaming program and the Republic of Slovenia (investment funding from the Republic of Slovenia and the European Union's European and Regional Development Fund); and Ministry of Education Youth and Sports in the Czech Republic [Grant Number #LL1909, ERC CZ].

REFERENCES

- Bruđi, E., and van Wassanaer P. (2001) Trees and statics: Nondestructive failure analysis. In: *Tree Structure and Mechanics Conference Proceedings: How Trees Stand Up and Fall Down*, ed. E.T. Smiley, and K.D. Coder. International Society of Arboriculture, Champaign, Illinois, U.S., pp. 53–69.
- Burdekin, D.A. (2012) Gale damage to amenity trees. *Arboricultural Journal*, **3**(3), 181-189
- Buza, Á.K., Divós, F. (2016) Root Stability Evaluation with Non-Destructive Techniques. *Acta Silvatica et Lignaria Hungarica*, **12**(2), 125-134.
- Čermák, J., Nadezhdina, N., Trcala, M., Simon, J. (2015) Open field-applicable instrumental methods for structural and functional assessment of whole trees and stands. *IForest - Biogeosciences and Forestry*, **8**(3), 226-278.
- Coutts, M. P. (1983) Root architecture and tree stability. *Plant and Soil*, **71**(1-3), 171-188.
- Crook, M.J., Ennos, A.R. (1996). The anchorage mechanics of deeprooted larch, *Larix europaea japonica*. *J. Exp. Bot.* **47**(303), 1509-1517
- Dahle, G.A. (2017) Influence of bark on the mapping of mechanical strain using digital image correlation. *Wood Science and Technology*, **51**(6), 1469-1477.
- Danquechin, D.A., Meredieu, C., Danjon, F. (2016) Anchorage failure of young trees in sandy soils is prevented by a rigid central part of the root system with various designs. *Annals of Botany*, **118**(4), 747-762.
- Detter, A., Rust, S., Rust, C., Maybaum, G. (2014) Determining strength limits for standing tree stems from bending tests. In: *Proceedings of Non-destructive Testing of Wood Conference (NDTW)*, Madison, Wisconsin, U.S
- Dupuy, L., Fourcaud, T., Stokes, A. (2005) A numerical investigation into the influence of soil type and root architecture on tree anchorage. *Plant and Soil*, **278**(1-2), 119-134.
- Dupuy, L.X., Fourcaud, T., Lac, P., Stokes, A. (2007) A generic 3D finite element model of tree anchorage integrating soil mechanics and real root system architecture. *American Journal of Botany*, **94**(9), 1506-1514.
- Fourcaud, T., Ji, J.-N., Zhang, Z.-Q., Stokes, A. (2008) Understanding the impact of root morphology on overturning mechanisms: A modelling approach. *Annals of Botany*, **101**(8), 1267-1280.
- Fraser, A. I. (1962) The Soil and Roots as Factors in Tree Stability. *Forestry*, **34**(2), 117-127.
- Ghani, M.A., Stokes, A., Fourcaud, T. (2009) The effect of root architecture and root loss through trenching on the anchorage of tropical urban trees (*Eugenia grandis* Wight) *Trees - Structure and Function*, **23**(2), 197-209.

- Gibbs, J.N., Greig, B.J.W. (1990) Survey of parkland trees after the great storm of October 16, 1987. *Arboricultural Journal*, **14**(4), 321-347.
- James, K., Hallam, C., Spencer, Ch. (2013) Tree stability in winds: Measurements of root plate tilt. *Biosystems Engineering*, **115**(3), 324-331.
- Koeser, A.K., Smiley E.T., Hauer, R.J., Kane, B., Klein, R.W. (2020) Landry, S.M., Sherwood, M. (2020) Can professionals gauge likelihood of failure? – Insights from tropical storm Matthew. *Urban Forestry & Urban Greening*, **52**, 1-7
- Klein, R.W., Koeser, A.K., Kane, B., Landry, S.M., Shields, H., Lloyd, S., Hansen, G. (2020) Evaluating the Likelihood of Tree Failure in Naples, Florida (United States) Following Hurricane Irma. *Forests*, **11**(5).
- Mancuso, Stefano, ed. (2012) *Measuring Roots*. Berlin, Heidelberg: Springer Berlin Heidelberg.
- Moore, G.M. (2014) Wind-Thrown Trees: Storms or Management? *Arboriculture & Urban Forestry*, **40**(2), 53-69.
- Peltola, H., Kellomäki, S., Hassinen, A., Granander, M. (2000) Mechanical stability of Scots pine, Norway spruce and birch: an analysis of tree-pulling experiments in Finland. *Forest Ecology and Management* **135**, 143-153.
- Peters, W. H., Ranson, W.F. (1982) Digital Imaging Techniques In Experimental Stress Analysis. *Optical Engineering*, **21**(3).
- Rahardjo, H., Harnas, F.R., Leong, E.C., Tan, P.Y., Fong, Y.K., Sim, E.K. (2009) Tree stability in an improved soil to withstand wind loading. *Urban Forestry & Urban Greening*, **8**(4), 237-247.
- Rahardjo, H., Gofar, N., Amalia, N., Leong, E.Ch., Ow, L.F. (2016) Structural cell contribution to resistance of trees to uprooting. *Trees - Structure and Function*, **30**(5), 1843-1853.
- Sebera, V., Praus, L., Tippner, J., Kunecký, J., Čepela, J., Wimmer, R. (2014) Using optical full-field measurement based on digital image correlation to measure strain on a tree subjected to mechanical load. *Trees -Structure and Function* **28**, 1173–1184.
- Sinn, G., Wessolly, L. (1989) A contribution to the proper assessment of the strength and stability of trees. *Arboricultural Journal* **13**(1), 45–65.
- Sutton, M.A., Ortu, J.J., Schreier, H.W. (2009) *Digital Image Correlation for Shape and Deformation Measurements Basic Concepts, Theory and Applications*. Springer-Verlag, Heidelberg
- Tippner, J., Praus, L., Brabec, M., Sebera, V., Vojáčková, B., Milch, J. (2019) Using 3D digital image correlation in an identification of defects of trees subjected to bending. *Urban Forestry & Urban Greening*, **46**.
- Vanomsen, P. (2006) *Der Einfluss der Durchforstung auf die Verankerung der Fichte hinsichtlich ihrer Sturmresistenz*. Doctoral dissertation, ETH Zürich.

Armillarioid root rot invasion: possibilities of silvicultural and chemical control

Liqiong Chen¹, Danish Shahab¹, Orsolya Kedves¹, Simang Champramary^{1,2}, Boris Indic², Viktor Dávid Nagy¹, Csaba Vágvölgyi¹, László Kredics¹, György Sipos²

¹ Department of Microbiology, Faculty of Science and Informatics, University of Szeged, Szeged, Közép fasor 52, H-6726 Szeged, Hungary; liqiongchen2016@163.com, danish18581@yahoo.co.in (D.S.), varga_orsi91@yahoo.com (O.K.); viktor.david.nagy@gmail.com (V.D.N.); csaba@bio.u-szeged.hu (C.V.); kredics@bio.u-szeged.hu (L.K.)

² Functional Genomics and Bioinformatics Group, Research Center for Forestry and Wood Industry, University of Sopron, Bajcsy-Zsilinszky str. 4., H-9400 Sopron, Hungary; boris.indjic@phd.uni-sopron.hu (B.I.); simang5c@uni-sopron.hu (S.C.); sipos.gyorgy@uni-sopron.hu (GS)

Keywords: Armillaria, management, silvicultural control, chemical control

ABSTRACT

Armillarioid mushrooms (*Armillaria* and *Desarmillaria* species) are among the most influential root pathogens worldwide, attacking more than 500 woody host plant species of both gymno- and angiosperms. Due to climate-related biotic and abiotic stress faced by different plant species, the invasion by armillaroid root rot, acting as an opportunistic indicator of root health, is becoming increasingly important in all forest ecosystems. Therefore there is an emerging need for efficient strategies to monitor, control and manage this problem. The aim of this review is to provide an overview about the classical means of armillaroid root rot management in forests, i.e., silvicultural and chemical control measures.

INTRODUCTION

Environmental factors, particularly soil conditions and climate change, affect host defence and enhance *Armillaria* infection. The root system in plants functions as a support and storage structure. It is also responsible for the absorption and transport of nutrients, water and mineral substances from the soil. Soil factors, including oxygen, water, organic and mineral content, pH and temperature, etc., play a vital role in plant's health, particularly the root system. Climate changes, such as flood, drought, storm or global warming, are significant causes of poor soil condition and tree stress. Climate change and poor soil either weaken plant vigour, rendering them sensitive to the infection of armillaroid fungi or directly influence the survival, development, reproduction and distribution of the pathogens, as well as indirectly change the abundance of competitors and stimulators of armillaroids in forests (Ayres and Lombardero 2000, Kliejunas et al. 2009, Pearce and Malajczuk 1990).

Natural forests usually establish a more adaptive and even harmonious relationship between plants and plant pathogens. Plant species in natural forests are generally considered less susceptible to *Armillaria* infection (Chapman et al. 2011). However, they still can be compromised by various kinds of impact factors such as natural hazards and animal attacks, and cannot escape *Armillaria* infection, not even to mention the less stable managed forests. Plantation forestry is of growing economic importance all over the world. With the plantation increasing, the threat of *Armillaria* root disease to these new timber resources is also rising. Tree mortality caused by *Armillaria* frequently occurs in discrete disease centers, and forest lands occupied by *Armillaria* pathogens are usually unavailable for fiber production (Labbé et al. 2015).

Below we intend to summarize the classical approaches of armillaroid root rot management in forests applying various silvicultural and chemical measures.

SILVICULTURAL CONTROL MEASURES

Physical control measures for any disease in plant protection seem cost-effective and environmentally friendly, but these methods may be laborious, time-consuming and often impractical for established forest trees (Morrison 1976). Crop rotation is widely used in agriculture to reduce losses from fungal disease, but this practice has a little impact on *Armillaria* inoculum control, as the rhizomorphs of *Armillaria* may persist in the soil for decades. Therefore, the most effective way to minimize the incidences of *Armillaria* root disease in the new stand is to remove infested wood debris which may serve as a reservoir of inoculum (Shaw III et al. 2012, Gutter et al. 2004), however, the cost of removal rarely exceeds the financial impact of crop losses occurring without this practice (Baumgartner et al. 2011). The inoculum removal followed by crop rotation showed improvement in seedling survival, reduced *Armillaria* root rot mortality and led to higher productivity of Douglas-fir, spruce, larch and birch trees in a 40-year study (Morrison et al. 2014). Other silvicultural practices include the planting of less susceptible tree species, stumping, push falling, using proper planting and mixture schemes, thinning when the spores are not dispersing, etc. Planting resistant tree species and removing inoculum sources like infected roots and stumps were found the most effective means of controlling *Armillaria* infections (Vasaitis et al. 2008, Sturrock 2000). Mixtures of resistant and susceptible tree species provided little benefit on reducing the impact of the disease in the susceptible species (Morrison et al. 2014, Sturrock 2000). These silvicultural measures are often difficult to apply in forests because of the longevity of both the inoculum and the crop tree species (Thies and Sturrock 1995, Cleary et al. 2008, 2011). Some specific plant breeding programmes were initiated to create new plant varieties with high tolerance capacity of fungal infections caused by *Armillaria* (Beckman et al. 1998, Guillaumin et al. 1991, Beckman and Pusey 2001, Beckman and Lang 2003) but the development of plants tolerant to the fungus is still a matter of further extensive research.

One of the silvicultural strategies is to isolate the infected plants from healthy ones by removing diseased trees and uprooting even neighbouring uninfected stumps (Shaw III et al. 2012, Morrison et al. 2014, Shaw III and Roth 1978, Schüti 1985, Fox 2000, Self and Mackenzie 1995). Sometimes clearcutting would be necessarily required when the stands are susceptible and severely infected. However, several problems appeared after implementing the traditional cut-regeneration method (Lee et al. 2016). Thus, clearcutting treatment was not a feasible option, and in most areas, clearcutting was not even permitted. Also, the partial-cut system seems to reduce the disease, but it is still full of controversy and needs further investigations on the *Armillaria* response to selective cutting and partial harvesting (Chapman et al. 2011, Morrison et al. 2001). Stand thinning was not effective but usually increased disease occurrence, apparently by providing new stumps for colonization (Bendel et al. 2006); thus although thinning is an essential activity of stand silviculture, it does not appear to be a good disease management option.

Mycelia or basidiospores of fungi colonized tree stumps during forestry operations and established disease center expanding to infect neighboring trees. Consequently, stump removal was also suggested as a measure for control of *Armillaria* root rot disease in regenerating stands (Vasaitis et al. 2008). It was suggested that the efficacy of stump removal to reduce the amount of inoculum and disease occurrence over a while could reach 80-100% for *A. solidipes* (Cleary et al. 2013).

Another recommended treatment option is to limit *Armillaria* spread by removing root systems beneath soil after harvest. The root removal treatment with excavator machine application has received acceptance in some areas of British Columbia (Sturrock 2000). However, this approach was time consuming and costly. Their investigation revealed that the pushover logging (tree felling combined with root removal) did not reduce the *Armillaria* disease incidence in post-harvest regeneration, compared with hand-falling logging in which the root was not removed. It is probably because that even removal of the roots during harvesting trees can reduce the levels of inoculum, the inocula left in the soil are still sufficient and have the ability to re-establish the infection disease cycle (Reaves et al. 1993). Overall, all the mentioned approaches belong to the inoculum reduction measure with different levels of sanitation. The thirty-five-year results from Shaw III et al. (2012), concluded that thorough removal of roots by machine or hand was generally more effective in controlling *Armillaria* root disease than less intense root removal. However, even the most intensive sanitation treatment still had 23% tree mortality.

Root collar excavation routinely applies compressed air to permanently remove soil from the base of the trunk of the infested tree to the depth at which primary roots originate. The compressed air dismantles the compact soil structures while causing minimal disturbance or damage to the root system, because, without

the proper flow of nutrients and water moving through the root system, trees become stressed (Kozłowski 1999, Kuht and Reintman 2004). Then, in turn, stress opens trees up to insect and disease conditions that they would otherwise be able to fight off. Root collar excavation by removing soil from around the base of the tree to a depth of 9 to 12 inches was practiced on deciduous trees and vineyards in Greece (Panagopoulos 2007). This method was used to control the root disease of the grapevine during the early stages of root collar infection caused by *A. mellea*. This approach caused mycelial fans to recede from the root collar and increased the weight and yield of symptomatic-excavated grapevines (Baumgartner 2004). Later on, applying root collar excavation for *Armillaria* root rot control was further improved and introduced for other commercial orchard trees, such as peach and citrus (Schnabel et al. 2012).

Soil heating is another method to control for *Armillaria* root rot disease, and it may be combined with the application of antagonists against *Armillaria* spp. for improving its efficacy. The application of antagonistic strains of *Trichoderma harzianum* in the soil surrounding the site of *Armillaria* inoculum, following soil solarization for five weeks, entirely removed the viability of inoculum which could be achieved in 10 weeks of solarization alone (Otieno et al. 2003a, b). Most of the species of genus *Armillaria* grow at temperatures between 10 and 31 °C, their optimum temperatures, however, lie between 20 and 22 °C (Rishbeth 1978, Keča 2005). The heating temperature must be higher than the maximum temperature still allowing the survival of the pathogens. Soil heating can be accomplished in warm climates by solarization, while in temperate countries like Germany, soil sterilization with steam (6 kg pressure for 30 minutes at 120 °C) is used. However, the disadvantages of the steam-based technique include the necessity of annual application and the adverse effects on beneficial soil microorganisms which might in-turn distract the native soil microbiota (Raziq 2000, West 1994).

In conclusion, it remains unclear what kind of role silvicultural treatments play in disease development in forested landscapes. Harmful *Armillaria* infections seem unlikely to be reduced by practices such as clearcutting, replantation, and thinning, which provide new stumps, roots and wood debris suitable for vegetative colonization or invasion by newly formed diploids from basidiospores (Kedves et al. 2021). On the other hand, the inoculum removal measures will reduce the level of *Armillaria* root rot disease, but they do not seem to guarantee the long-term controlling effect and warrant their cost.

CHEMICAL CONTROL MEASURES

Most of the fungicides commonly available in the market did not significantly control *Armillaria* species (Tomlin 1994, West and Fox 2002). Soil fumigation is a pre-plant chemical treatment of soil, commonly used in high value cropping systems to control soil-borne pests and diseases using a pesticide that converts to a volatile gas during its application (Noling 2008). Soil fumigants, such as carbon disulfide, methyl bromide or chloropicrin, seem to effectively control *Armillaria* infections even in susceptible plants. The latter two fumigants have certain drawbacks, i.e., methyl bromide is a greenhouse gas that may contribute to global warming; therefore its use is banned, while the penetration of chloropicrin through the soil is quite difficult to achieve. Carbon disulfide is a cost-effective fungicide with lower toxicity and high penetrating ability even 3 meters into the soil, which might be a unique option to control *Armillaria* spp. (Fox 2003). Pre-plant soil fumigation with sodium tetrathiocarbonate, a liquid that breaks down into carbon disulfide gas, may also improve the control of *Armillaria* root rot (Adaskaveg et al. 1999).

The use of fumigants such as metham-sodium and methyl bromide to kill *Armillaria* pathogens in managed forests is, however, very costly and labour intensive, and it also presents occupational health risks for the labourers and farmers (Robinson and Smith 2001). Due to environmental concerns and operator safety issues during the application of some chemicals such as carbon disulfide; sodium tetrathiocarbonate (STTC or Enzone) which is an environmentally safe compound was used as an alternative. This liquid formulation can be used as a pre-plant fumigant or as a post-plant treatment, by gradually releasing carbon disulfide to kill *Armillaria* at application sites (Adaskaveg et al. 1999).

Phenolic emulsions are quite effective in controlling *Armillaria* spp. in the field. Nevertheless, inactive components of the mixtures of phenolic brands such as Armillatox or Bray's Emulsion, even the latter's active ingredient (cresylic acid) were found phytotoxic (West 1994, Fox 2003, Pawsey and Rahman 1976). In turn, several other chemicals, such as flutriafol (a triazole), fenpropidin (a piperidine), guazatine (a guanide), and phenyl phenol (a phenolic compound), were observed as non-phytotoxic fungicides more effective than Bray's emulsion used as a standard under *in vitro* conditions (Fox 2003, Gohet et al. 1991,

Aguín et al. 2006). In a field experiment, phenyl phenol and cresylic acid did not reduce the infection, while they showed toxic effects on plants (West 1994); furthermore, cresylic acid even showed a stimulating effect on *A. mellea* growth and therefore found to be counter-productive (West 1994). Other non-toxic fungicides like flutriafol, fenpropidin and guazatine, etc., are not tested yet against *Armillaria* infection under field conditions; therefore, no evidence on the effect of their application is available (Turner and Fox 1988, Turner 1991).

The fungicide cyproconazole is a sterol biosynthesis inhibitor (SBI), which revealed its effectiveness against *A. mellea* *in vitro* on malt extract agar (MEA) (Gohet et al. 1991, Aguín et al. 2006). During field experiments conducted in commercial apple (8-years-old; M26), walnut (6-years-old) and kiwifruit (9-years-old; Hayward) orchards located in Macedonia and Greece, this fungicide proved itself a potent chemical against *A. mellea* (Thomidis and Exadaktylou 2012). Other SBIs, such as hexaconazole, propiconazole and tetraconazole have also been reported as efficient fungicides against *Armillaria* spp. in vineyards and peach orchards (Adaskaveg et al. 1999, Aguín et al. 2006). Propiconazole was found to be translocated in peach roots when transfused into the trunk, indicating that the trunk transfusion could be helpful for targeted *Armillaria* root disease management (Amiri et al. 2008, Amiri and Schnabel 2012). Inhibition of fungal pathogens of woody plants by plant growth regulators also seems quite fascinating. The gibberellin inhibitor paclobutrazol (PBZ) is a triazole plant growth regulator that inhibits stem elongation (Davis et al. 1988) and has been used as an effective fungicide against *A. gallica*, as it can reduce spore germination and rhizomorph production (Jacobs and Berg 2000).

However, several problems appeared during the application of chemicals. Chemical fungicides, especially the fumigants, do not penetrate the soil deeply enough to kill all *Armillaria*-infected roots. Methyl bromide is one of the chemical fumigants used to kill *A. mellea* in residual roots, but it does not guarantee long-term control (Munnecke et al. 1976). Even though it was reported that soil fumigation treatment of methyl bromide significantly eradicated *A. mellea* from infected root segments at both depth of 0.3 m and 1.2 m (Adaskaveg et al. 1999), other fumigants including vapam, carbon disulfide, chloropicrin, and vorlex were proved to be effective in eradicating *A. mellea* from infected stumps (Filip and Roth 1977). However, grapevines growing in fumigated soil maintained health only for a few years. Eventually they became infected as their roots reached the inoculum in the deep soil that escaped the effects of the chemical fumigants. Phenolic fungicides only initially showing fungicidal effects on the mycelium of *A. mellea* eventually stimulated the *Armillaria* growth and failed to reduce the incidence of infection (West and Fox 2002). Besides, *Armillaria* pathogens, as wood decay fungi, usually hide beneath the infected root bark, to decompose wood and cause damage to the vascular system. Hence, eradicating *Armillaria* pathogens from a living host can be less efficient due to failing to deliver a fungicide directly to the infected roots (Adaskaveg et al. 1999). Indeed, fungicide injection on diseased trees infected by *Armillaria* was only effective based on the extent it actually reached the infected tissue. Thus intravascular trunk infusion has been introduced to directly target propiconazole, a DMI fungicide, into the infected tissues of *Prunus* species to inhibit mycelial growth of *D. tabescens* (Amiri et al. 2008). This systemic fungicide has been labeled for oak wilt control against fungi colonizing the vascular system (Appel and Kurdyla 1992). As most of the currently available chemical means for controlling *Armillaria* are either ineffective, phytotoxic or have some environmental consequences, there is an emerging need for effective biological control strategies applied either alone or in integration with other control measures (Raziq 2000, West 2000).

FUTURE PERSPECTIVES

Concerning the environmental threats posed by chemical fungicides, as well as the dangerous and unendurable effects from silvicultural control treatments, biological control strategies can be applied as an alternative (Proserpio et al. 2021). Biological control of fungal pathogens is environmentally friendly, therefore better to adopt. An understanding of interactions between plant pathogens and other microorganisms in natural environments is crucial for the identification of potential biocontrol agents (BCAs) as well as for risk assessment analysis. Several microbes have been identified as antagonists of different fungal pathogens by reducing the inoculum density in the infected areas. The application of naturally occurring fungal antagonists, e.g., members of the genus *Trichoderma* (Chen et al. 2019) and bacteria, e.g., *Pseudomonas* and *Bacillus* strains has substantial potential for successfully reducing the pathogenic activities of *Armillaria*. Native microorganisms derived from the rhizosphere, soil, or plant roots

usually have a better adaptation potential to the given plant and soil environment, and thus can display more efficient control of diseases, than introduced exotic microorganisms (Kedves et al. 2021).

The availability of whole-genome level sequences for an increasing number of armillarioid species (Sipos et al. 2017; Sipos et al. 2018) and identifying species-specific pathogenicity factors will further aid in developing more efficient root rot control strategies. In addition, the dual differential gene expression and enrichment analysis performed for different stages of interactions between potential biocontrol agents and *Armillaria* species have the great potential to confirm the specific role of various genes/gene families that could be involved in possible multi-stage interactions.

ACKNOWLEDGMENTS

The preparation of this review was funded by the Hungarian Government and the European Union within the frames of the Széchenyi 2020 Programme (GINOP-2.3.2-15-2016-00052).

REFERENCES

- Adaskaveg, J.E., Förster, H., Wade, L., Thompson, D.F. and Connell, J.H. (1999) Efficacy of sodium tetrathiocarbonate and propiconazole in managing *Armillaria* root rot of almond on peach rootstock. *Plant Disease*, **83**(3), 240-246.
- Aguín, O., Mansilla, J.P. and Sainz, M.J. (2006) *In vitro* selection of an effective fungicide against *Armillaria mellea* and control of white root rot of grapevine in the field. *Pest Management Science*, **62**(3), 223-228.
- Amiri, A. and Schnabel, G. (2012) Persistence of propiconazole in peach roots and efficacy of trunk infusions for *Armillaria* root rot control. *International Journal of Fruit Science*, **12**(4), 437-449.
- Amiri, A., Bussey, K.E., Riley, M.B. and Schnabel, G. (2008) Propiconazole inhibits *Armillaria tabescens* *in vitro* and translocates into peach roots following trunk infusion. *Plant Disease*, **92**(9), 1293-1298.
- Appel, D.N. and Kurdyla, T. (1992) Intravascular injection with propiconazole in live oak for oak wilt control. *Plant Disease*, **76**(11), 1120-1124.
- Ayres, M.P. and Lombardero, M.J. (2000) Assessing the consequences of global change for forest disturbance from herbivores and pathogens. *Science of the Total Environment*, **262**, 263-286.
- Baumgartner, K. (2004) Root collar excavation for postinfection control of *Armillaria* root disease of grapevine. *Plant Disease*, **88**, 1235-1240.
- Baumgartner, K., Coetzee, M.P. and Hofmeister, D. (2011) Secrets of the subterranean pathosystem of *Armillaria*. *Molecular Plant Pathology*, **12**, 515-534
- Beckman, T.G. and Lang, G. (2003) Rootstock breeding for stone fruits. In: *XXVI International Horticultural Congress: Genetics and Breeding of Tree Fruits and Nuts* **622**, 531-551.
- Beckman, T.G. and Pusey, P.L. (2001) Field testing peach rootstocks for resistance to *Armillaria* root rot. *HortScience*, **36**(1), 101-103.
- Beckman, T.G., Okie, W.R., Nyczepir, A.P., Pusey, P.L. and Reilly, C.C. (1998) Relative susceptibility of peach and plum germplasm to *Armillaria* root rot. *HortScience*, **33**(6), 1062-1065.
- Bendel, M., Kienast, F., Bugmann, H. and Rigling, D. (2006) Incidence and distribution of *Heterobasidion* and *Armillaria* and their influence on canopy gap formation in unmanaged mountain pine forests in the Swiss Alps. *European Journal of Plant Pathology*, **116**(2), 85-93.

- Chapman, W.K., Schellenberg, B. and Newsome, T.A. (2011) Assessment of *Armillaria* root disease infection in stands in south-central British Columbia with varying levels of overstory retention, with and without pushover logging. *Canadian Journal of Forest Research*, **41**(8), 1598-1605.
- Chen, L., Bóka, B., Kedves, O., Nagy, V.D., Szúcs, A., Champramary, S., et al. (2019) Towards the biological control of devastating forest pathogens from the genus *Armillaria*. *Forests*, **10**, 1013.
- Cleary, M.R., Arhipova, N., Morrison, D.J., Thomsen, I.M., Sturrock, R.N., Vasaitis, R., Gaitnieks, T. and Stenlid, J. (2013) Stump removal to control root disease in Canada and Scandinavia: A synthesis of results from long-term trials. *Forest Ecology and Management*, **290**, 5-14.
- Cleary, M., Sturrock, R. and Hodge, J. (2011) Laminated root disease-stand establishment decision aid. *Journal of Ecosystems and Management*, **12**(2), 17-20.
- Cleary, M., van der Kamp, B. and Morrison, D. (2008) British Columbia's southern interior forests *Armillaria* root disease stand establishment decision aid. *Journal of Ecosystems and Management*, **9**(2), 60-65.
- Davis, T.D., Steffens, G.L. and Sankhla, N. (1988) Triazole plant growth regulators. *Horticultural Reviews*, **10**, 63-105.
- Filip, G.M. and Roth, L.F. (1977) Stump injections with soil fumigants to eradicate *Armillariella mellea* from young-growth ponderosa pine killed by root rot. *Canadian Journal of Forest Research*, **7**(2), 226-231.
- Fox, R.T.V. (2000) *Armillaria* root rot: Biology and control of honey fungus. *New Zealand Journal of Forestry Science*, **31**(1), 150-152.
- Fox, R.T.V. (2003) Managing *Armillaria* root rot. *Journal of Food, Agriculture and Environment*, **1**, 95-100.
- Gohet, E., Van Canh, T., Louanchi, M. and Despréaux, D. (1991) New developments in chemical control of white root disease of *Hevea brasiliensis* in Africa. *Crop Protection*, **10**(3), 234-238.
- Guillaumin, J.J., Pierson, J. and Grassely, C. (1991) The susceptibility to *Armillaria mellea* of different *Prunus* species used as stone fruit rootstocks. *Scientia Horticulturae*, **46**(1-2), 43-54.
- Gutter, W.D., Baumgartner, K., Browne, G.T., Eskalen, A., Latham, S.R., Petit, E. and Bayramian, L.A. (2004) Root diseases of grapevines in California and their control. *Australasian Plant Pathology*, **33**(2), 157-165.
- Jacobs, K.A. and Berg, L.C. (2000) Inhibition of fungal pathogens of woody plants by the plant growth regulator paclobutrazol. *Pest Management Science*, **56**(5), 407-412.
- Keča, N. (2005) Characteristics of *Armillaria* species development and their growth at different temperatures. *Glasnik Sumarskog Fakulteta*, **91**, 149-162.
- Kedves, O., Shahab, D., Champramary, S., Chen, L., Indic, B., Bóka, B., Nagy, V.D., Vágvölgyi, C., Kredics, L. and Sipos, G. (2021) Epidemiology, biotic interactions and biological control of armillarioids in the northern Hemisphere. *Pathogens*, **10**(1), 76.
- Kliejunas, J.T., Geils, B.W., Glaeser, J.M., Goheen, E.M., Hennon, P., Kim, M.S., Kope, H., Stone, J.L., Sturrock, R. and Frankel, S.J. (2009) *Climate and forest diseases of Western North America: a literature review*. United States Department of Agriculture, Forest Service, Pacific Southwest Research Station, General Technical Report, PSW-GTR-225.
- Kozłowski, T.T. (1999) Soil compaction and growth of woody plants. Scand. *Scandinavian Journal of Forest Research*, **14**(6), 596-619.

- Kuht, J. and Reintman, E. (2004) Soil compaction effect on the soil physical properties and the contents of nutrients in spring barley (*Hordeum vulgare L.*) and spring wheat (*Triticum aestivum L.*). *Agronomy Research*, **2**(2), 187-194.
- Labbé, F., Marcais, B., Dupouey, J.L., Bélouard, T., Capdevielle, X., Piou, D., Robin, C. and Dutech, C. (2015) Pre-existing forests as sources of pathogens? The emergence of *Armillaria ostoyae* in a recently planted pine forest. *Forest Ecology and Management*, **357**, 248-258.
- Lee, C.A., Dey, D.C. and Muzika, R.M. (2016) Oak stump-sprout vigor and *Armillaria* infection after clearcutting in southeastern Missouri, USA. *Forest Ecology and Management*, **374**, 211-219.
- Morrison, D.J. (1976) Vertical distribution of *Armillaria mellea* rhizomorphs in soil. *Transactions of the British Mycological Society*, **66**(3), 393-399.
- Morrison, D.J., Cruickshank, M.G. and Lalumière, A. (2014) Control of laminated and *Armillaria* root diseases by stump removal and tree species mixtures: amount and cause of mortality and impact on yield after 40 years. *Forest Ecology and Management*, **319**, 75-98.
- Morrison, D.J., Pellow, K.W., Nemeč, A.F., Norris, D.J. and Semenov, P. (2001) Effects of selective cutting on the epidemiology of *Armillaria* root disease in the southern interior of British Columbia. *Canadian Journal of Forest Research*, **31**(1), 59-70.
- Munnecke, D.E., Wilber, W.D. and Darley, E.F. (1976) Effects of heating or drying on *Armillaria mellea* and *Trichoderma viride* and the relation to survival of *A. mellea* in soil. *Phytopathology*, **66**, 1363-1368.
- Noling, J.W. (2008) Soil fumigation. In: *Encyclopedia of Entomology*. Capinera, J.L. (Ed.) Springer Science, pp. 3452-3463.
- Otieno, W., Jeger, M. and Termorshuizen, A. (2003a) Effect of infesting soil with *Trichoderma harzianum* and amendment with coffee pulp on survival of *Armillaria*. *Biological Control*, **26**(3), 293-301.
- Otieno, W., Termorshuizen, A., Jeger, M. and Othieno, C.O. (2003b) Efficacy of soil solarization, *Trichoderma harzianum*, and coffee pulp amendment against *Armillaria* sp. *Crop Protection*, **22**(2), 325-331.
- Panagopoulos, C. (2007) *Diseases of Deciduous Trees and Vineyard (Greek)*, forth ed. Stamoulis Publisher, Athens, Greece, 76-88.
- Pawsey, R.G. and Rahman, M.A. (1976) Field trials with *Armillatox* against *Armillariella mellea*. *International Journal of Pest Management*, **22**(1), 49-56.
- Pearce, M.H. and Malajczuk, N. (1990) Factors affecting growth of *Armillaria luteobubalina* rhizomorphs in soil. *Mycological Research*, **94**, 38-48.
- Prospero, S., Botella, L., Santini, A. and Robin, C. (2021) Biological control of emerging forest diseases: How can we move from dreams to reality? *Forest Ecology and Management*, **496**, 119377
- Raziq, F. (2000). Biological and integrated control of *Armillaria* root rot. In: Fox, R.T.V. (Ed.) *Armillaria root rot: biology and control of honey fungus*. Intercept, Andover, UK, pp. 183-201.
- Reaves, J., Shaw, III. C.G. and Roth, L.F. (1993) Infection of *Ponderosa* pine trees by *Armillaria ostoyae*: Residual inoculum versus contagion. *Northwest Science*, **67**(3), 156-162.
- Rishbeth, J. (1978) Effects of soil temperature and atmosphere on growth of *Armillaria* rhizomorphs. *Transactions of the British Mycological Society*, **70**(2), 213-220.

- Robinson, R.M. and Smith, R.H. (2001) Fumigation of regrowth karri stumps with metham-sodium to control *Armillaria luteobubalina*. *Australian Forestry*, **64**(4), 209-215.
- Schnabel, G., Agudelo, P., Henderson, G.W. and Rollins, P.A. (2002) Aboveground root collar excavation of peach trees for *Armillaria* root rot management. *Plant Disease*, **96**, 681-686.
- Schüti, P. (1985) Control of root and butt rots: limits and prospects. *European Journal of Forest Pathology*, **15**(5-6), 357-363
- Self, N.M. and MacKenzie, M.A. (1995) Intensive site-preparation to control *Armillaria* root disease in second-rotation *Pinus radiata*. *New Zealand Journal of Forestry Science*, **25**(1), 111-116.
- Shaw, III. C.G. and Roth, L.F. (1978) Control of *Armillaria* root rot in managed coniferous forests 1: A literature review. *Journal of Forest Pathology*, **8**(3), 163-174.
- Shaw, III. C.G., Omdal, D.W., Ramsey-Kroll, A. and Roth, L.F. (2012) Inoculum reduction measures to manage *Armillaria* root disease in a severely infected stand of ponderosa pine in south-central Washington: 35-year results. *Western Journal of Applied Forestry*, **27**(1), 25-29.
- Sipos, G., Prasanna, A.N., Walter, M.C., O'Connor, E., Bálint, B., Krizsán, K. et al. (2017) Genome expansion and lineage-specific genetic innovations in the forest pathogenic fungi *Armillaria*. *Nature Ecology and Evolution*, **1**, 1931-1941.
- Sipos, G., Anderson, J.B., Nagy, L.G. (2018) *Armillaria*. *Current Biology*, **28**, R297-R298.
- Sturrock, R.N. (2000) Management of root diseases by stumping and push-falling. *Pacific Forestry Centre, Canadian Forest Service*, **16**.
- Thies, W.G. and Sturrock, R.N. (1995) *Laminated root rot in western North America*. Gen. Tech. Rep. PNW-GTR-349. Portland, OR: U.S. Department of Agriculture, Forest Service, Pacific Northwest Research Station, In cooperation with: Natural Resources Canada, Canadian Forest Service, Pacific Forestry Centre. 32 p.
- Thomidis, T. and Exadaktylou, E. (2012) Effectiveness of cyproconazole to control *Armillaria* root rot of apple, walnut and kiwifruit. *Crop Protection*, **36**, 49-51.
- Tomlin C. (1994) *The Pesticide Manual-10th Edition*. The British Crop Protection Council and The Royal Society of Chemistry.
- Turner JA and Fox RT. (1988) Prospects for the chemical control of *Armillaria* species. In: *Proceedings of the British Crop Protection Conference - Pests and Diseases*.
- Turner, J.A. (1991) Biology and control of *Armillaria*. *Doctoral dissertation, University of Reading*.
- Vasaitis, R., Stenlid, J., Thomsen, I.M., Barklund, P. and Dahlberg, A. (2008) Stump removal to control root rot in forest stands. A literature study. *Silva Fennica*, **42**(3), 457.
- West, J.S. (1994) Chemical control of *Armillaria* root rot. *Doctoral dissertation, University of Reading*.
- West, J.S. (2000) Chemical control of *Armillaria*. In Fox, R.T.V. (Ed.): *Armillaria Root Rot: Biology and Control of Honey Fungus*, Intercept, Andover, pp. 173-182.
- West, J.S. and Fox, R.T.V. (2002) The response of *Armillaria mellea* to phenolic fungicides. *Annals of Applied Biology*, **140**(3), 291-295.

Porosity of beech and oak heartwood degraded by *trametes versicolor*, L. Lloyd (*Fagus sylvatica*, L. and *Quercus petraea*, Matt. Liebl)

Barbora Slováčková

Department of Wood Science, Technical University in Zvolen T.G. Masaryka 24, 96001 Zvolen, Slovakia,
xslovackova@tuzvo.sk

Key words: beech wood, oak heartwood, porosity, degraded wood, *Trametes versicolor*

ABSTRACT

Thermal properties of both wood species degraded by *Trametes versicolor*, L. Lloyd were studied in a previously published research. Degraded wood has a lower thermal conductivity than undegraded wood and the decrease of mass loss and the increase in porosity due to degradation have also an influence on thermal conductivity among other factors. Thermal insulating materials are usually very porous and have a low density. Thus, the main objective of this study is the porosity of beech wood and oak heartwood degraded by the white-rot fungus *Trametes versicolor*, L. Lloyd. Wood degraded by wood decaying fungi has often a decreased density. Wood degraded by *Trametes versicolor*, L. Lloyd was found to have thinned out cell walls and bore holes in cell walls. Thinned out cell walls and bore holes could cause an increase of the wood porosity. Median mass losses for the researched wood species after degradation were 44.50% for beech wood and 35.74% for oak heartwood. Median porosity values of the researched wood species were 76.85% for degraded beech wood and 70.06% for degraded oak heartwood. Porosity was calculated by weighing the samples in different environments; at their maximum moisture content in the environment of water, at their maximum moisture content in the environment of air and at oven dry density. This method can not determine the size and ratio of pores in wood like the mercury intrusion porosimetry method, but it is a simple and low cost way of determining the overall porosity of wood.

INTRODUCTION

Wood is a natural, porous material. Pores in wood ensure the transport of water and nutrients in living trees. This ability to transport masses through pores remains active even after the tree is logged. It is important in many manufacturing processes – drying, vacuum drying, impregnating wood with chemicals, gluing – to mention a few.

Pores in wood are of various sizes, positions (longitudinal, radial or tangential–orientation) and geometry. These properties vary in different wood species. Some wood species' pores can be clogged by tyloses or other barriers, which greatly affects the ability to transport mass in wood. The ratio of pore volume in oven-dried wood volume is called porosity. Porosity of wood is defined as the volume of pores in a unit of wood. When mentioning pores, cavities and voids created by lumens or intercellular voids with a capillary radius higher than 100 nm and voids in cell walls with a capillary radius lower than 100 nm are meant (Požgaj et al. 1997).

Factors influencing porosity of wood are density and moisture content of wood. With an increasing density, porosity is decreasing. Until the fibre saturation point, porosity is increasing with increasing moisture content (Kúdela and Čunderlík 2012). Porosity and density of wood are important parameters that significantly influence material properties such as flow, adsorption and impregnability but also heat conductivity and tensile and bending strength (Plötze and Niemz 2011).

Pores in wood can be filled with water in its liquid or its gaseous state. The ratio of empty pores is decreasing with increasing moisture content in the whole moisture content range. The pores ratio is zero when the wood reached maximum moisture content. This porous system is important in the transport of liquids in wood. From this point of view, size of the pores, their count and morphology are important. In beech wood, vessel lumens take the highest ratio in porosity (Kúdela and Čunderlík 2012).

The white-rot fungus *Trametes versicolor* L. Lloyd is known to thin out cell walls, cause ruptures in cell walls through creating bore holes and eventually make even cells disappear. *Trametes versicolor* primarily attacks lignin, followed by cellulose and hemicelluloses (Bari et al. 2015, 2018). Thinning of cell walls and

the formation of cavities in cell walls due to degradation could greatly increase the porosity. Moreover, a partial removal of lignin is believed to increase porosity and open new pathways for the transport of solutions deep inside the material, which should facilitate a subsequent impregnation step for further functionalization (Vitas 2019, Donaldson et al. 2015, Jakes et al. 2015).

Porosity beech wood (*Fagus sylvatica* L.) and sessile oak heartwood (*Quercus petraea* Matt. Liebl.) intentionally degraded by white-rot fungus *Trametes versicolor* L. was the main focus of this paper. Porosity of the degraded wood species is expected to be higher compared to porosity of undegraded wood species. The results and experiments presented in this paper are a part of a larger, ongoing experiment on thermal properties on degraded wood and proposing a new bio-based thermal insulation material based on degraded wood. Thermal properties of the decayed wood species were described in another article (Slováčková 2021).

EXPERIMENTAL METHODS

Samples preparation

The lumber used to prepare beech (*Fagus sylvatica*, L.) and oak heartwood (*Quercus petraea*, Matt. Liebl.) samples was stored at the Department of Wood Science and Technology. The samples were cut into following dimensions (in L × R × T direction): 8 × 50 × 50 mm³; 50 × 8 × 50 mm³ and 50 × 50 × 8 mm³. As it was mentioned in the introduction, other physical properties were measured on these samples as well, so the dimensions were limited by calculations for the measurement of these properties. Measurements of diffusion coefficients and thermal properties required samples with one smaller dimension than the two other dimensions. The smallest dimension was cut accordingly to the anatomical direction of wood since the other physical properties were determined for all anatomical directions. Porosity is not influenced by the anatomical direction in wood, so the different sample size does not have a significant impact on the results. A total of 47 beech wood and 45 sessile oak heartwood samples were used in this experiment.

The samples were oven-dried, then weighed and their dimensions were measured. They were then intentionally degraded with *Trametes versicolor* L. Lloyd. The intentional degradation was performed in the laboratory of Department of Wood Technology. Kolle flasks were sterilized in an autoclave prior to the experiment. A malt extract prepared accordingly to the STN EN 113 was poured into the Kolle flasks and inoculated with growing fungal cultures. The fungus was incubated until the whole malt extract surface was fully covered with mycelium. The oven-dried samples were submerged into distilled water 24 hours prior to the degradation experiment. Four to five samples were inserted into the Kolle flasks and they were placed on “U” shaped stainless steel support. The exposition duration was 6 months.

After the exposure time passed, the samples were taken out of Kolle flasks, cleaned off visible mycelium and they were submerged into containers with distilled water. Submerging the samples caused all cavities to fill up with distilled water and it removed all air left in samples. Since there was not any air left, the fungus was not able to survive in these conditions and it stopped its activity. According to Rypáček (1957) wood decaying fungi need at least 5–20 % air in wood in order to be able to survive.

One container per wood species was used. The containers with samples were stored in a dark room with constant temperature to prevent any photochemical reactions. Distilled water was changed periodically, about every two weeks. The samples were kept in the water until they reached maximum moisture content. Reaching of the maximum moisture content was checked by double weighing the samples in water.

Calculation of the porosity

To calculate the porosity, the samples were weighed in different conditions. After the samples reached maximum moisture content, they were weighed at their maximum moisture content. First, in the environment of water (apparent mass) and then in the environment of air. The samples were then dried and their mass at oven-dried density was measured.

Porosity was calculated according to (Eq. 1):

$$p = \left(1 - \frac{\rho_0}{\rho_s}\right) \cdot 100 \quad (1)$$

where ρ_0 [$\text{kg}\cdot\text{m}^{-3}$] is the oven-dried density of the samples and ρ_s [$\text{kg}\cdot\text{m}^{-3}$] is density of wood substance. Density of wood substance was calculated according to (Eq. 2):

$$\rho_s = \frac{1}{\frac{1}{\rho_{gv}} \frac{w_{max}}{\rho_{H2O}}} \quad (2)$$

Density at green volume was calculated according to (Eq. 3):

$$\rho_{gv} = \frac{m_0}{V_{max}} \quad (3)$$

where m_0 [kg] is the mass at oven-dried state and V_{max} [m^3] is the maximum volume of the samples. The maximum volume of the samples was calculated according to (Eq. 4):

$$V_{max} = \frac{m_{max} - m_{zmax}}{\rho_{H2O}} \quad (4)$$

where m_{max} [kg] is the mass at maximum moisture content weighed in the environment of air, m_{zmax} [kg] is the mass at maximum moisture content weighed in the environment of water (apparent mass) and ρ_{H2O} [$\text{kg}\cdot\text{m}^{-3}$] is the density of water at a certain temperature.

Laboratory scale by RADWAG, Analytical Balances, model XA 60/220/X with accuracy of $1 \cdot 10^{-5}$ g was used to weigh the samples. Dimensions measurement was done with a caliper by Mitutoyo, model Absolute Digital Digimatic with an accuracy of 0.1 mm.

RESULTS AND DISCUSSION

Results of porosity calculations are summarized in Table 1. Densities after the intentional degradation as well as mass losses after the degradation are stated in Table 1 as well. Medians of all values are stated, quartiles Q1 and Q3 are below the median values in brackets. Density values were calculated for oven-dried samples. Average densities before intentional degradation were $695.4 \text{ kg}\cdot\text{m}^{-3}$ for beech wood and $736.1 \text{ kg}\cdot\text{m}^{-3}$ for sessile oak heartwood.

Table 1: Porosities, densities and mass losses of the samples.

Wood species	Porosity [%]	Density after degradation [$\text{kg}\cdot\text{m}^{-3}$]	Mass loss [%]
Degraded beech wood	76.85 (76.01 – 78.32)	346.0 (327.7 – 364.1)	44.50 (41.76 – 47.93)
Degraded sessile oak heartwood	70.06 (59.79 – 72.94)	452.8 (420.9 – 619.7)	35,74 (15.63 – 40.91)

Degraded beech wood had a higher porosity than degraded sessile oak heartwood. The mass loss was higher in degraded beech wood than in degraded sessile oak heartwood. According to the quartile values, degraded sessile oak heartwood samples showed a substantial variability in porosity and mass loss results.

Density is one of the factors influencing porosity of wood. Because there were significant fluctuations of densities in the degraded sessile oak heartwood samples, significant fluctuations of porosity values for this wood species were expected. For comparison, the minimum density among degraded beech samples was $193.4 \text{ kg}\cdot\text{m}^{-3}$ and the maximum density was $403.3 \text{ kg}\cdot\text{m}^{-3}$, whereas the minimum density among degraded sessile oak heartwood samples was $246.3 \text{ kg}\cdot\text{m}^{-3}$ and the maximum density was $770.1 \text{ kg}\cdot\text{m}^{-3}$. Minimum porosity in degraded beech wood samples was 73.41% and maximum porosity value was 87.17%. The minimum porosity value in degraded sessile oak heartwood was 50.20% and the maximum porosity value was 83.32%. That makes a 13.76% difference between minimum and maximum porosity values in degraded beech wood and 33.12% difference in degraded sessile oak heartwood. The density of wood definitely affects its porosity.

Porosity values for undegraded beech and oak wood were found in studies by Krackler et al. (2011), Plötze and Niemz (2011), Vitas et al. (2019) and Diaz-Maroto and Tahir (2019).

Porosity value of undegraded beech wood as stated by Krackler et al. (2011) is 58.9 % and density of the samples was $666 \text{ kg}\cdot\text{m}^{-3}$. Plötze and Niemz (2011) presented a beech wood porosity value of 46.93 % at a density of $401 \text{ kg}\cdot\text{m}^{-3}$ (samples were air-dried at 20°C and relative air humidity 65%). Vitas et al. (2019) presented a beech wood porosity of 52 %. All measurements in these papers were made by mercury intrusion porosimetry. Porosity of degraded beech wood is significantly higher. The porosity of degraded beech wood increased by 20–30 % compared to porosity values of undegraded beech wood found in references.

Diaz-Maroto and Tahir (2019) researched the porosity of 3 oak species. According to their research, average porosity and oven-dried density values were as follows: *Q. pyrenaica* heartwood – 53 % and a density of $661 \text{ kg}\cdot\text{m}^{-3}$, *Q. robur* heartwood – 55 % at a density of $646 \text{ kg}\cdot\text{m}^{-3}$ and *Q. petraea* heartwood – 56 % with a density of $629 \text{ kg}\cdot\text{m}^{-3}$. Plötze and Niemz (2011) presented a value of porosity for *Q. robur* – 53.81 % at a density of $706 \text{ kg}\cdot\text{m}^{-3}$ (samples were air-dried at 20°C and relative air humidity 65%). Porosity of degraded oak heartwood increased by 10 – 13 % compared to porosity of undegraded oak heartwood.

CONCLUSION

Porosity of beech wood and sessile oak heartwood degraded by the white-rot fungus *Trametes versicolor* were researched in this paper. Porosity of both wood species increased in comparison to porosities of undegraded wood found in references. Density of wood is a significant influence on porosity. It was confirmed, that porosity increases with decreasing density.

ACKNOWLEDGEMENTS

This work was supported by the Slovak Research and Development Agency under contract no. 16-0177.

REFERENCES

- Bari, E., Nazarnezhad, N., Kazemi, S., M., Ghanbary M., A., T., Mohebbi, B., Schmidt, O., Clausen, C., A. (2015) Comparison between degradation capabilities of the white rot fungi *Pleurotus ostreatus* and *Trametes versicolor* in beech wood. *International Biodeterioration & Biodegradation*, **104**, 231–237.
- Bari, E., Mohebbi, B., Naji, H., R., Oladi, R., Yilgor, N., Nazarnezhad, N., Ohno, K., M., Nicholas, D., D. (2018) Monitoring the cell wall characteristics of degraded beech wood by white-rot fungi: Anatomical, chemical, and photochemical study. *Maderas Ciencia y Tecnologia*, **20**(1), 35–56, ISSN 0718-221X.
- Diaz-Maroto, I., J., Tahir, S. (2019) Test of Wood Properties in Oak Species (*Quercus robur* L., *Quercus petraea* (Matts) Liebl. and *Quercus pyrenaica* Willd.) for Wine Aging. Part III: Porosity versus Void Ratio. *Wood Research* **64**(5), 833-846.

- Donaldson, L., A., Kroesse, H., W., Hill, S., J., Franich, R., A. (2015) Detection of wood cell wall porosity using small carbohydrate molecules and confocal fluorescence microscopy. *Journal of Microscopy*, **259**, 228-236.
- Krackler, V., Camathias, U., Ammann, S., Niemz, P. (2011) Untersuchungen zum Feuchtverhalten und zur Porosität von thermisch modifiziertem Holz. *Bauphysik* **33**(6), 374-381 (in German).
- Kúdela, J., Čunderlík, I. (2012) *Bukové drevo – štruktúra, vlastnosti, použitie*. Zvolen, Technická univerzita vo Zvolene, 152 p, ISBN 978-80-228-2318-0 (*Beech wood – structure, properties, use*, in Slovak).
- Jakes, J., E., Hunt, C., G., Yelle, D., J., Lorenz, L., Hirth, K., Gleber, S. –C., Vogt, S., Grigsby, W., Frihart, C., R. (2015) Synchrotron-based X-ray Fluorescence Microscopy in Conjunction with Nanoindentation to Study Molecular-Scale Interactions of Phenol-Formaldehyde in Wood Cell Walls. *ACS Applied Materials & Interfaces*, **7**, 6584-6589.
- Plötze, M., Niemz, P. (2011) Porosity and pore size distribution of different wood types as determined by mercury intrusion porosimetry. *European Journal of Wood and Wood Products*, **69**, 649–657.
- Požgaj, A., Chovanec, D., Kurjatko, S., Babiak, M. (1997) *Štruktúra a vlastnosti dreva*. Bratislava, ISBN 80-07-00960-4 (*Structure and Properties of Wood*, in Slovak).
- Reynolds, T., P., S., Burridge H., C., Johnston, R., Wu, G., Shah, D., U., Scherman, O., A., Linden P., F., Ramage, M., H. (2018) Cell geometry across the ring structure of Sitka Spruce. *Journal of the Royal Society Interface* **15**, 20180144.
- Rypáček, V. (1957) *Biologie Dřevokazných hub*, Nakladatelství Československé Akademie Věd, Praha, Česká republika (*Biology of Wood decaying fungi*, in Czech).
- Slováčková, B. (2021) Thermal conductivity of spruce, beech and oak heartwood degraded with *Trametes versicolor* L. Lloyd. *Acta Facultatis Xylologiae Zvolen*, **63**(1), 1-7. Zvolen, Technická univerzita vo Zvolene, ISSN 1336 – 3824.
- Vitas, S., Segmehl, J., S., Burgert, I., Cabane, E. (2019) Porosity and Pore Size Distribution of Native and Delignified Beech Wood Determined by Mercury Intrusion Porosimetry. *Materials*, **12**, 416

